Afrida Binth Iqbal

Learning from the catastrophic 1979-flood in Jostedalen in Norway

Bridging past and future across Jostedalsbreen with high-resolution hydrological modelling

Master's thesis in Natural Resources Management
Supervisor: Irina Rogozhina
Co-supervisor: Andrés Daniel Castillo Llarena
December 2022

Master's thesis

NTNU
Norwegian University of Science and Technology
Faculty of Social and Educational Sciences
Department of Geography

NTNU
Norwegian University of
Science and Technology

Afrida Binth Iqbal

Learning from the catastrophic 1979-flood in Jostedalen in Norway

Bridging past and future across Jostedalsbreen with high-resolution hydrological modelling

Master's thesis in Natural Resources Management
Supervisor: Irina Rogozhina
Co-supervisor: Andrés Daniel Castillo Llarena
December 2022

Norwegian University of Science and Technology
Faculty of Social and Educational Sciences
Department of Geography

NTNU
Norwegian University of
Science and Technology

Abstract

The last few decades have been marked by increasing intensity and frequency of heavy rainfall and extreme glacier melt events due to climate change. Through this development, regions dependent on glacier-fed river systems have become more vulnerable to repeated floods. The Jostedalsbreen National Park is in the region with highest annual precipitation in Norway and is home to the largest mainland glacier in Europe. Due to its history of major floods and a key tourism attraction, the Jostedalen valley has been monitored closely since the largest flood in the documented history of the region on August 15, 1979. The valley has experienced many modifications and developments over the years in attempt to reduce its vulnerability to floods and flood-related erosion.

Based on the evidence of the flood impacts on local communities, this study has been designed to estimate future flood risks and their possible impacts on the valley compared to the historical event of 1979. The overarching objective of this study is to reconstruct the history and impacts of the tragic past flood in Jostedalen and assess to which extent the governmental response to the past hazard protects local people from upcoming future disasters. Furthermore, the study presents model-based projections of flood exposure and vulnerability in the less documented Hjelledalen valley on the northern side of the national park to emphasize differences in the existing protective measures and their impacts. As part of this analysis, the region's sensitivity to minor versus high-intensity floods (median, 10-, 20-, 50-, 100- and 200-year floods) were tested to map and identify areas at risk under different flood. The experiments presented in this thesis are based on the high-resolution hydrological modelling using HEC-RAS (Hydrologic Engineering Centre River Analysis System) with topographic and runoff forcings from the detailed Digital Terrain Model and water flux data from gauging stations and the Regional Flood Frequency Analysis (RFFA).

The simulations show that most areas along the Jostedøla river are at risk of flooding even during minor floods (median, 10- and 20-year floods), albeit with low societal impacts. As the magnitudes of floods grow, the extents of flood damage increase drastically, showing high water levels throughout most of the populated sections of the valley. When assessing the effect of flood mitigation measures under future flood scenarios, this study has found that mitigation measures at Myklemyr are very effective even under high-magnitude floods, while the existing installations at Hesjevoll, Sperle, Fossen, Alsmo and low-lying parts of Gaupne need extensive upgrades and maintenance. The Hjelledalen valley appears to be at a very high risk of flooding from high magnitude floods, especially in the highly touristic areas at Folva and Hjelle. However, the study demonstrates that introduction of additional protective installations along vulnerable parts of the river will significantly increase the resistive capacity of the valley.

Sammendrag

De siste tiårene har vært preget av en økning i intensitet og hyppighet av kraftig regn og ekstrem smelting av isbreer på grunn av klimaendringene. Det har ført til økt sårbarhet for flom i regioner langs elveløp som kommer fra isbreer. Jostedalsbreen nasjonalpark er en av regionene med høyest årlig nedbør i Norge og er hjem til den største fastlands isbreen i Europa. Jostedalen er på grunn av dalens historie med flommer og mange turist attraksjoner blitt overvåket siden den siste store flommen som førte til store ødeleggelser i dalen den 15 August 1979. Dalen har opplevd mange forandringer og utviklet seg mye gjennom årene i et forsøk på å redusere sårbarheten mot flommer og medfølgende erosjon.

Denne studien estimerer flom risiko i fremtiden og mulige påvirkninger på samfunnet sammenlignet med den historiske hendelsen i 1979. Det overordnede målet er å rekonstruere historien og påvirkningene til den ødeleggende flommen i Jostedalen og å vurdere i hvilken grad statlig respons og tiltak etter hendelsen beskytter lokalsamfunn fra fremtidige katastrofer. Dessuten presenterer denne studien modell-baserte projeksjoner av flom utsettelse og sårbarhet i Hjelledalen, en dal på andre siden (nord) av nasjonalparken, for å analysere forskjeller i eksisterende beskyttende tiltak og deres effekter. Regionens sensitivitet til flommer av mindre og større intensitet (median, 10-, 20-, 50-, 100- og 200-års flommer) blir analysert for å kartlegge områder som er i fare under forskjellige flom-scenarioer og for å identifisere høy-risiko soner. Eksperimentene i denne oppgaven er basert på hydrologisk modellering med høy oppløsning i HEC-RAS (Hydrologic Engineering Centers River Analysis System) med topografisk info fra den Norske Digitale Høydemodellen og avrennings data fra målestasjoner og den Regionale Flom Frekvens Analysen (RFFA).

Simulasjonene viser at de fleste områdene langs Jostedøla er i fare for oversvømmelser allerede under mindre flommer (median, 10- og 20-års flom), riktignok med lav samfunnspåvirkning. Med økende flom intensitet øker flomskadene drastisk og viser høy vannstand i de fleste bebodde områdene i dalen. Analysen av effekten av tilpasnings tiltak mot flom under forskjellige scenarioer viser at tiltakene som har blitt gjort i Myklemyr er veldig effektive under alle scenarioer mens betraktelig oppdatering og vedlikehold er nødvendig i Hesjevoll, Sperle, Fossen, Alsmo og Gaupne for å motstå fremtidige flom hendelser. Flere områder i Hjelledalen, spesielt Folven og Hjelle, står i stor fare for oversvømmelser fra høy-intensitets flommer. Imidlertid demonstrerer studien at ytterligere beskyttende installasjoner i utsatte områder langs elva vil øke resistensen mot flom hendelser.

Acknowledgements

The completion of this thesis marks the end of my Masters in Natural Resource Management. Words are not enough to describe how incredible and enlightening this journey has been. Having moved to a new country in the midst of a global pandemic has tested my strength, resilient and emotional limits. With the support of the incredible friends, mentor, and colleagues, I can say I have made it through the hardest of time.

I would like to thank my supervisor, Dr. Irina Rogozhina for her unwavering support and dedication towards making this thesis the best version of itself. Her constant encouragement and trust made me experience the most incredible fieldworks. Thank you for making me believe I can do anything if I set my mind to it. I am grateful for all the guidance and feedback that kept me motivated to work hard to complete this thesis successfully.

I would like to convey my gratitude to my co-supervisor, Andrés Daniel Castillo Llarena, for the guidance and support he provided whenever I hit a dead end. Thank you for your valuable insights and solutions to my technical problems.

A special thanks to the GOTHECA team for always showing support and giving advice throughout my journey. I could not have gone through the fieldworks and the experience of writing this thesis without the help of my dear friend and project partner, Jogscha, thank you for always keeping me encouraged.

This master's journey would have been a dull one without the incredible friends I have made at NTNU and Trondheim. I will forever be grateful to have such an amazing and supportive group of friends, who bring out the best in me. Thanks to Julie, Amy, Aljona, Su, Peter, Rakeb, Steff, Tima, Ben, and Zuza for the incredible 2.5 years and keeping me motivated every step of the way. A special thanks to my best friend thousands of miles away, Anika, for always being there to respond to my frustrations and celebrate my achievements.

Finally, I want to thank my parents and siblings who guided and supported me to reach this stage of my life. Thanks to for always believing in me and encouraging me in achieving my academic goals.

Table of Contents

List of Figures

List of Tables

List of Abbreviations (or Symbols)

BC	Boundary Condition
DEM	Digital Elevation Model
DTM	Digital Terrain Model
EG	Energy Gradient
GOTHECA	Glacier impacts On The Hydrological systems in Europe and Central Asia
HEC-HMS	Hydrologic Engineering System-Hydrologic Modelling System
HEC-RAS	Hydrologic Engineering System- River Analysis System
IC	Initial Condition
LiDAR	Light Detecting and Ranging
NEVINA	Nedbørfelt-Vannføring-INdeks-Analyse
NIBIO	Norsk institutt for bioøkonomi
NVE	Norges vassdrags- og energidirektorat
RFFA	Regional Flood Frequency Analysis

1 Introduction

1.1 Background

Part of the cryosphere that plays a vital role in the land-atmosphere energy exchange are glaciers (Vaughan, Comiso, & Allison, 2013). Evidence of the warming climate is best seen in the changes in mountain glaciers. Due to elevation dependent warming, glaciers are more susceptible to responding to climate change than low-laying areas (Pepin et al., 2015). With the increase of global temperatures in the past decades, the pace of ice thinning, glacier retreat, sea-ice retreat and diminishing snow-cover has increased since the dawn of 21st century (Demiroglu, Dannevig, & Aall, 2018; Zemp et al., 2015). The rapid melting of glaciers causes a change in the hydrological regime which leads to increased glacier run-off and growth of glacial lakes resulting in sudden floods and deadly mass movements downstream. Such phenomena are increasing in Norway resulting in repeated flood and flood warnings in downstream areas towards the end of ablation seasons.

Norway, being in a temperate climate zone is exposed to the North Atlantic Current which moves temperate ocean currents to the Norwegian coast. Abundant precipitation from the Atlantic ocean and the north sea is carried by the mild air masses causing heavy precipitation and frequents floods in the windward side of the mountain ranges and the rain shadow on the leeward sides of the country (Roald, 2021). The Norwegian Water Resources and Energy Directorate (NVE) highlights eight causes of floods in Norway: Snowmelt floods, Rainfall floods, ice run floods, floods caused by slides, Jøkullhlaup- floods from glacier dammed lakes, floods due to condition of the ground, effects of lake, and backwater and bifurcations. However, majority of floods in Norway is caused by rainfall in combination with snowmelt (Roald, 2021). Besides this combination, some areas in the country are prone to Jøkullhlaup or glacier lake outburst flood (GLOF) and sudden drainage of the glacier lakes with little to no warnings.

With the increased glacier melt and precipitation due to global warming, there is however a threat to of sudden high impacts floods and glacier induced hazard in several regions of Norway where communities and businesses are dependent on glacier fed rivers and valley. The most eminent being hydropower in Norway, which accounts for more than 95% of power production within the country. The hydropower production is highly dependent on runoff from glacierized river basins (Gong & Rogozhina, 2021). The western Norway is one of these regions that are highly valuable to hydropower reservoirs, prone to frequent floods caused by increased melt and dependence on the downstream rivers for local businesses.

The largest mainland ice cap in Europe, Jostedalsbreen, is one of the glaciers that has been studied for the longest. So has been its largest and best-known outlet glacier, Nigardsbreen (Oerlemans, 1992, 1997, 2007; Østrem, Liestøl, & Wold, 1976). On the contrary, the glacier north of Jostedalsbreen, Tystigbreen has be rather studied less compared to most of the glaciers in the Jostedalsbreen national park. Tystigbreen, currently has 2 known active glacier lakes that drain almost every year causing risk of flooding in the downstream valley. For this master thesis, the focus will be on the Nigardsbreen glacier, the River Jostedøla, the valley Jostedalen on the southern part of the Jostedalsbreen glacier and Tystigbreen glacier and the valley Hjelledalen in the North of Jostedalsbreen. The Jostedøla catchment area has a well-documented history of glacier advances and retreat as well as floods along the Jostedalen valley. The largest flood in the Jostedalen occurred in August 1979 due to intense rainfall in the area. This has been the most devastating flood till date causing re-routing of tributaries of the river, erosion of riverbed, damage of roads, infrastructure, and farmlands in the area. There were no fatalities, but residents had to be evacuated and displace. The valley suffered a loss of 32 million NOK (Hoel, 2013; NVE, 1981). The flood was caused by intense rainfall from the south combined with melting of the glaciers. Several other floods have occurred since the 1979 but not as intense. The region is still prone to frequent floods due increased glacier melt and runoff and abundance of precipitation. NVE has been carrying out mass balance observation of Nigardsbreen since 1962 and the glacier length change measurement since 1899. The glacier's first known written history can be traced back to 1735 (Østrem et al., 1976). The surface ice velocity of the glacier along with the water levels and water discharge of the river in several gauge stations along the River Jostedøla is currently being monitored (Miriam Jackson, 2014; Roald, 2021). Roald (2021) has an inventory of the ten largest observed floods at three gauging stations in Jostedalen dating back to 1969 until 2014. The well documented observations and data on the glacier and the valley are an important asset to analyse what are the significant climate drivers of the re-current floods in the area. While Jostedalen valley has a well-documented history, Hjelledalen is the opposite. This valley has very few documentations of the glacier retreat. But, due to the presence of the Summer Ski Centre on the Tystigbreen glacier, information of the changing glacier and the glacier lakes are available as well as observations and data collected by the GOTHECA team.

The diverse availability of flood estimation models, high resolution digital elevation models and observed data has enabled a great opportunity to recreate the past floods and analyse the impacts caused by the intense floods and how this can be used to mitigate and adapt to present and future floods. With access to elevation models and climate data and various computational models such as HEC-RAS, HEC-HMS, MIKE FLOOD, MIKE SWMM, MIKE11, and InfoWORKS, it now possible to simulate velocity, depth, and several other characteristics of floods that occur in snow and glacier-fed basins. One of the best hydrodynamic models for flood simulation and analysis that currently exists and have been used by several studies around the world is the Hydrologic Engineering Centre River Analysis System (HEC-RAS) (Hayat et al., 2021). HEC-RAS is developed by the U.S. Army Corps of Engineers to perform one-dimensional steady flow hydraulics; one and two-dimensional unsteady flow river hydraulics calculations; quasi-Unsteady and full unsteady flow sediment transport-mobile bed modelling; water temperature analysis; and generalized water quality modelling in 1995 and several updates and versions has been released since then (Brunner, 2021a). 2D modelling in HEC-RAS can create flood simulations and help identify potentials areas at risk from floods. It can be used to reconstruct past floods and future flood scenarios using appropriate hydrological and climate data.

In Norway, flood frequency estimation has been going on since 1976 for regulations of dams and rivers. The two-flood estimation methods that are used by NVE are Flood frequency analysis and Rainfall-runoff modelling (Wilson et al., 2011). Flood frequency analysis is performed based on the observed historical flood events and an estimated magnitude of the floods with a return period. The Rainfall run-off model converts rainfall into surface run-off using a catchment response model and calibrates the model based on observed data or estimated catchment characteristics (Wilson et al., 2011). A Flood frequency model is more applicable to the interests of this research since it is performed using observed flood data at site of interest or from several comparable gauged basins within the region. Therefore, for this study, Regional Flood Frequency Analysis or RFFA-2018 flood values and observed data from gauging stations in Jostedalen and Hjelledalen, has been used to perform 2D unsteady flow analysis in HEC-RAS to create frequent Median, 10- year and 20- year flood scenarios, reconstruct the major past flood of 1979 and construct future 50-, 100-, and 200- year flood scenarios. The simulations aimed at testing the resistive capacity of the valleys in handling the floods and the effectiveness of the mitigation measures against the floods.

1.2 Objectives and Research Questions

Local communities in the Luster and Stryn Municipalities have lived for centuries side-by-side with glaciers and have been using glacier runoff to sustain their livelihoods and local economies. The municipalities are also among areas with the highest topography and markedly high precipitation in Norway where weather-related flood hazards and consequent slope hazards are common. Many floods affected the areas in the past and, it has become vital to study the impacts of the glacier changes, change in water discharge and climate forcings leading to these changes in the regions where communities are vulnerable to the hazards and have their livelihoods dependent on the glacier fed hydrological systems.

This thesis is setting a stage for the studies of future impacts of climate changes, glacier melting and possible glacier hazards on the hydrological systems in the Jostedøla and Hjelledøla rivers within the GOTHECA project. The main objective of this study is however not directly linked to the glaciers themselves but to the largest historical flood in western Norway, the terrifying impacts of which on local people are thoroughly documented along one of the two rivers and represent invaluable constraints on model-based flood reconstructions. Linking the impacts of historical and potential future floods on the infrastructure, agricultural lands, and settlements along Jostedøla and Hjelledøla is therefore of vital importance for the local people and businesses since these areas are some of the most touristic places in Norway today. The methodological objective of this study is creating such link between past and future by setting up hydrological modelling experiments to reconstruct the historical floods and perform future projection of flood with higher magnitude. Through the implementation of this methodological objective, the thesis is addressing its overarching objective by focusing on the story of the region with the documented signatures and consequences of the tragic past flood and assessing the extent to which the governmental response to the hazard has protected local people from the upcoming future disasters. The scientific objective of the study is to link the reconstructed floods to the available observations and identify the range of uncertainties and with this range, perform future projections of the impacts of comparable or even stronger floods on the involved communities.

The study has been set to address its overarching goal by answering the following research questions:

1. To which extent can the impacts of the 1979 flood on the valley downstream be reproduced and explained using a high-resolution hydrological model? What are the critical limitations that we experience when designing such historical experiments and what conclusions can we draw about the magnitude of this historical event from the analysis of model-based reconstructions against existing documentation of the induced damage?
2. How efficient are the flood protection installations and terrain modifications introduced after the 1979 flood to prevent damage to private property and infrastructure in the valley under future flood scenarios of similar and even larger magnitudes?
3. What can we learn from the historical and future simulations of the Jostedøla floods to identify and protect other vulnerable sectors in the Jostedalsbreen National Park from similar future weather extremes and glacier melt events, using Hjelledalen as a case study?

1.3 Study Area

The drainage basin comprising Nigardsbreen and other surrounding glaciers in the south-east of Jostedalsbreen has its water flowing into the Jostedalen valley through the Jostedøla river and its many tributaries (Figure 1). For this study, the focus will be on Nigardsbreen and the river Jostedøla due to their long history of prevailing floods and their impacts on the communities living down the valley. In the Hjelledalen region, the glacier lakes from Tystigbreen drain into the Hjelledøla river through the tributaries Videdøla (in the east) and Sunndøla (in the south) (Figure 1). Prevalence of minor floods due to precipitation and snow melt combined with glacier lake drainages in this region imply that habitants may suffer from loss and damage in the future and have done so in the past, making these two rivers important targets for this study.

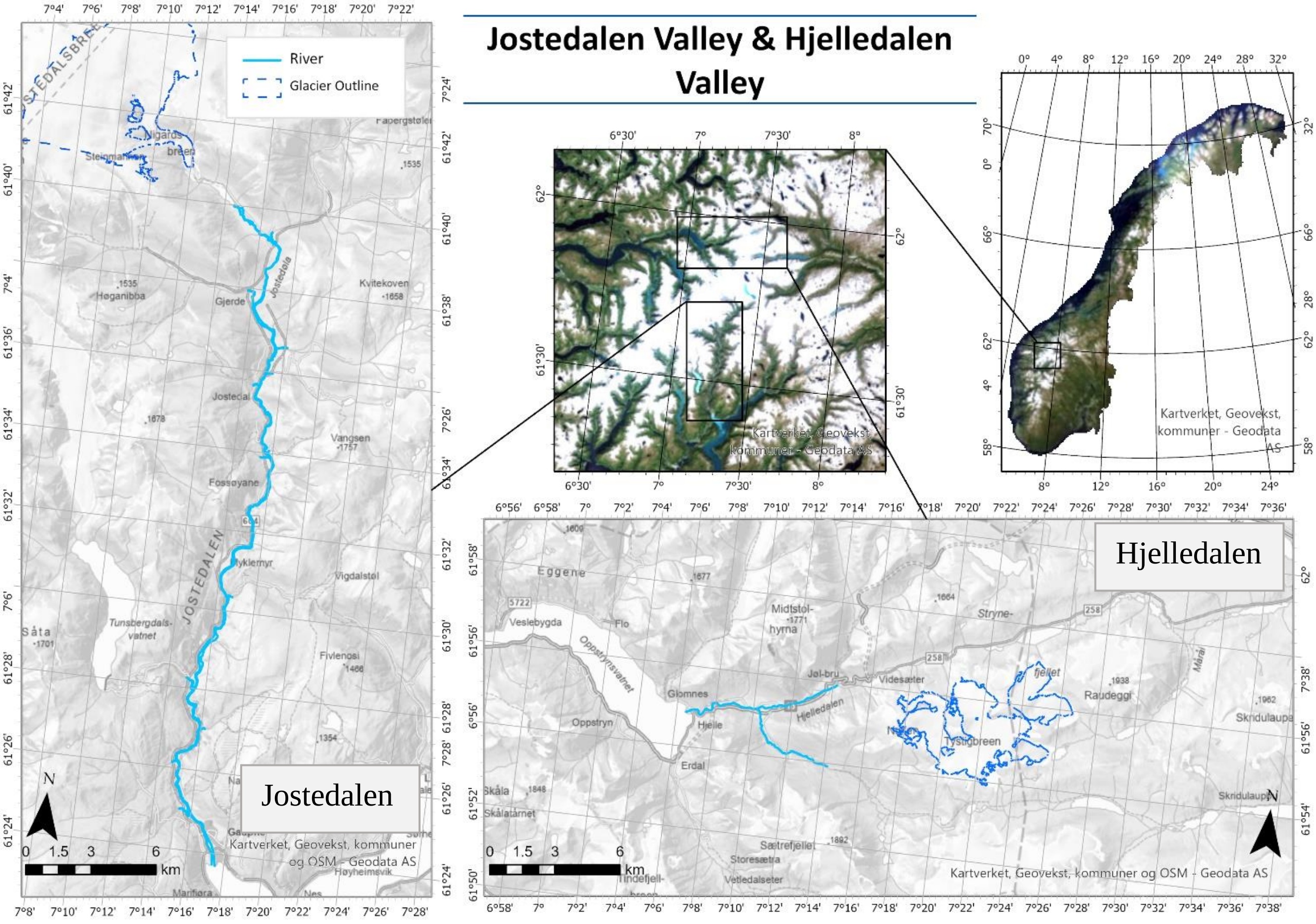

Figure 1: Study Area map of Jostedalen and Hjelledalen Valleys

The two valleys situated on the north and south of the Jostedalsbreen national park have different precipitation patterns and different historical records of floods and flood damage. While both valleys are prone to floods, the focus of governmental protective projects has been on Jostedalen due to its higher population and tourism attraction when it comes to monitoring its rivers. Hjelledalen with its smaller community still has a lot of tourism in the valley but has received little attention in terms of flood monitoring.

The 1979 flood is a key focus of this study, due to its large extent of damage and combined trigger from high temperature, glacier melt and heavy precipitation. This combination makes it interesting to look at why only the valley of Jostedalen was impacted so much and not the northern valleys of Jostedalbreen, including Hjelledalen. The interviews performed in Jostedalen and the post-flood briefing by NVE (1981) state that the flood in the valley was triggered by a temperature increase leading to the excessive glacier melt and by heavy precipitation during the night before. Based on this information, this study has looked at the weather patterns within the two valleys and across the Jostedalsbreen national park in August of 1979 to infer why the flood occurred only in Jostedalen. Figure 2 shows temperature changes during the week before the flood on 15th August 1979 based on the SeNorge data (SeNorge, 2022). Temperatures in both valleys were gradually increasing until the maximum values on the 15th of August, potentially increasing glacier run off. From the air temperature maps, it can be seen that temperature has reached very high values (above 20 degrees along most parts of the valleys) within both values during 3 consecutive days prior to the flood, even though upstream of Hjelledalen shows less increase in temperature. It is clear that the primary trigger for the flood was a heavy rainfall that is clearly captured as a very local event in the precipitation map for August 14, 1979 (Figure 3), with precipitation patterns being very different for the two valleys. One week before the flood Jostedalen received 29.1 mm of rainfall, whereas in Hjelledalen there was much less precipitation, namely 1.3 mm (Figure 3G). As the week progressed towards the flood, the region remained dry until the 14th of August, when the entire Jostedalbreen area received heavy precipitation ranging from 20-40 mm. In the Figure 3H, it is quite evident that the southern part of Jostedalsbreen received much more precipitation than the north. Focusing on the two study areas, it can be seen that the Jostedalen valley received 66.8 mm rainfall on the 14th of August, whereas in Hjelledalen it was only a 1.9 mm mean rainfall. Therefore, it is clear why there is so much evidence for the largest and most devastating flood in Jostedalen but no evidence for any flood in the northern part of the national park, including Hjelledalen.

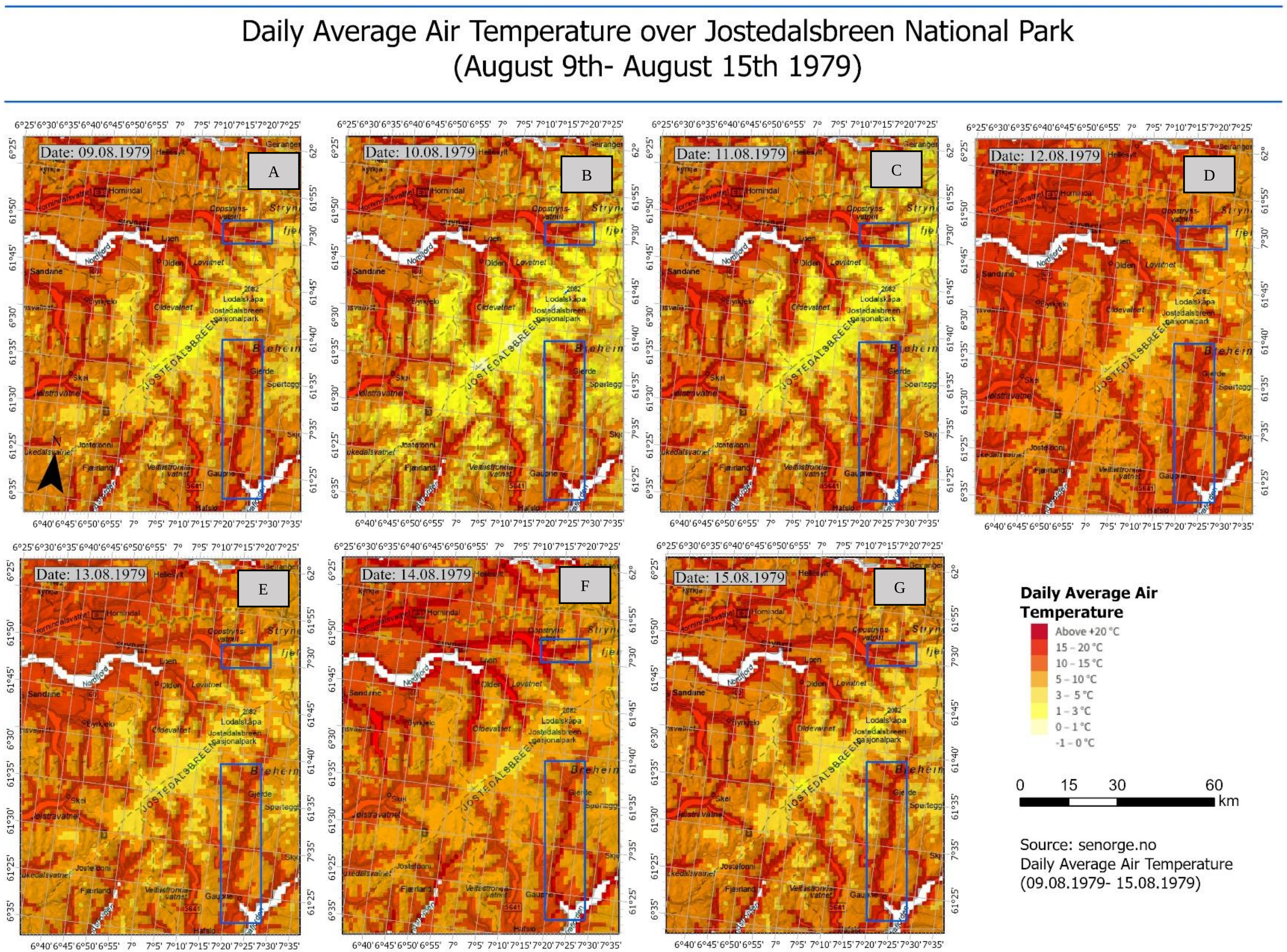

Figure 2: Daily Average Temperature over Jostedalsbreen National Park: 9th August- 15-August 1979, (Source: senorge.no)

Daily Average Precipitation over Jostedalsbreen National Park
(August 9th- August 15th 1979)

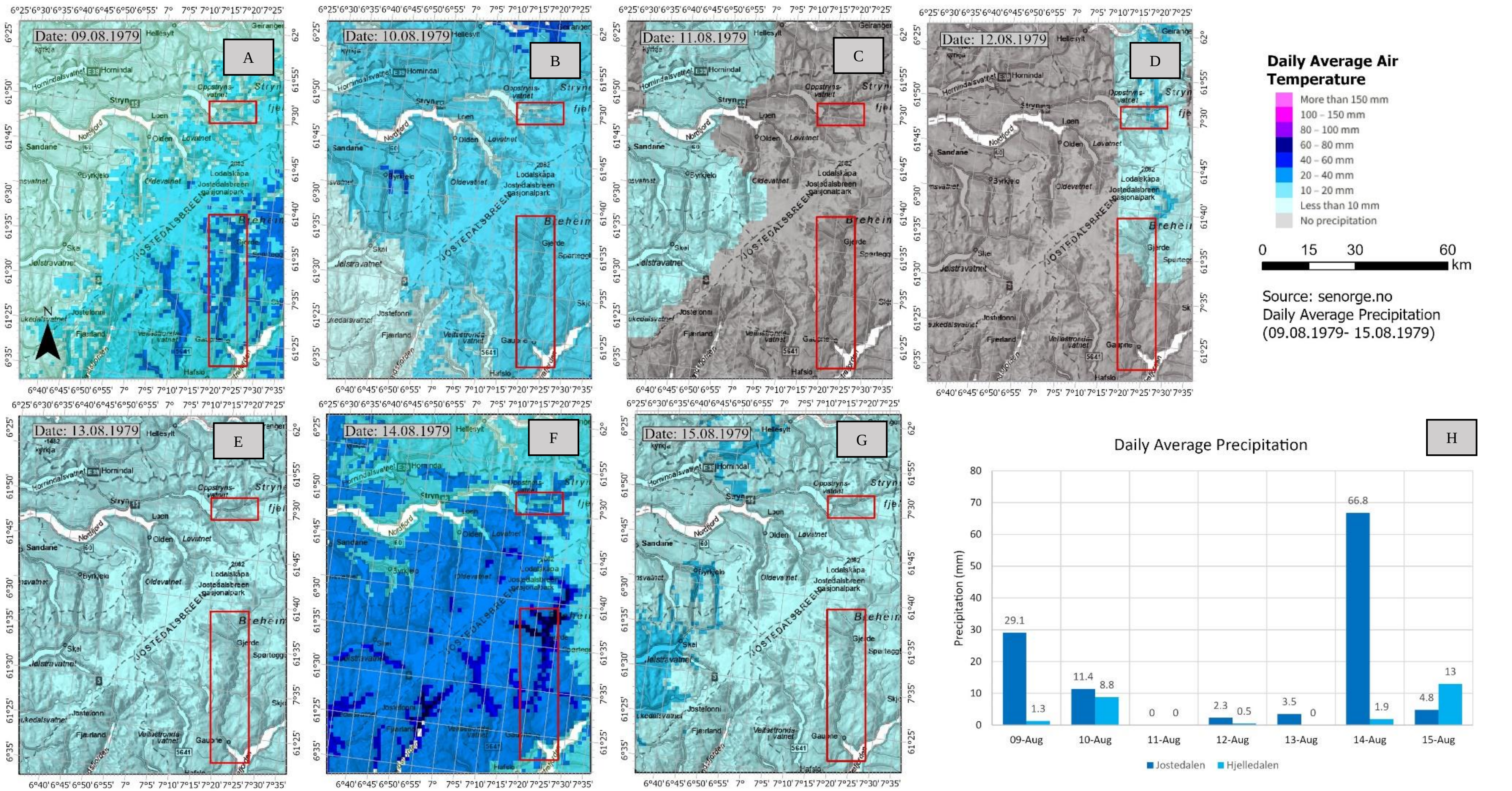

Figure 3: Daily Average Precipitation over Jostedalsbreen National Park: 9th August- 15-August 1979, (Source: senorge.no)

1.3.1 Jostedalen Region

1.3.1.1 Nigardsbreen Glacier

Nigardsbreen is located on the south-east (61°42′N, 7°08′E) of the largest mainland glacier in Europe, Jostedalsbreen. It is the most known and one of the largest outlet glaciers of Jostedalsbreen with an area of 44.9 km^2 (2020). The area accounts for 10% of the total area of Jostedalsbreen and stretches from an extend of 398m asl to 1955m asl (Bjarne Kjøllmoen, 2021).

The glacier area reduced from 46.6 km^2 in 2013 to 44.9 km^2 in 2020. The length of the glacier was 10.3 km (Oerlemans, 2007) but the tongue of the glacier receded between 300-400m from 2013 to 2020 and a total of 2.5km change in length since the length measurement started in 1899. The largest retreat occurred during 1940-1970, however, between 1988-2003 the length increased 280m but from 2003 onwards the retreat continued (NVE, 2020). The glacier one of the most climate sensitive glaciers in southern Norway. According to Oerlemans (1992) ice-flow model, Nigardsbreen is predicted to retreat by 6.5km for 1 K warming and advance 3km for 1 K cooling, because of the large sensitivity of the glacier due to its dynamic geometry.

The written history of Nigardsbreen can be traced back to the 1735 and images of the retreat of the glacier can be found from as far as the 1869. During 1735 the glacier had a dramatic advance which led to destruction of valuable grasslands in the valley (Figure 4). The ice from the glacier damaged cultivated land and infrastructure of the farms. The glacier ceased to advance in 1748, has never since reached so far down the valley (Oerlemans, 1997). Photo inventory of the glacier retreat can be found from 1869 until 2021 in the NVE Glacier periodic photo webpage (NVE, 2022a). Figure 5 shows photos of the glacier tongue taken from the same position from summer of 1951 until summer of 2021.

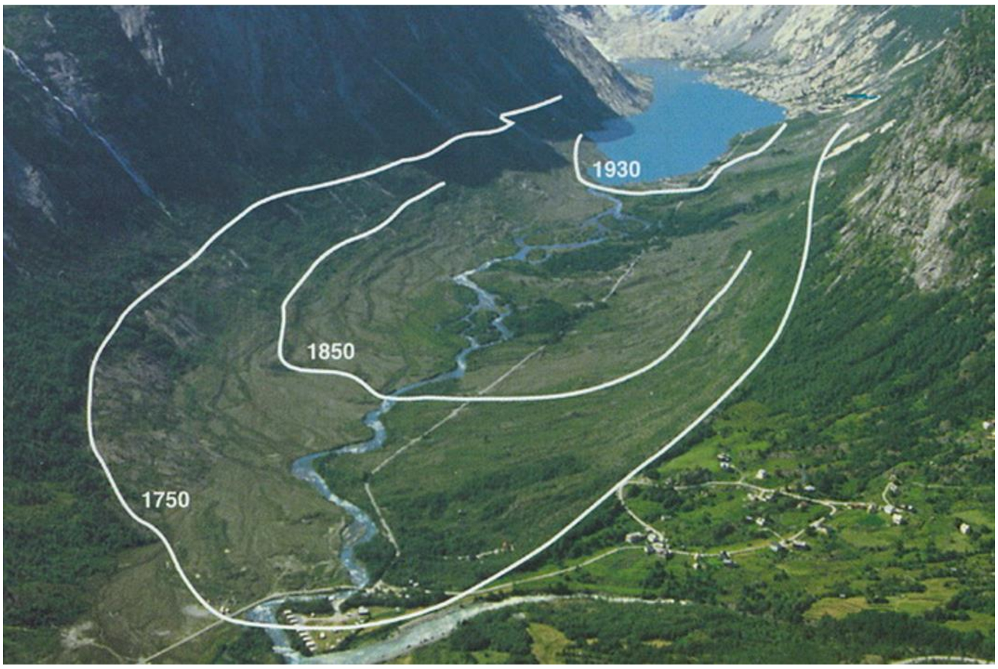

Figure 4: Outline of glacier tongue from 18th, 19th and 20th century, Photo: Carstens (2015)

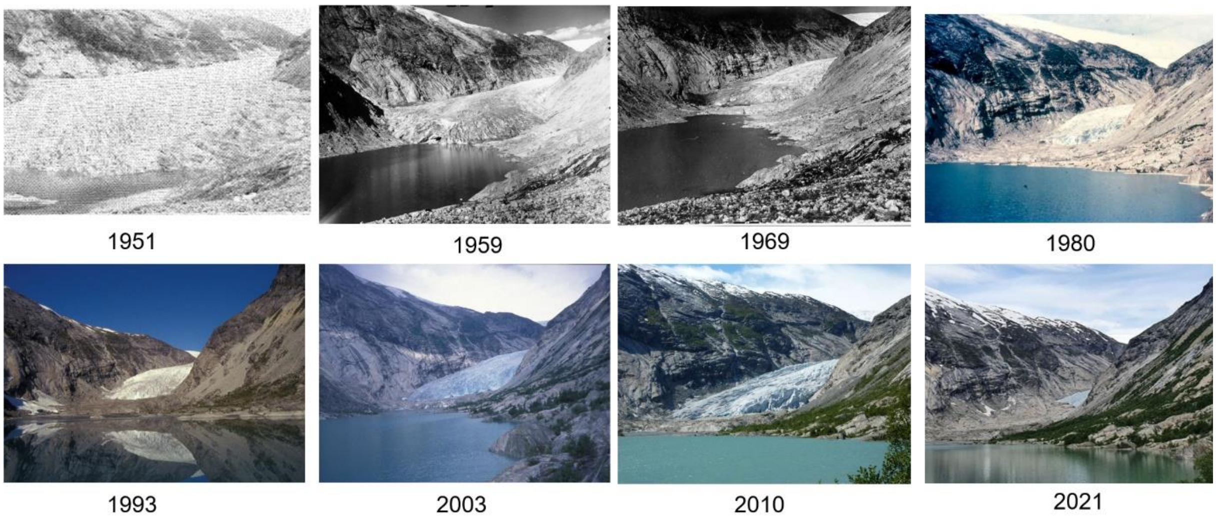

Figure 5: Retreat of Nigardsbreen 1951-2021, Photo: NVE (2022a)

1.3.1.2 Jostedalen valley and Jostedøla River

Jostedalen valley runs through the town of Gaupne, population of 1233 (SSB, 2022), in Luster municipality into the Lusterfjorden. The river Jostedøla and several of its tributaries from the Jostedalsbreen glacier flows through the valley making it an ideal settlement for farming and tourism (Figure 6). The valley highly impacted by the Jostedalsbreen glacier on its west, therefore, the river has been monitored since 1949 by several gauging stations located throughout the river and the Nigardsbreen lake (Roald, 2021).The two active gauging stations in the river are currently located in the Nigardsbreen lake outlet and Myklemyr. The inactive gauging stations data are however still accessible.

Figure 6: Jostedøla river and the valley (Photo: Afrida Iqbal)

1.3.1.3 Regulation and hydropower reservoirs

Currently there are no hydropower reservoir in the chosen study area, but there are two hydropower reservoirs, one located north of Nigardsbreen in Syggevatnet and one South of Nigardsbreen in Tunsbergdalsvatnet. The river Leirelva downstream of Tunsbergdalsbreen, in the east of Jostedøla has been regulated due to large number of jøkullhlaup from Brimkjelen causing floods in Jostedøla (Roald, 2021).

1.3.1.4 Historical Floods in the Jostedalen valley

The latest NVE report (Roald, 2021), gives an account of the 10 largest floods that has been observed gauging stations in the Jostedøla river. Table 1 has the dates and ranks from the largest observed floods (daily values) from the gauging stations Nigardsbrevatn and Myklemyr.

Table 1: 10 largest floods observed in gauging station in Jostedøla (Roald,2021)

76.5 Nigardsbrevatn			76.10 Myklemyr		
1962-2014			1979-2014		
Year	Date	Rank	Year	Date	Rank
1969	30/7	8	1979	15/8	1
1970	25/6	10	1981	1/10	10
1979	15/8	2	1985	1/10	3
1997	30/8	1	1989	21/9	6
2003	15/8	9	1997	30/8	2
2005	21/7	5	2007	15/8	8
2007	15/8	6	2009	1/9	9
2010	22/7	4	2010	22/7	5
2011	28/8	7	2011	29/6	4
2014	6/8	3	2014	28/10	7

The largest one-day flood observed in river was in Myklemyr on 15 August 1979 with a discharge of 409.1 m^3/s corresponding to 711 $l/s/km^2$ or to a runoff of 61.4 mm/day. This was the most devastating flood in the region since 1898. Both the major flood occurred on 15 August 1898 and 1979 respectively. The flood in 1979 was 1.35 meters higher than the one in 1898. Flood markers for both the major floods can be found in the valley (Figure 7).

Figure 7: Flood Markers from 1898 and 1979 (Photo: Rasmus Benestad)

Brief documentation of the 1979 Flood

The flood in 1979 was triggered due to heavy precipitation, high temperatures and warm air with strong winds causing severe glacier melt (NVE, 1981). Rainfall of 77.8 mm, which came during a 12-hour period caused the heavy water flow and rise in water level in the river and the tributaries leading to the most damaging flood the valley had ever suffered. The report published by NVE 2 years after the flood stated that the flood was as rare as a 100-year flood (NVE, 1981). However, according to modern calculations by NEVINA, the flood in August 1979 is now categorised as a 50-year flood. The flood caused severe damage to the infrastructure, commercial and residential buildings, and the riverbed. The flood water inundated the first floors of several houses, approximately 100 residential buildings and 30-40 commercial buildings were damaged. Large and small bridges as well as the national road to the Jostedalen valley was heavy damaged, as a result the valley was isolated for 2 weeks. A total of 150 acres of cultivated land was destroyed. The total damage in the region rounded up to NOK 32 million. There were no loss of life or injury during the flood, but several residents and many tourists were trapped in the valley (Hoel, 2013).

Due to the completion of the Leirdøla Power Plant the year before and the reservoir in Tunsbergdalsvatnet, the water that would have come in from the Leirdøla river was captured, preventing major damages in Gaupne (Hoel, 2013).

Recent flood warning

In the recent years, the flood warnings have increased in frequency according to the locals in the area. During the field visit by GOTHECA in 2021 an interview with a local suggested that the flood warnings have increased in years since 2009. The interviewee also mentioned that the camping place near the river has suffered damage in 2009 due to sudden rise in water levels and guests had to be evacuated due to flood warnings in summer of 2010. The same scenario was experienced by the GOTHECA team during their 2019 visit. The water levels in the river were extremely high and there was an evacuation warning in the area.

1.3.1.5 Previous and ongoing work on Nigardsbreen and Jostedøla

NVE has been performing mass balance investigation of Nigardsbreen since 1962. The latest report by NVE, Bjarne Kjøllmoen (2021), has an account of the glacier boundary for 2020. The same report also investigates the mass balance for 2020 and annual mass balance for 1962-2020 period as well as surface ice velocity of the glacier for the period of 2019-2020. Oerlemans (1992, 1997) studied the climate sensitivity of the glacier by applying the energy-balance model and using the flow-line model for Nigardsbreen projected the future length of the glacier based on dynamic calibration from historic records.

NVE also has several gauging stations along the Jostedøla river and in the valley to measure hourly and daily water level, water flow and water temperature of the river. The data for both active and inactive stations are publicly available in NVE's Sildre website (NVE, 2022c). A Flood calculation project was carried out by NVE in 2001 in 3 flood prone locations in the valley at Gaupne, Myklemyr and Fossøy (Drageset, 2001)

1.3.2 Hjelledalen Region

1.3.2.1 Tystigbreen glacier

Tystigbreen is in the north of Jostedalsbreen (61°55′ N, 7°21′E) at the border of Stryn municipality in Vestland and Sjak municipality in Innlandet on the Tystigen mountain. The glacier is about 16.5 km^2 is area and the highest altitude is 1900 m a.s.l (Hagen, 2019). The glacier is best known for the Stryn Summer Ski resort located right next to it. The glacier is accessible by the ski lift and is readily used during the summer for sports and tourism. The glacier has 2 active glacial lakes located on its south-east wing that has precedent of drainage almost every year (Figure 8).

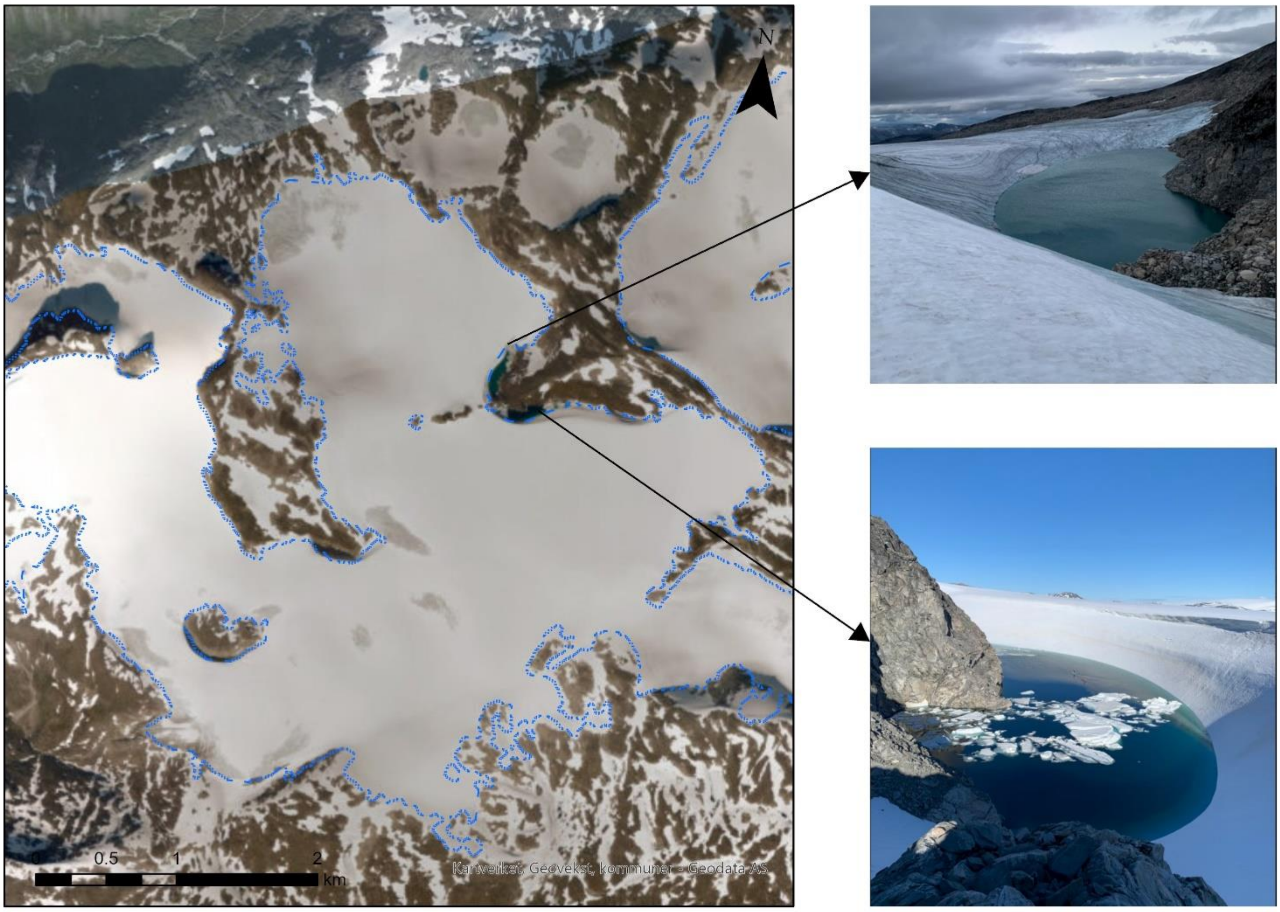

Figure 8: Tystigbreen and the 2 glacial lakes (Lake Photos: Jogscha Miriam Abderhalden)

1.3.2.2 Videdøla river, Sunndøla river and Hjelledalen Valley

The glacier being located at a high altitude, it drains through several streams running down the mountain into the Videdalen valley in Videdøla river (Figure 9A). The glacial lake on the north side drains into the Videdøla river (Figure 9B) while the lake on the lower side drains through the Sunndøla river in the Sunndalen valley southeast of the glacier. Both the rivers join in Hjelledøla flowing through Hjelledalen into the Oppstrynsvatnet lake.

1.3.2.3 Floods in Hjelledalen

According to NVE inventory on floods (Roald, 2021), the major historical floods in the valley occurred in 1722 and 1726. There is very little information on the extend of these floods. Nevertheless, interviews with some of the locals in the area suggest that there are rarely any floods in the valley. The river system is wide enough to hold the drainage from the glacial lakes. However, there has been floods in the region according to historical records and given the rapid and frequent drainage of the glacial lakes in Tystigbreen, there is a risk of flood in the valley.

1.3.2.4 Previous work on Tystigbreen and Hjelledalen

Tystigbreen is one of the key study areas of the GOTHECA project. The glacier is of particular interest due to its two glacial lakes. A recent master thesis by the project analysed extent of risk that GLOF of the both lakes at Tystigbreen can cause if they drain at the same time (Svendsen, 2022).

The river flow monitoring system in the area is low. Currently there are no active gauging stations in either of the rivers in the valley. However, during the period of 1967-2017, NVE had some active gauging station in the valley in expectations for development of hydropower. The stations were, however, later shut down due to cancellation of hydropower development plans (Roald, 2021). The data for the inactive gauging stations are available for use on their Sildre website.

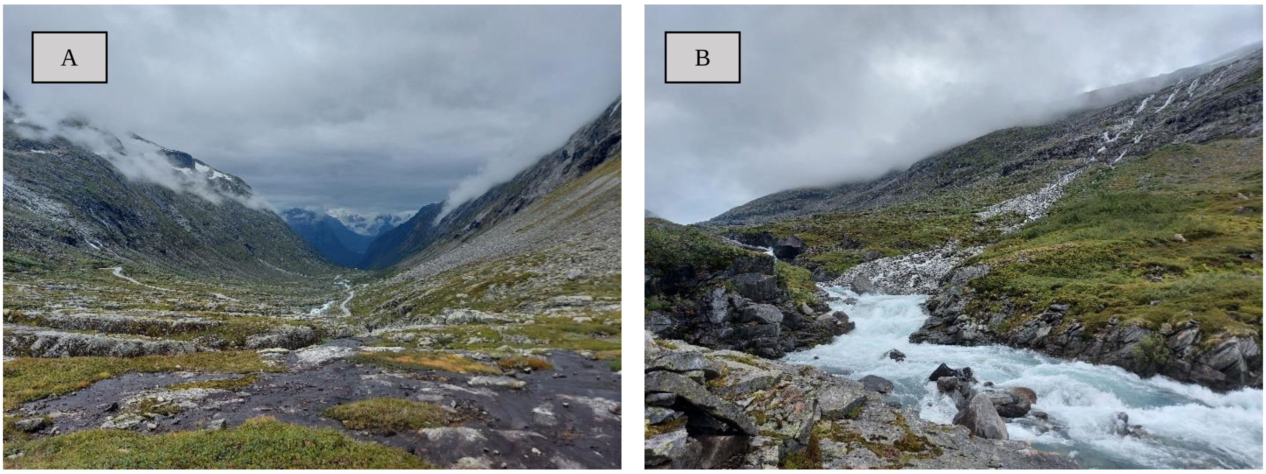

Figure 9: A) Videdalen Valley upstream of Hjelledalen, B) Stream from Tystigbreen flowing into Hjelledøla (Photo: Afrida Iqbal)

2 Methods

This chapter contains the information about the data used in performing the hydrological simulations developing the hydrological model, the process explaining the steps of developing the numerical simulations the model in HEC-RAS and sensitivities of the model based on different parameters. The data includes the LiDAR based DTMs, hydrographs made from waterflow data to simulate floods, orthophotos to identify terrain modification since the 1960's and interviews from the valley to validate impacted locations during the 1979 flood. Tthe performed simulations development of the model in HEC-RAS has been discussed in detail in sub-chapter 2.2 along with the modifications that were done to the terrain model.

2.1 Data collection

2.1.1 Elevation models

Elevation data for the study was downloaded from the Norwegian mapping authority, Kartverket services (hoydedata.no). The elevation models for the study areas, Stryn, Skjåk and Luster municipalities were downloaded in GeoTIFF format from the national elevation model project which creates Digital Terrain Models (DTMs) from airborne Light detection and Ranging (LiDAR) data collected throughout Norway. LiDAR is a remote sensing method that pulse laser in order to measure range or distance to the surface of the earth. The lasers in combination with other variables recorded by airborne system creates accurate 3-dimensional information about the structure of the earth and the characters of its surface (Lim, Treitz, Wulder, St-Onge, & Flood, 2003; NOAA, 2021).

Table 2: Data source for Digital terrain models (DTM)

	Jostedalen	*Hjelledalen*
Dataset	National Elevation Model DTM 1	National Elevation Model DTM 1
Resolution	1 meter	1 meter
Year	2020	2020
Format	GeoTIFF	GeoTIFF
Source	https://hoydedata.no/LaserInnsyn/	https://hoydedata.no/LaserInnsyn/

The DTMs used for this study (Table 2) were 1-meter resolution, even though for hydrological modelling 1 m resolution is not optimal due to its coarse resolution but these are the most precise and updated DTMs available for the study areas. For Jostedalen four DTM were merged to create one terrain model, whereas for Hjelledalen, one DTM was used. This was solely due to the variation in the size of the 2 locations.

2.1.2 Water flow data

The waterflow data used in the study were collected from NVE hydrological data services, (sildre.nve.no) and NEVINA. The website sildre.no has a collection of all the active and inactive gauging stations throughout Norway. It provides a time series for water level, water flow and water temperature as well as snow and groundwater data for certain locations. Depending on the gauging station, the data is available dating back to 1950s until today. The data varies from weekly to hourly water flow, water level and temperature.

For the Jostedalen valley, most of the data were collected from the 2 active stations 76.5.0 Nigardsbrevatn and 76.1.0 Myklemyr (Table 3). For Hjelledalen, most of the station in the valley has been inactive, since the cancelling of hydropower development plans (Roald, 2021), however there is still waterflow and water level data available from the 2 stations 88.16.0 Hjelledøla and 88.14.0 Sunndøla.

Table 3: Gauging stations along Jostedalen and Hjelledalen

Station name	*Valley*	*Station Number*	*Active years*	*Earliest available data*
Nigardsbrevatn	Jostedalen	76.5.0	1962-present	1998
Myklemyr	Jostedalen	76.1.0	1978-present	1978
Hjelledøla	Hjelledalen	88.16.0	1982-present	1982
Sunndøla	Hjelledalen	88.14.0	1967-1989	1967

Given the constrain on the availability of real time waterflow data for the tributaries of both the rivers in Jostedalen (Figure 17) and Hjelledalen, another webservice by NVE was used. NEVINA, Nedbørfelt-Vannføring-INdeks-Analyse or Rainfall and waterflow index analysis, is a mapping service that generates catchment boundaries of watercourses, calculate field parameters, climate and hydrological parameters and estimates low water indices and flood values. The annual runoff and Regional Flood Frequency Analysis or RFFA-2018 were acquired for the tributaries of the two valleys.

2.1.3 Orthophotos

The largest floods documented in Jostedalen dates to 1979 (Roald, 2021). The landscape and land use in the area have changed drastically in the last 43 years. The change in land-use and development of infrastructures for flood protection and hydropower has a major impact on the rivers in the valley. Therefore, to identify and to account for the changes in the valley aerial photographs from the past were used. Norge i Bilder, (www.norgeibilder.no) is a webservice in collaboration with Statens Vegvesen, NIBIO (Norwegian institute for Bioeconomics) and Staten Kartverk (Norwegian National Mapping Authority) that provides an overview of orthophotos of Norway. The most recent high resolution aerial photos available for Jostedalen is from 2019 with 0.1m resolution and the oldest available aerial image is from 1964 with a resolution of 0.2m. As for Hjelledalen the most recent aerial photos are from 2020 with a resolution of 0.1m and oldest images are from 1966 with a resolution of 0.4m.

2.1.4 Interview and observations from GOTHECA fieldwork in the Valleys

The study includes information collected from informal interviews with the owner of one of the camping sites in the Jostedalen valley in 2021 and observations from the GOTHECA team members during one of the fieldworks in 2019 on the extent of flood damage and rise in water levels in the river during the months of June-August. Similar interviews were conducted with an ex-museum national park employee and a farmer in the Hjelledalen region in Summer 2021 about their experiences of the previous floods that effected the area.

2.2 Set up of the hydrological model HEC-RAS

The software HEC-RAS, Hydrological Engineering Center-River Analysis System, was developed by the U.S. Army Corps of Engineers in the 1995 and have released several updated versions until 2020. For this thesis HEC-RAS versions 5.0.7 and 6.3.1 has been used. The version 6.3.1 was used to implement the terrain modifications. The enables users to perform 1-dimension steady flow, 1- and 2-dimension unsteady flow calculations, mobile bed /sediment transport computations, and water quality/ water temperature modelling (Brunner, 2021a).

The software is designed for multitasking and interactive use. The modelling system includes a graphical user interface, separate analysis components, data storage and management abilities, graphics, mapping, and reporting system (Brunner, 2021a). The river analysis components of HEC-RAS include:

1) One-dimensional steady flow water surface profile computation
2) One-dimensional and two-dimensional unsteady flow simulation
3) Quasi-unsteady or fully unsteady flow movable boundary sediment transport computation, 1D and 2D
4) One-dimensional water quality analysis

All the four component of the software uses the same geometric data representation and common geometric and hydraulic computation routines. HEC-RAS also has a spatial data integration and mapping system called RAS Mapper, which enables users to view, edit and export simulation results and maps to other software like ArcGIS Pro.

For this study, 2-dimensional unsteady flow simulation was used to construct floods in the 2 valleys of Jostedalen and Hjelledalen. HEC-RAS 2D unsteady flow model is best suited for large river systems which are flood prone and have an inconsistent water flow. Several studies have proven that this model produces the most accurate simulations of flood compared to other flood mapping models (Hayat et al., 2021). Figure 10 gives a brief overview of the steps that were taken while setting up the model. Sub-chapters 2.2.1-2.2.6 discusses in detail how the following steps were implemented.

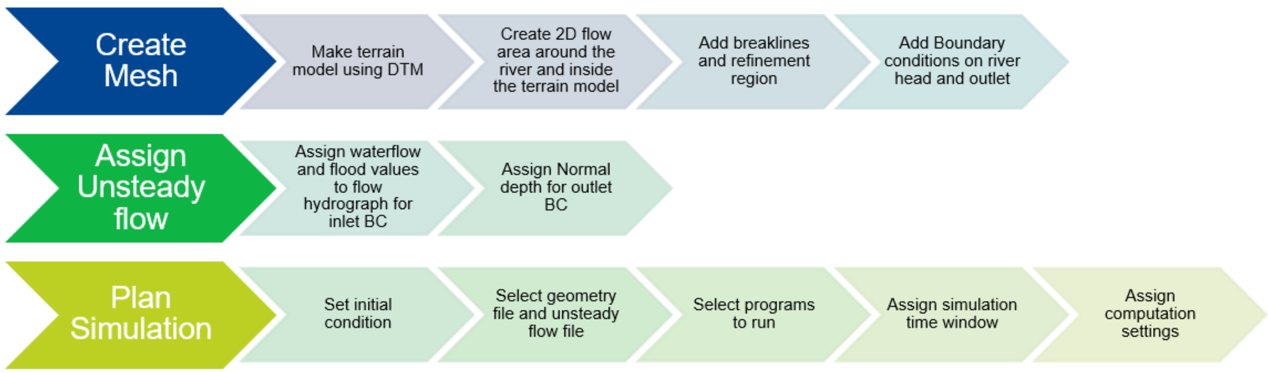

Figure 10: Overview of Steps to Perform 2D unsteady Flow analysis

2.2.1 Terrain Model

The terrain model is developed in the HEC-RAS, RAS mapper option. It is an essential requirement for 2D modelling to establish the geometric and hydraulic properties of the 2D cells and 2D faces. It is also a requirement for flood mapping in HEC-RAS mapper. To create a terrain model, the appropriate projection file, and (DTM) of the study area is imported into the RAS Mapper. For this study, the projection file was same as the projection of the DTMs. The use of a DTM over digital elevation model (DEM) ensures that the model runs over the elevation of the earth's surface and does not include the vegetation, buildings, and other infrastructures.

2.2.2 Terrain Modification

It is important to make the bathymetry of the terrain model as accurate as possible since some of the narrower places in the river might not be accurately represented in courser DTMs. Changing the bathymetry of the terrain model using 1D geometry is a way to do so. However, the DTM used to create the terrain model for Jostedalen and Hjelledalen has been created after being validated against river profile depth of the river Jostedøla and Hjelledøla by NVE (NVE, 2018). Therefore, no major bathymetry changes were needed. The depths of the terrain model were validated against the observed depth of the river profiles made by NVE. However, one of the DTMs used for the Jostedalen terrain model had a bridge that was not removed, therefore it was manually edited and removed (Figure 11) using the methods from Brunner (2021c) and Goodell (2019).

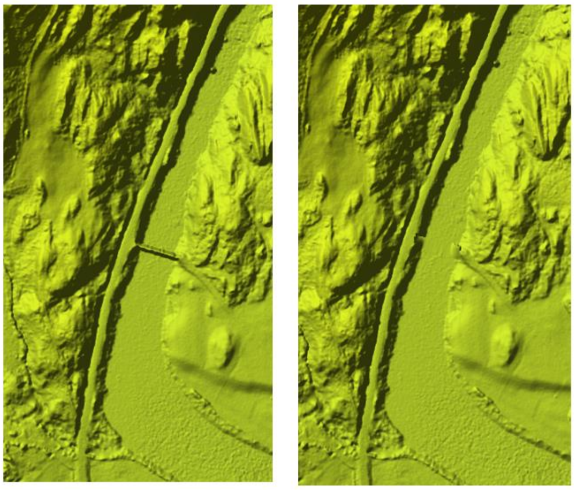

Figure 11: Correction of terrain model

In order to recreate the flood of 1979, some parts of the terrain had to be modified to match the terrain of the region 50 years ago. The DTM used was from 2020 (Table 2) and there has been several installations and modification made along the river over the years. Based on interviews, markers of flood in the valley and aerial photos from 1964, several locations along the river were went through terrain alteration for flood mitigation measures. Figure 12 shows the difference in topography of two areas GOTHECA team visited and interviewed that has changed since the flood in 1979.Therefore, to match the real scenario of the flood, protections were removed in these locations and the terrain was modified (Figure 13) using the terrain modification tool in HEC-RAS 6.3.1 (Gibson, 2022). The terrain modification tool is the latest update added to the HEC-RAS modelling system. The line modification option allows specific elevation along a line drawn over the terrain, it creates an interpolated 3D line with a shape of template wither a channel or a high ground. Depending on the length of the shape and the elevation of the surrounding the model interpolates along the profile to create a surface and merges it with the terrain. The tool also allows the users to edit the height and width of the newly added shape which can be used for both terrain elevation and reduction.

Figure 12: Change in terrain and land use from 1964 to recent years (Photos: Norge I Bilder)

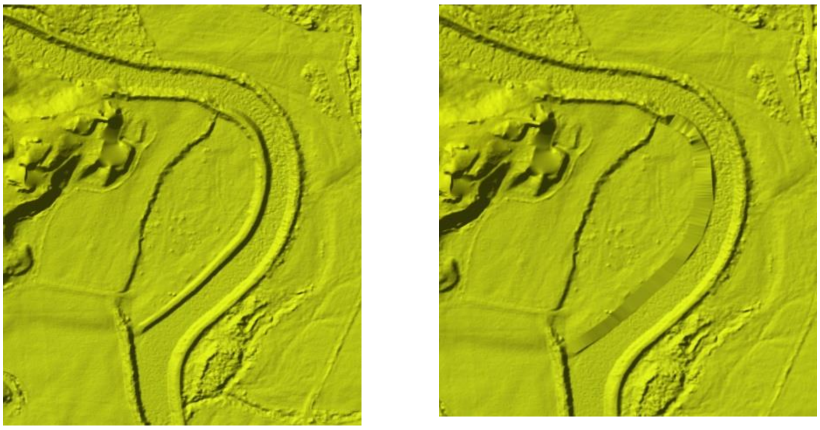

Figure 13: Terrain modification at the flood protection site in Jostedal Camping- removal of flood installation

Similarly, terrain modifications were done on Hjelledøla but in the reverse fashion. Where in Jostedøla flood protections were removed to recreate the past flood, in Hjelledalen, flood protections were installed in terrain using modification tool to simulate scenarios on how the floods behave which mitigation measures (Figure 14). The high-ground modification tool was used to add levees along the banks of Hjelledøla. Along the riverbanks, between 1-2 m terrain height was increased to test the flood protection system. The levees were installed on along the breaches identified along the river during the flood simulations over regular present-day terrain.

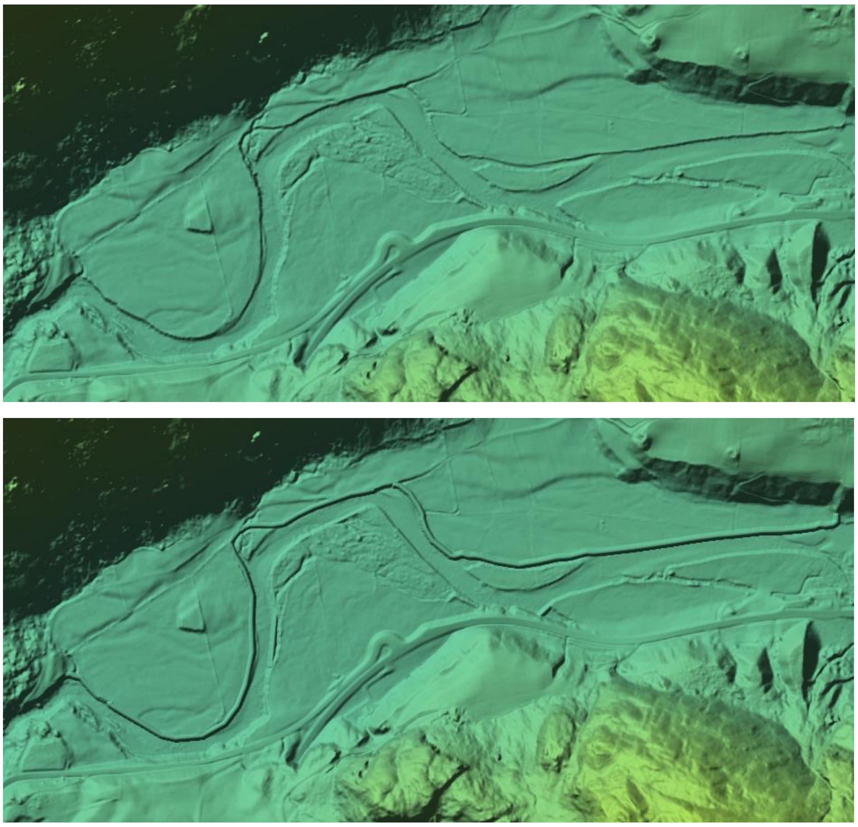

Figure 14: Terrain modification at banks of Hjelledøla, installing flood protection

2.2.3 2D Geometry

A 2D flow area is made in the geometry editor by drawing a polygon around the boundaries of the desired river/s and inside the terrain model. Then breaklines are drawn within the flow area to identify the riverbanks and significant barriers to the flow, such as: levees, roads, embarkments, overbanks, etc. Since the DTM used to create the terrain model already removed any bridges, only riverbanks were added as breaklines. The cell spacing of breaklines needs to be assigned, for this study spacing of 5x5 was used to fit best with the 1m resolution terrain.

Once the breaklines are added, using 2D flow area editor, 2D computational mesh is created for the 2D flow area. It is important to use the appropriate Manning's N value for the mesh. The Manning's N value depends on the roughness and type of the riverbed (Brunner, 2021b). The river Jostedøla falls under the category of Mountain streams, no vegetation in channel, banks usually steep, with trees and brush on the banks submerged, bottom: gravels, cobbles, and few boulders. For rivers with this characteristic the normal Manning's N value used is 0.040, minimum 0.030 and maximum 0.050. The Manning's N value used to make the model was 0.04. This can be changed to calibrate the model against the observed depth. In order to calibrate the model, all 3 values were used and compared to the observed depth at the Nigardsbrevatn station, Manning's N value of 0.040 shows the smallest difference with observed water depth compared to 0.030 and 0.050. After defining the Manning's N value, the computation cell size must be assigned for the mesh. Cell size can vary from 100x100 m to 50x50 m depending on the resolution of the terrain model and need of the user. For accurate and best result several cell sizes were tested out, cell spacing of 10x10 was used for Jostedalen and 20x20 for Hjelledalen valley in the study. Jostedalen was prescribed a finer mesh because several narrow tributaries were present in the area.

One of the drawbacks of using finer cell size is that there are higher number of errors fitting the breaklines and the 2D flow area that needs to be edited manually. Errors on a mesh occur when one cell has more than 8 sides, and this is more prominent when cell size 10x10 neighbours finer breaklines cells 5x5. However, to reduce errors and manual editing, a refinement region can be added. A refinement region is a smaller 2D computational mesh that acts as a bridge between the courser flow area and finer breaklines. The refinement region automatically adjusts the size of the cells to accommodate the 5x5 grid with the 10x10 grid with 8 sides, reducing errors in the computational mesh. A refinement region was created for along the sides of the river and into the areas where the flood water may come in with a cell spacing of 5x5. The computational cells increase after adding the refinement region making the mesh more precise and reducing leakage considerably (Figure 15).

Figure 15: Screenshot of one of the Mesh designed for the model

2.2.3.1 Leaks and gaps in 2D geometry

One of the more common errors in HEC-RAS is leaks in the computational mesh, when the mesh is not properly aligned with the terrain underneath or the cell sizes in the mesh are too course (Brunner, 2021c). While calculating the water flow in a higher elevation cell, the software faces barrier and instead on detecting the barrier within the cell it makes the water flow through the neighbouring cells. The software uses height of each cell to calculate the flow and motion of fluids, therefore the error occurs. Hence, if the height of cells around the higher elevation is same, the neighbouring cells are calculated as wet, causing leaks outside the defined region (Brunner, 2021c; Goodell, 2015).

This problem of leak can be solved by editing the 2D computational mesh and cell faces is areas that show leaks and aligning it with the underlying terrain. By altering the mesh, water will either stop before higher ground, like it would in real, or recourse through lower ground in the mesh. Leakage and gaps in flow has been a major problem while creating the 2D flow area for the Jostedøla river. Figure 16C shows the leak in the model in the marked area, this is because the cells in this specific part of the mesh have higher elevation (Figure 16A), therefore after manually adding more cells in the area (Figure 16B), the model then identifies the higher and lower grounds and does not generalize the entire area as high ground. Figure 16D shows the flow after adding more computation points.

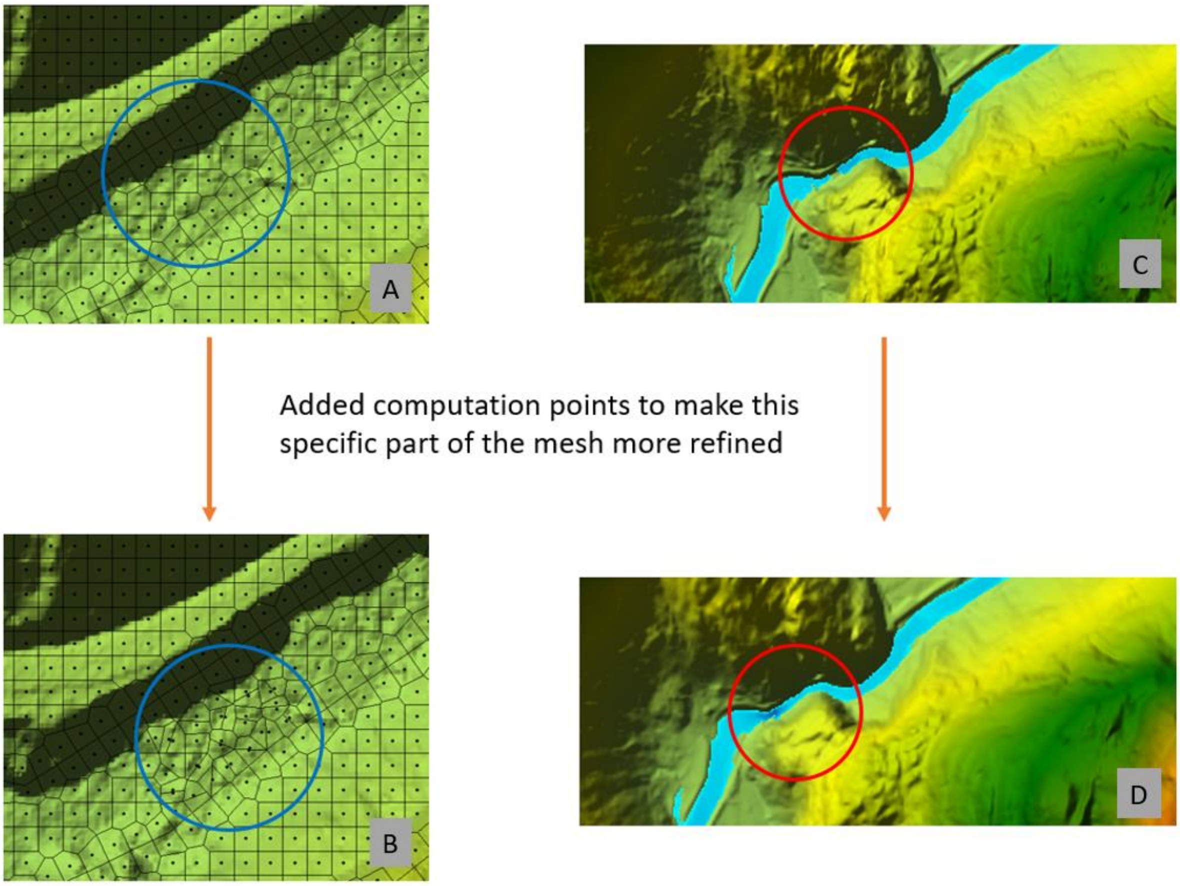

Figure 16: Change in flow after adding computation points

2.2.4 River sections and tributaries

Due the difference in size and characteristics of the two study areas, different approaches were taken to design the models. The 2D flow area for Hjelledalen was designed as one big mesh of the 8 km long river Videdøla. On the contrary, the 2D flow area for Jostedalen was separated into 6 different meshes. The 37 km long river Jostedøla and its tributaries were too large and dynamic to be set in one mesh. Therefore, to minimize errors and computation time, the river was divided into 6 sections with overlapping transition zones. The transition zones were selected to be in flatter riverbed, as the depth and velocity of 2 consecutive models matched the most in flatter regions (Sub-chapter 2.2.5 and 3.1 has more details in the transition zones). Each section of the river was on average 6.3 km. The tributaries of the river were also considered while developing the model. 12 tributaries were identified throughout the main river of Jostedøla (Figure 17), each of these tributaries contributed significantly to the main river during the floods.

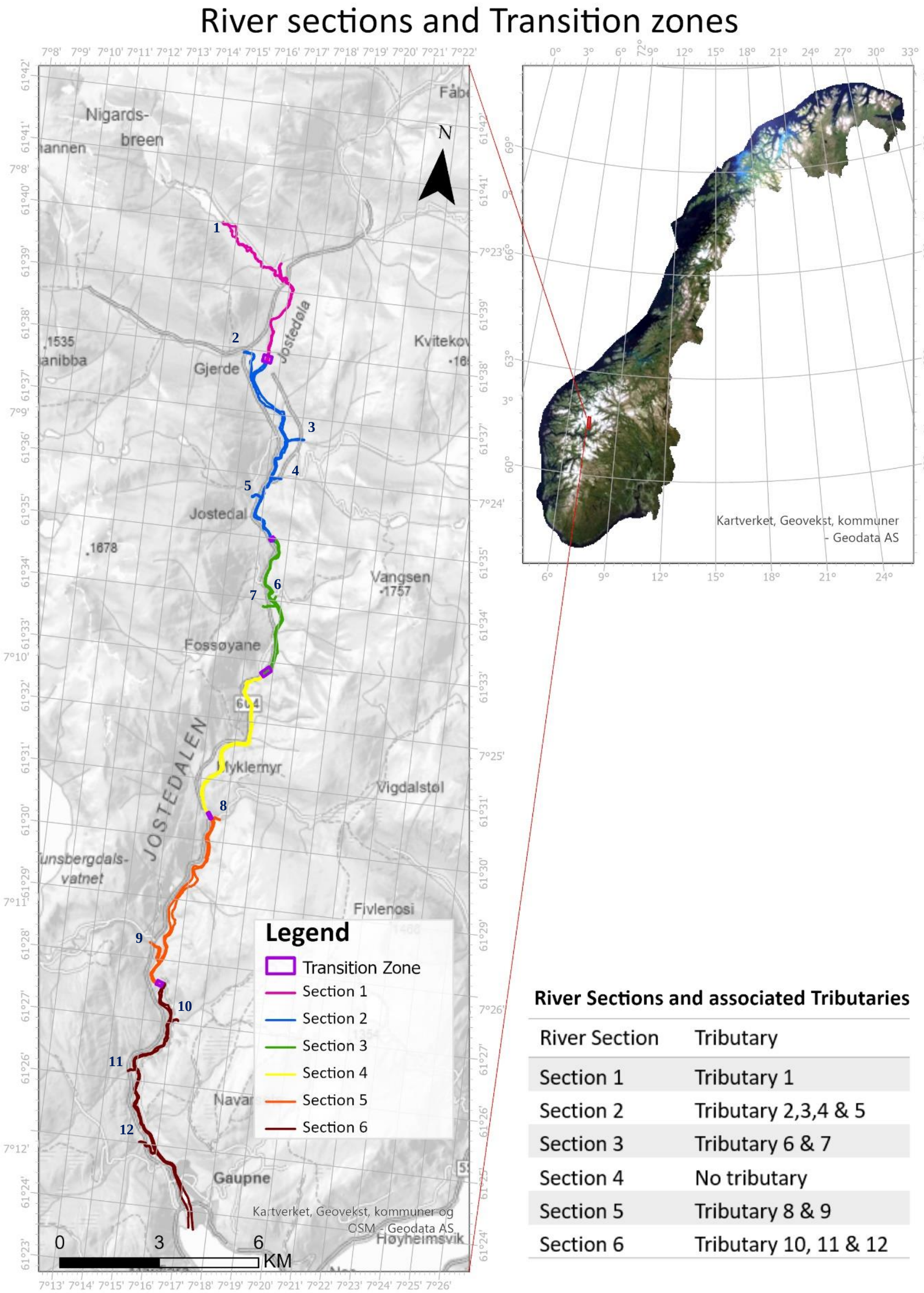

River Sections and associated Tributaries

River Section	Tributary
Section 1	Tributary 1
Section 2	Tributary 2,3,4 & 5
Section 3	Tributary 6 & 7
Section 4	No tributary
Section 5	Tributary 8 & 9
Section 6	Tributary 10, 11 & 12

Figure 17: Map of river sections, tributaries, and transition zones

2.2.5 Boundary Conditions and Water Flow data

Adding Boundary Conditions (BC) is the next essential step to the unsteady flow analysis. External boundary conditions are added along the perimeters of the 2D flow area. Boundary conditions are usually added at the head of the river/s and tributaries where the water enters the model and at the outlet of the river/s where the water leaves the model. The BC at the head of the river is assigned through a hydrograph and energy gradient (EG) slope and the BC at the outlet is assigned through normal depth by specifying the slope of the terrain (friction slope) at the exit. The slope gradients of the boundary conditions are important to run the unsteady flow analysis. The slope gradients, EG slope and Friction slope, can be found using the measure tool in the geometry editor (Goodell, 2014).

The BC for Jostedalen were assigned differently than in Hjelledalen. Since the river was sectioned, the BC had to be assigned for each of the sections separately. The BC for the first section was the observed value and the maximum water flow from the Nigardsbrevatn gauging station during the largest flood in the valley. The BC for the second section was at the transition zone between Section 1 and Section 2. The value assigned here was the flow that was exiting the previous section, or the model for section 1 of the river, this was done for all the 6 sections of the river (Figure 18). Several experiments were performed on the transition zones and the water flow of the river sections and validated against observed water flow on the downstream gauging station to get the most accurate and best possible outcome. The slope gradient for each of the river sections were different therefore they were measured separately for each of the models using the method suggested by Goodell (2014). Table 3 shows the slope gradients and water flow entering each of the river sections at the transition zone during the floods. The second gauging station along the river was in section 4, which was used as a validation point for the model. For Hjelledalen BC were assigned at the head of Videdøla (on the east) and Sunndøla (on the south) before they joined at the junction and the outlet was assigned at the fjord (Figure 1).

No observed values were available for the Jostedøla, its tributaries 2 to 12, Videdøla and Sunndøla, therefore annual mean runoff, and Regional Flood Frequency Analysis or RFFA-2018 flood values were used to create the hydrographs for the BCs for the tributaries. RFFA-2018 is a simplified model of local and regional mean flood which is calculated as a weighted average of the estimates from regression equation and local flood data for 24 hours (Engeland, 2020). The RFFA-2018 flood values and annual mean runoff were acquired from waterflow index analysis service by NVE, NEVINA. The mean annual flow was calculated using the annual mean runoff and the associated drainage area of the tributaries. Table 4 gives an overview of the slope gradient, annual flow and flood values used for the BC of each of the tributaries and the main river.

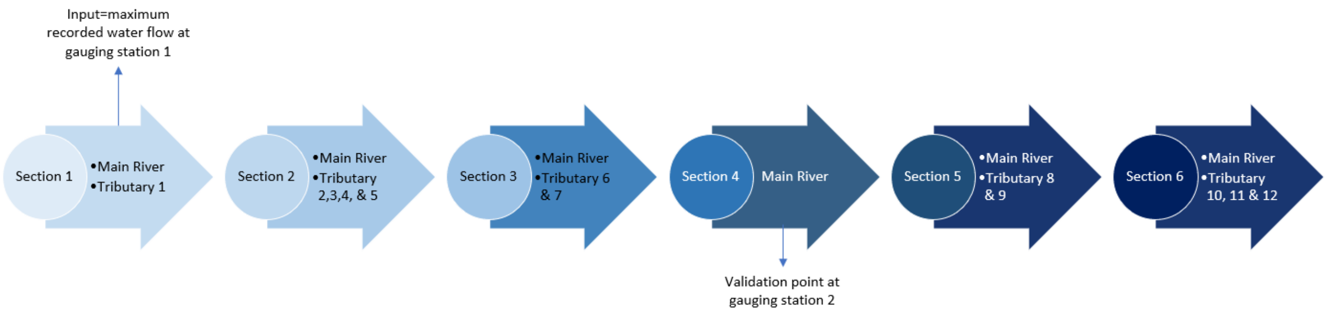

Figure 18: Waterflow data transition from one section to the next

2.2.6 Computational Settings and Initial condition

Assigning the computation setting is the last and one of most important components of performing unsteady flow analysis. The computational settings for unsteady flow analysis primarily comprise of 4 setting options: Computational interval, Hydrograph output interval, Detailed output interval, and Mapping output interval.

Computational interval

Computational interval is used in the calculation of unsteady flow analysis and is a major component in running the simulations accurately. The important factor while assigning computation interval is that the interval must be small enough to precisely describe the rise and fall of the hydrograph. Brunner (2021a) suggests the general rule of thumb, the interval should be equal or less than the time needed for the hydrograph to peak divided by 20. For example, if a flood reaches from base flow to peak flow in 10 hours, then the interval should be equal or less than 30 minutes. If the river route contains major hydraulic structures like bridges, culverts or gates, the water upstream can rise suddenly, therefore, to give the model some time to handle this, the time stamp should be reduced to an even smaller interval. Since both the study areas in this study had bridges over the river, experiments were conducted to get the best and minimum possible computational intervals. The software offers computational intervals from 0.1 seconds to 24hours. According to the HEC-RAS manual (Brunner, 2021a) and the experiments performed, the model gets better with smaller intervals, however, the computation time to perform the analysis significantly increases after certain interval time. For instance, performing a simulation with 10 second interval can take around 40 minutes whereas a simulation with 1 second interval can take up to 4 hours, depending on the size of the 2D flow area and number of rivers in the flow area. Therefore, to ensure time efficiency and accuracy of the model, the computational interval of 3 second was chosen for all the simulations performed which took on an average 3 hours to complete.

Hydrograph output interval

Hydrograph output interval defines the interval in the computed stage and flows hydrographs in the output file produced, HEC-DSS. The interval defines the shape of the computed hydrograph; therefore, it should be chosen as not to lose any information regarding the peak or the volume of the hydrograph. This is usually equal or larger than the computational interval, for this study it was chosen to be 10 minutes.

Detailed output interval

Detailed output interval makes profile of water surface elevation and flow at given intervals. To reduce storage space, profiles are only made for specified intervals and not all computational time step. This also runs post processor and computes detailed hydraulic information for each of the profiles. The interval is usually to be equal or greater than computational interval. However, (Brunner, 2021a) suggests this interval to be large to reduce post-processing and storage space for detailed hydraulic output. The detailed output interval for this study was chosen to be 4 hours.

Mapping output interval

Mapping output interval is used to visualize the mapping output in the RAS mapper. The user can visualize the spatial mapping output of the simulation based on this interval. For this study, a mapping output interval of 10 minute was selected.

Another important parameter of the model is to set the initial condition (IC) ramp up time. Initial condition setting makes sure that the model does not assume that the river is empty/dry before the simulation starts. Therefore, if the IC ramp up time is set to 10 hours, then the model will run a steady flow for 10hours to wet the river and start the simulation. The warm-up helps the model establish water surface elevations and consistent flow (Brunner, 2021c). It is also vital to assign the fraction of time, BC ramp up fraction, that the model will use to ramp up from 0 to the first water-flow value of the BC that enters the 2D flow area. The default ramp-up fraction is set to 0.1, which means, that the model will use 10% of the 10 hour (60 minutes) IC ramp up time to reach from 0 to the first flow value. The IC and ramp value for Jostedalen and Hjelledalen were set to be 6 hours and 0.5 ramp up fraction. The model is sensitive to both these values since this contributes greatly to leaks in the model. Experiments were performed to find the best fit IC and ramp fraction. Section 2.4 has more details on the impacts of different IC and ramp fraction.

2.3 Simulations and experiments

2.3.1 Simulation with Average conditions (No excess flow)

Simulations were performed using constant flow to test the accuracy and stability of the model before the flood values were added. Prior to adding the flood values to the model, the model had to be tested to find the parameters that were best fit for the unsteady flow analysis. Therefore, a flow of $35m^3/s$ was selected for the Nigardsbrevatn gauging station to run throughout the valley to test the most efficient computation settings and the most appropriate position for the transition zones between each of the sections. These experiments were set up for each of the 6 sections with waterflow from the previous river section and no tributaries were added. Only the main river was used to perform the experiments to see the effect on how much the tributaries contribute to the main flow. Table 4 gives an account of the water flow in each of the transition zones. The outflow of each of the section is the inflow of the next section. The inflow for section 1 was $35m^3/s$ and the outflow at the end of the river in section 6 was $31m^3/s$. There was some water loss from section 1 because some water was stuck in some the smaller channels right after the Nigardsbreen lake.

Table 4: Waterflow in Jostedalen river sections with average conditions

Transition Zone	River Sections	Inflow	Outflow	Waterflow m3/s
No Transition zone	Section 1	Y	-	35
Transition zone 1	Section 1	-	Y	31
	Section 2	Y	-	
Transition zone 2	Section 2	-	Y	31
	Section 3	Y	-	
Transition zone 3	Section 3	-	Y	31
	Section 4	Y	-	
Transition zone 4	Section 4	-	Y	31
	Section 5	Y	-	
Transition zone 5	Section 5	-	Y	31
	Section 6	Y	-	
No Transition zone	Section 6	-	Y	31

**Y= measurements inflow/outflow of a section in transition zone*

The second gauging station along the river was in section 4, Myklemyr station, where the observed water flow during the same time as Nigardsbrevatn station was 243 m3/s, which shows that the tributaries have significant contribution to the water flow in the main river. It is also important to mention again that tributary flowing from Nigardsbreen lake was considered the river head for the experiments as observed gauging station data was required to validate with the next gauging station data. The main river started from the Nigardsbreen lake and end at Gaupne where the river flows into the fjord with the gauging station Myklemyr in the middle.

Figure 19 shows the water depth at the transition zone of two consecutive river sections. In transition zone 3,4 and 5, the profiles overlap almost perfectly. Transition zone 1 and 6 however, have some difference, but the maximum difference observed was only 6cm. Therefore, these transition zones were used for the rest of the simulations.

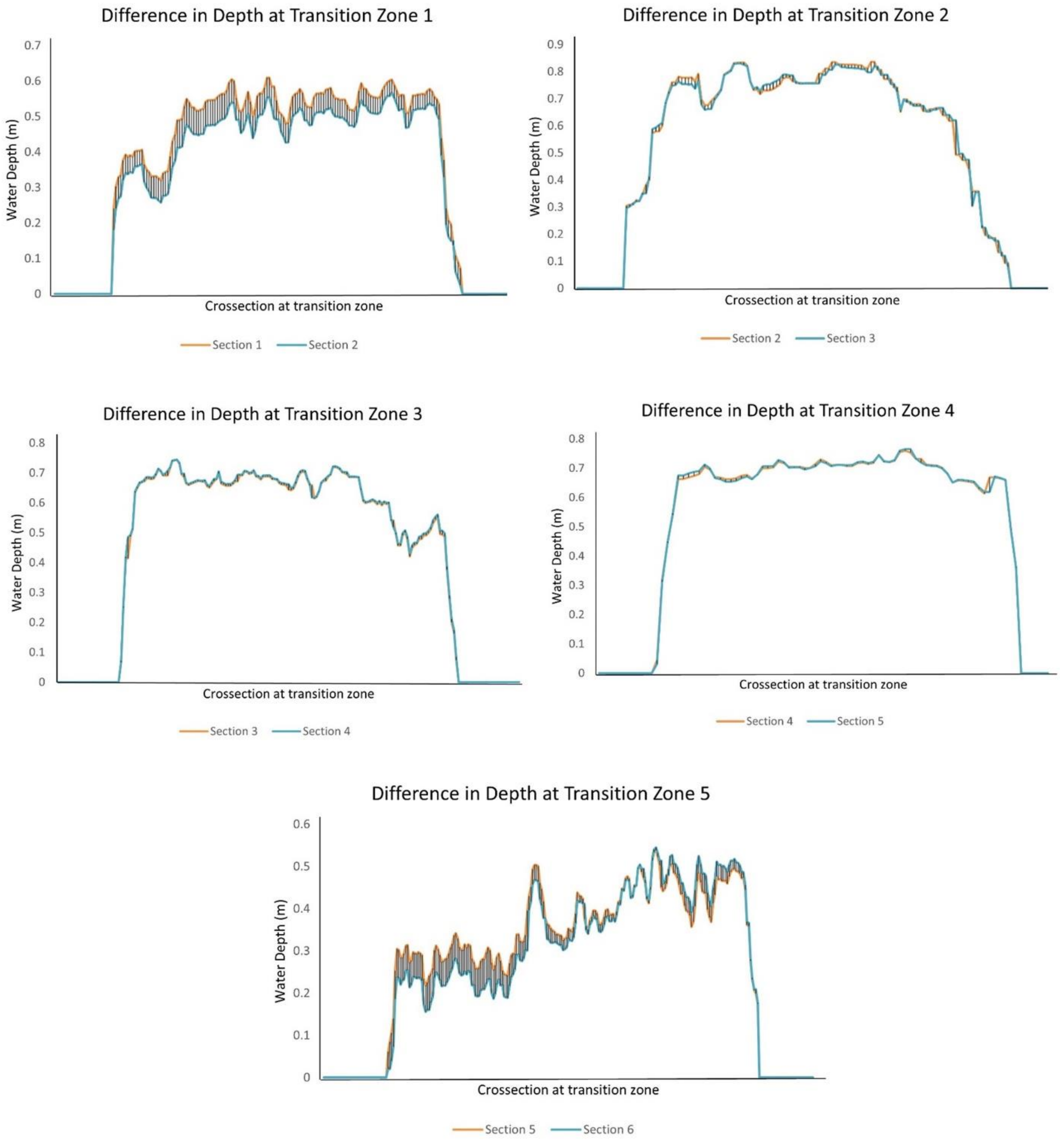

Figure 19: Water depth of profiles across each of the transition zones

2.3.2 Simulation with flood values

As the river was divided into 6 sections, several simulations had to be performed to cover the entire valley starting from the lake at Nigardsbreen until the river reaches the fjord at Gaupne. Flood value used in the simulation was the maximum recorded water flow in the Nigardsbrevatn station. This set-up was repeated 6 times in each of the 6 river sections with different flood waterflow added in the tributaries. The 6 flood values used for each of the tributaries were median flood, 10-year flood, 20- year flood, 50-year flood, 100-year flood and 200-year flood. The largest recorded flood in the Myklemyr gauging station was 409.09 m^3/s on 15th August 1979, which according to NEVINA was a 50-year flood. Tables 5 and 6, gives an overview of the water flow input in the rivers and the tributaries.

Table 5: Slope of river sections at the beginning and end of each section

River Section	E.G. Slope	Friction Slope
Jostedalen		
Section 1	0.01	0.01
Section 2	0.01	0.01
Section 3	0.01	0.004
Section 4	0.002	0.03
Section 5	0.002	0.01
Section 6	0.02	0.003
Hjelledalen		
Videdøla	0.01	0.001
Sunndøla	0.1	

Table 6: Mean annual flow, flood value and slope of Tributaries

Tributary	Mean flow (m^3/s)	Flood Value (m^3/s)						Slope
		Median	10-year	20-year	50-year	100-year	200-year	
Jostedalen								
Main River	20.0	125	175	194	220	240	260	0.07
Tributary 2	5.5	41	57	64	72	78	85	0.08
Tributary 3	2.3	17	25	28	31	34	37	0.2
Tributary 4	0.7	6	9	10	11	12	13	0.05
Tributary 5	0.8	7	10	11	13	14	15	0.2
Tributary 6	0.3	3	4	4	5	5	6	0.08
Tributary 7	1.6	12	18	20	22	24	26	0.2
Tributary 8	3.5	25	36	40	46	50	55	0.3
Tributary 9	11.5	76	105	116	131	143	164	0.05
Tributary 10	0.7	7	11	12	14	15	17	0.6
Tributary 11	1.1	11	16	18	21	23	25	0.1
Tributary 12	0.6	7	10	11	13	15	16	0.2
Hjelledalen								
Videdøla	10	-	-	-	125	137	149	0.01
Sunndøla	5	-	-	-	65	71	77	0.1

*Tributary 1 the channel coming out of the Nigardsbreen lake where, observed values have been used

**For Videdøla and Sunndøla only higher intensity floods were simulated

2.4 Sensitivity of the model

The hydrological 2D unsteady flow model has some uncertainty from the mesh structure, parameter, the boundary conditions, and the computation settings of the model. Therefore, in order to have a model with the least possible uncertainties, several sensitivity tests were performed.

2.4.1 Sensitivity to 2D flow area

The 2D flow area one of the most important components of the HEC-RAS 2D unsteady flow analysis. Therefore, it is vital to have a 2D geometry that causes least number of leaks and gaps in the model. To find the most appropriate flow area setting several tests were performed. The first being the cell spacing of the mesh. Hydrological models are very sensitive to terrain model resolution as well as resolution of the 2D flow area. Experiments were performed with 10x10, 5x5 and 1x1 mesh resolutions. Using 10x10 mesh resulted in several leaks and gaps throughout the river, as the mesh couldn’t aligned properly with the 1m resolution terrain and the bathymetry. The 1x1 mesh, on the other hand, resulted in computation time over 24hours and caused the software to shut down before completing the simulation due to the heavy size of the file. The 5x5 mesh gave the best possible outcome. The gaps and leaks reduced drastically from 10x10 mesh, and the computation time varied between 1-2 hours.

The second experiment was done to see if gaps in the model reduces by manually adding computation points in areas that showed gaps (Figure 16). This was done in several narrow areas throughout the river to improve the accuracy of the model in identifying the uneven bathymetry of the river.

2.4.2 Sensitivity to water flow data

Some of the tributaries in the rivers showed patches and gaps in the flow even after refining the mesh. Therefore, to test the waterflow data, experiments were done with steadily increasing the flow data using flow of 0.1 m3/s , 1 m3/s , 10 m3/s , 20 m3/s , 40 m3/s , 80 m3/s and 90 m3/s. This resulted in showing that flow below 1 m3/s is not ideal for the models set up (Figure 20).

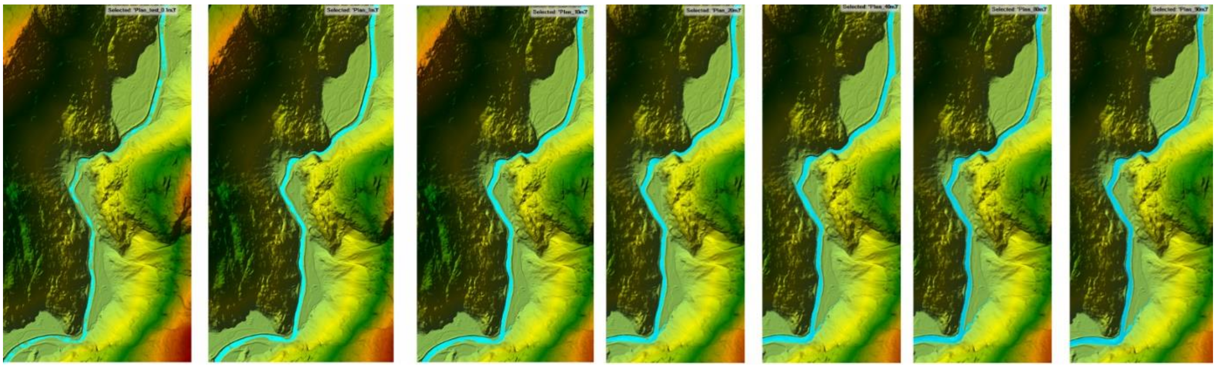

Figure 20: Screenshot of experiments performed with different waterflow

2.4.3 Sensitivity to computation settings and initial conditions

The computation settings and the initial condition of the model has significant impacts on the output and the leaks. After several trial and errors, the best computation settings and initial conditions were assigned. Figure 21 shows how drastically the model improves with appropriate IC and computation settings. If the IC is more than the chosen time the model leaks water into the surrounding after the river has been wet, and if the IC time is less than the model doesn’t get enough time to wet the river before the water flow comes in.

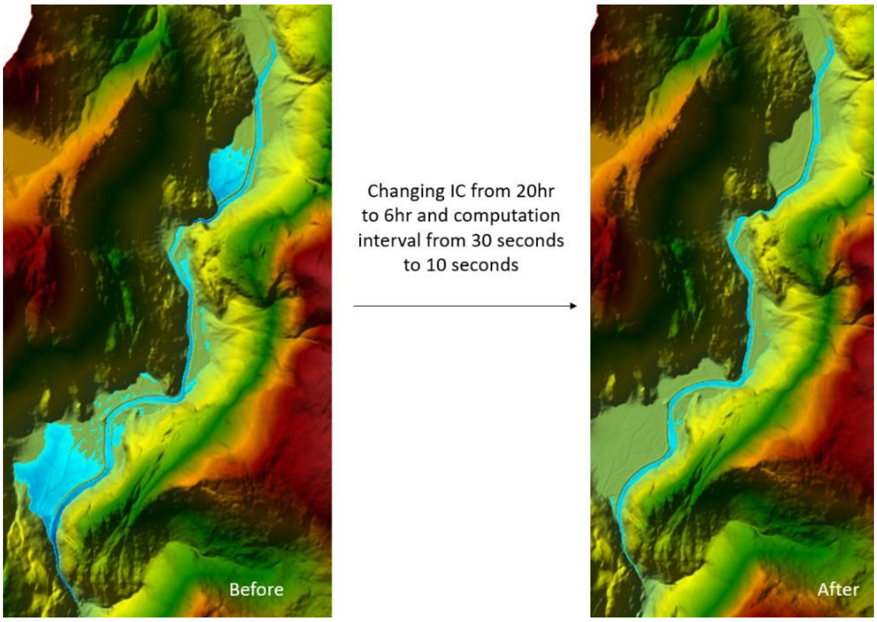

Figure 21: Screenshot of experiment with IC and computation interval

3 Results

This chapter contrasts the results of minor frequent model-based floods and future simulations with increasing intensities of flood scenarios to infer the most probable magnitude of flood that hit Jostedalen in 1979 and evaluate to which extent NVE's protective installations will shield local population from future hazards of higher magnitudes. Furthermore, photographic evidence and interviews with local citizens on both northern and southern sides of Jostedalsbreen have been used to test the efficiency of NVE's installations – existing and hypothetical – to protect currently exposed vulnerable infrastructure.

The outputs from the flood simulations are detailed in the sub-chapters 3.1-3.3. The results of the flood simulations are presented according to increasing intensity of flood scenarios. First 2 sub-chapter shows the change in river water depth of Jostedøla and effected areas for median flood, 10-year flood, 20-year flood, 50-year flood, 100-year flood and 200-year flood. The last sub-chapter focuses on the other side of Jostedalsbreen, at Hjelledalen and presents the higher intensity 50-, 100- and 200- year floods and their impacts.

Results presented in sub-chapters 3.1 and 3.2 are in order of the River Jostedøla flowing downstream. The first flood map for each flood scenario is confluence between the River Jostedøla and the Tributary 1 from Nigardsbreen lake and the last flood map is at Gaupne, where the river flows into the Gaupnefjorden. Similarly, in 3.3 for Videdøla and Sunndøla, the results are presented as both rivers flow into Hjelledøla and downstream to Hjelle and into Oppstrynvatnet.

3.1 Model Responses to Minor Floods

The first section of the results chapter presents a comprehensive overview of minor floods that occur in Jostedalen at a relatively frequent rate (up to every 20 years) and what signatures such floods leave throughout the valley, starting from a median flood and going up to 10-year and 20-year floods. The first part of the analysis compares the water flow induced by floods to the mean annual flow throughout the river. These experiments and analyses are used to assess the river sensitivity to relatively minor changes in the hydrological forcings within different river segments.

The mean annual flow of the river and the tributaries along with the RFFA-2018 flood values have been used for median flood, 10-year flood and 20-year flood from NEVINA to create hydrographs for each of the flood simulations (Section 2.2.5). Figures 22A, 22B, 22C-23A, 23B and 23C depicts mean annual flow throughout the valley prior to the flood occurrence, with the mean annual flow varying between 20 m^3/s and 72 m^3/s throughout the main river and between 0.3 m^3/s and 11.5 m^3/s in the tributaries (Table 6). The water depth is below 2 m throughout the river, with the exception of the narrow parts of the river, where water depth reaches a maximum of 3.6 m. The standard mean annual weather and hydrological conditions imply that tributaries 3, 5, 6, 7, 8, 9 and 10 remain inactive/dry, since they only activate during the melting season, high precipitation and floods. The following sections demonstrate how these tributaries fill up during summer months and act as hydrological forcings for the main river flow and flood extents. The following maps corresponding to the floods of minor magnitudes show the close-up of the river with mean annual flow (referred as ‘before’ in the text) against median, 10-year and 20-year floods.

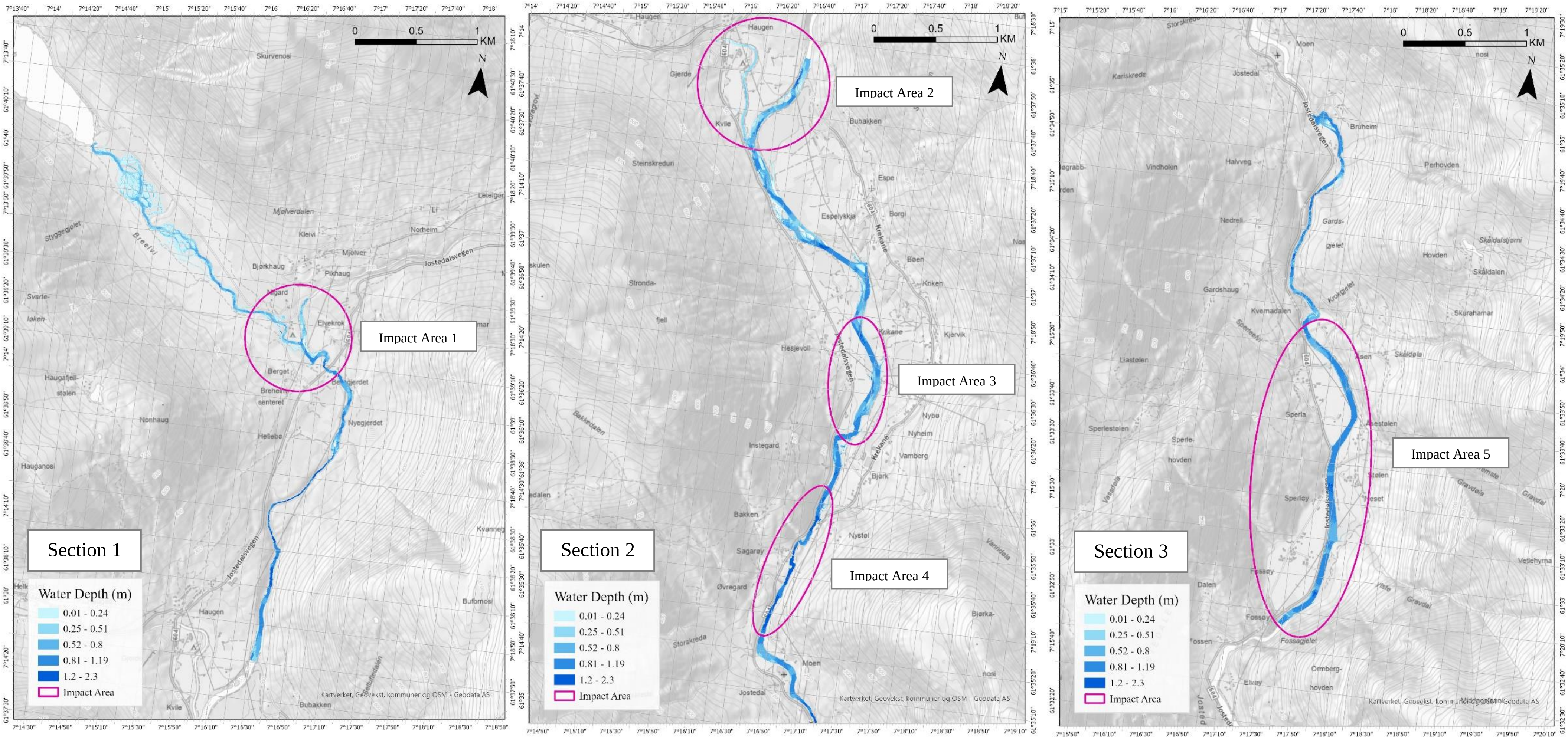

Figure 22: Full extent of Mean Annual Water Level and Flood Impact Areas in Section 1 (A) Section 2 (B) and Section 3 (C)

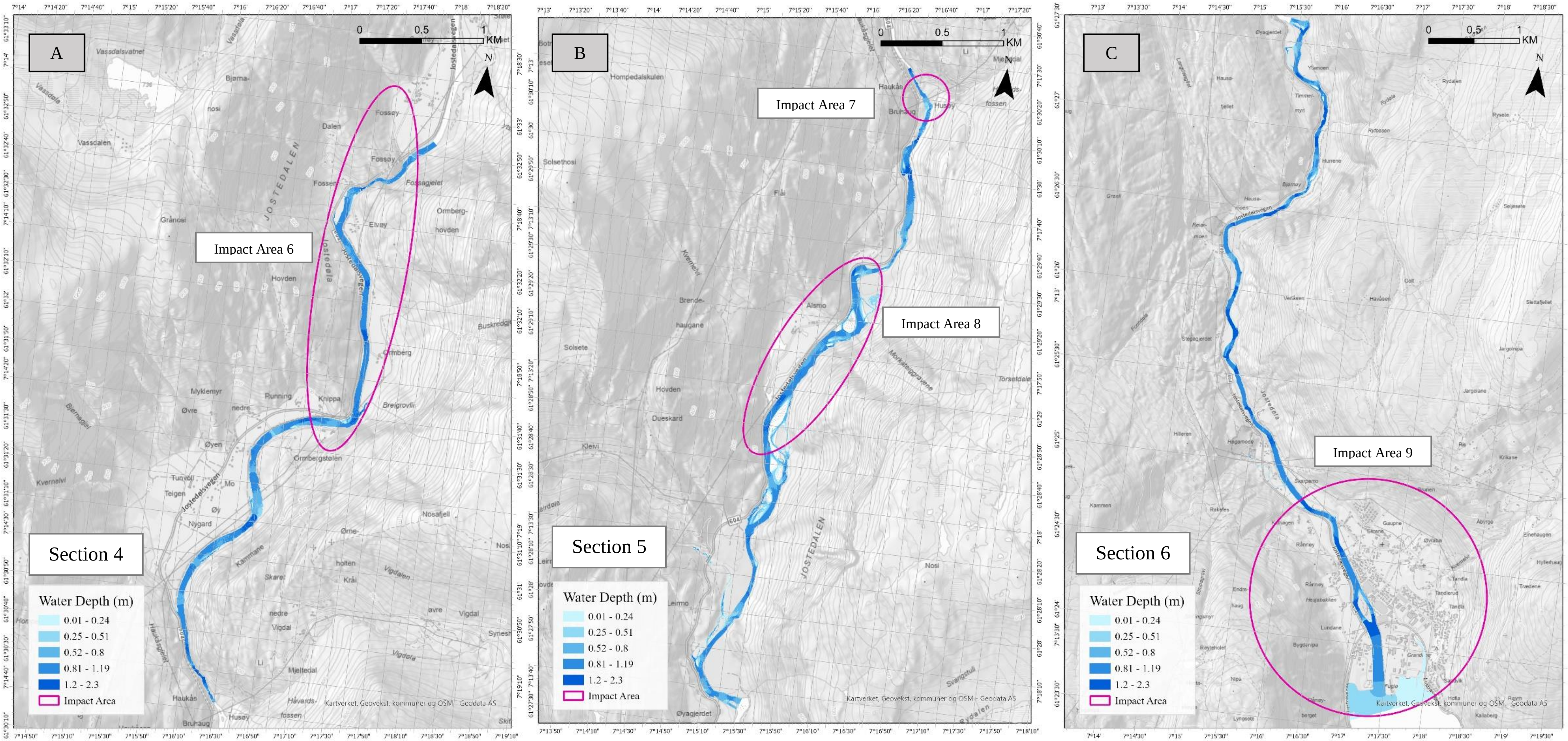

Figure 23: Full extent of Mean Annual Water Level and Flood Impact Areas in Section 4 (A) Section 5 (B) and Section 6 (C)

Sensitivity simulations along Jostedøla have identified 9 areas at risk of getting negatively affected even under minor flood conditions. Although under these flood scenarios the affected regions experience generally low water levels, the flooding increases as the hydrological forcing becomes more intense.

Impact Area 1, Section 1 (Figure 24): Figure 24 shows the region where the main river Jostedøla joins Tributary 1, Breelvi, from the Nigardsbreen lake. One of the camping places, Nigardsbreen Camping, is located at the junction between the main river and its tributary. This segment of the river includes two bridges connecting two sides of the valley. Water levels in the river are predicted to rise from the range of 0.48-1.11 m to 1.12-1.88 m when the median flood occurs. In this case, water volumes and water levels are still mostly contained by the river, with some of the excess water masses spreading across the adjacent flood plains (Figure 24B). Regardless, in the areas of flood plains, water levels remain very low, within the range of 0.01-

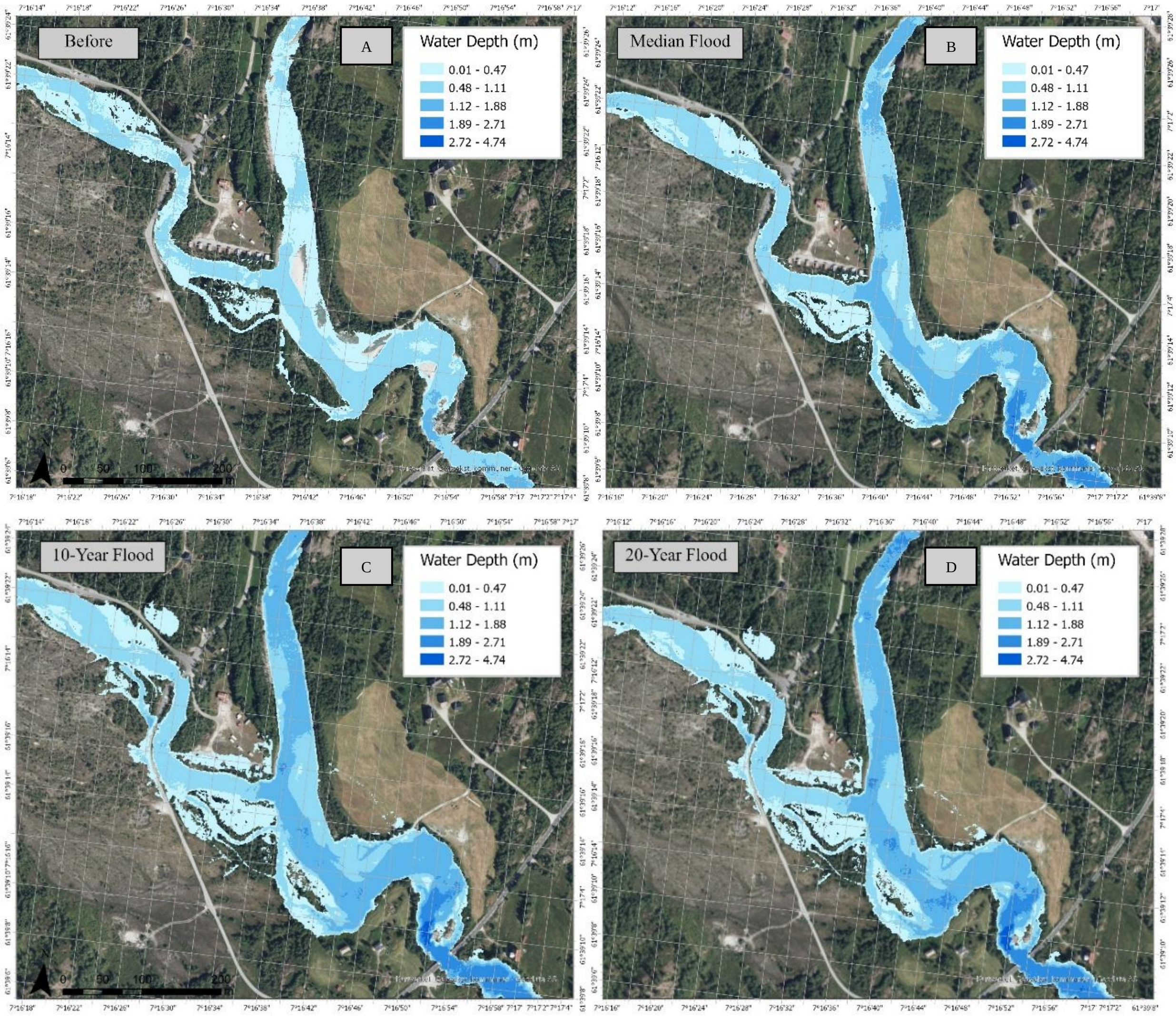

Figure 24: Impact Area 1- Nigardsbreen Camping and Confluence of Rivers Jostedøla and Breelvi (Tributary 1 from originating the Nigardsbreen lake) with mean annual water levels (A) versus water levels for the median (B), 10-year (C) and 20-year (D)floods.

0.47 m. A part on the camping place is slightly impacted by water flowing into its eastern confines. Yet the water inflow is still characterized by a low energy, within the lowest water depth range.

Naturally, the extents of affected areas increase for the 10- and 20-year flood simulations as it is seen in Figure 24C and 24D where new areas get flooded in the north-western part of the region, both to the north and to the south of the Breelvi, before it meets Jostedøla. Some more water has also entered the camping area but still with low water levels. In the meantime, water levels in the river have risen from the range of 1.89-2.71 m for the median flood to the range of 2.72-4.74 m in the 10- and 20-year simulations. Water levels have particularly increased near the Elvekrok Bridge in the south-eastern part of the map. For comparison, water has extended a bit more for the 20-year flood (Figure 24D), although the difference is not immediately noticeable; however, it produces higher water levels in the river, bringing more water onto the farmlands along the eastern riverbanks.

Impact Area 2, section 2 (Figure 25): The river then flows downstream to meet the second tributary of Jostedøla flowing down from the west of Gjerde (Figure 25). The second camping place of Jostedalen, Jostedal Camping, is located here, along the western bank of Tributary 2. Figure 25 shows two rivers joining together, and water levels and extents before and after the three types of floods occur. This section of the river is clearly more affected by floods, albeit still with low impacts, as the water flow downstream is a result of the combined effects of two rivers, which are inflated upstream. Some parts of the farmlands in the centre and in the western confines of the impact area 2 seem to have water flowing in already under the conditions of the median flood, which becomes increasingly worse with increasing flood levels. However, water levels over most of the flooded farmlands remain within the lowest range of 0.01-0.56 m under all flood scenarios. The farmland along the western bank of the tributary 2 has a channel coming from the river into the southern field border, locally increasing water levels to the range of 0.56-

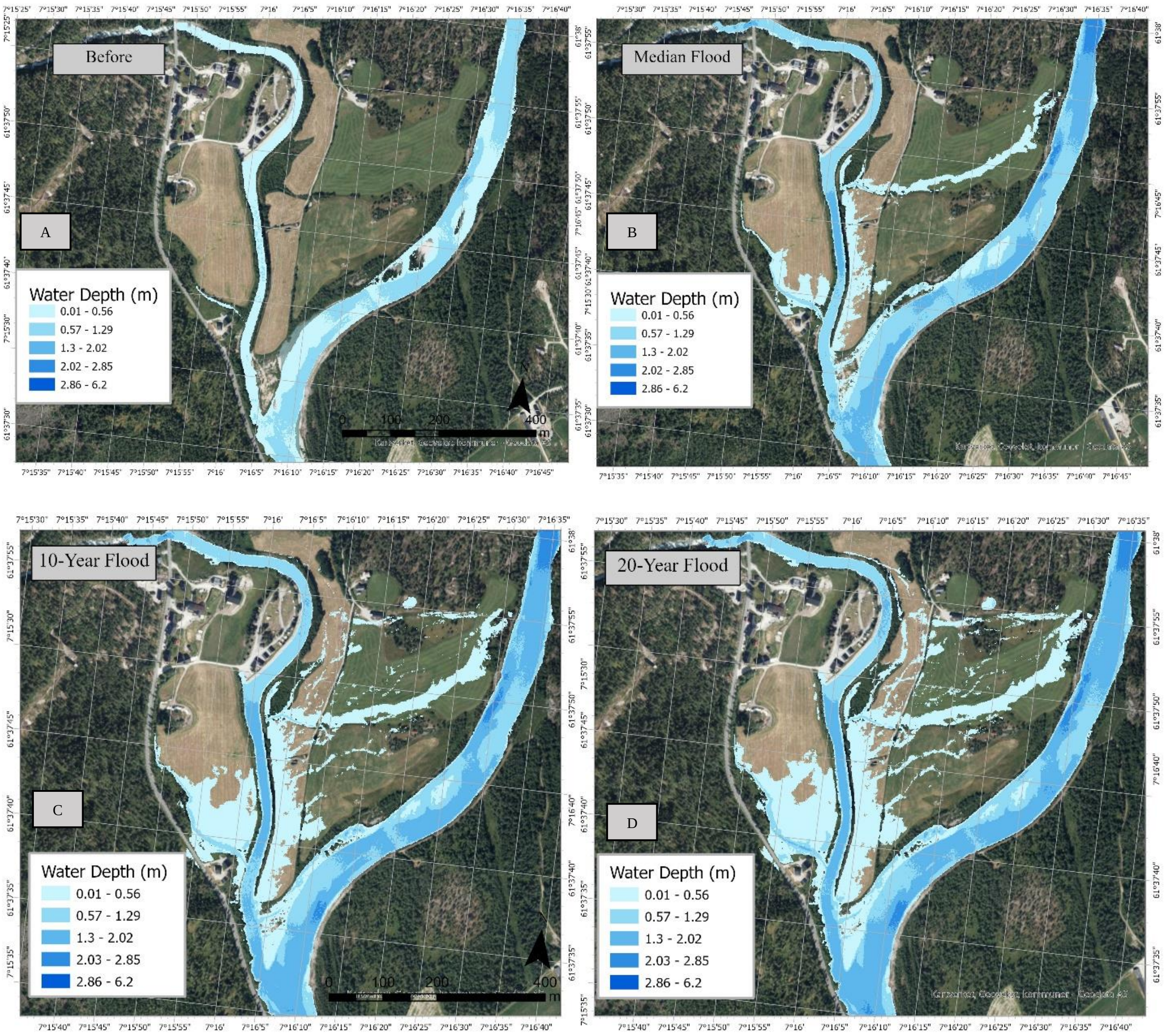

Figure 25: Impact Area 2- Jostedal Camping and Confluence of Jostedøla and Tributary 2 on the west with Mean annual water levels (A), Median (B), 10-year (C), and 20-year (D) floods

1.16 m. Here, increasing floods levels progressively push water to higher elevations towards the farmers' houses. Water depths near the camping place increase from the mean annual range of 0.01-0.56 m (Figure 25A) to the range 0.57-1.29 m for the median flood and above 1.5 m for the 20-year flood, gradually moving up the riverbanks towards the campgrounds. Overall, the impacts of 10- and 20-year floods are more extensive area-wise, with slightly higher water levels in the main river than predicted for the median flood. Larger areas of the two farmlands become submerged under water, flood is slowly marching towards the camping site from the south, but still with very low water levels. The roads on the westside seem to be affected with water flowing over the road and into the other side.

Impact Area 3, Section 2 (Figure 26): Figure 26 shows increase in water levels with Median flood in the river and the flood water infiltrating the smaller channels from the river into the farmlands at Hesjevoll with low water levels. Some parts of the farmland seem to be affected on the northern part of the Figure 26B. For the 10-year and 20-year floods more affected areas can be seen compared to the Median flood. The 10- and 20-year flood has further extent of water flowing into the farmlands (Figure 26C and 26D). The water levels in the river rises more than that during the median flood in certain parts. As the river flows downstream and Tributary 3 joins in from the east, the water flow and volume of the river increases. A drastic change can be seen in tributary 3 during the median, 10- and 20-year floods, the river is completely full, with water levels ranging from 1.72 m to 4.85 m whereas it was fairly empty and dry with the mean annual flow. The lower parts of the farmlands in Hesjevoll have a larger affected area in all the flood scenarios. The river depth increases significantly from 0.5-1.29 m range before the flood to 2.02-2.85 m range in Median flood. Larger parts of the farmland are affected yet again with low impact. The water levels are still in the 0.01-0.56 m range with a bit high water levels in some of the areas. For the 10- and 20-year scenarios water covered more area of the lands compared to Median flood. This could be due to the Geistedøla river contributing huge volume of water to the main river and overflowing into the farmland. The water levels on the farmland reaches the upper range of 0.57-1.29 m and up to 2.02-2.85 m with 20-year flood. Both the floods also cover the main road by the farms.

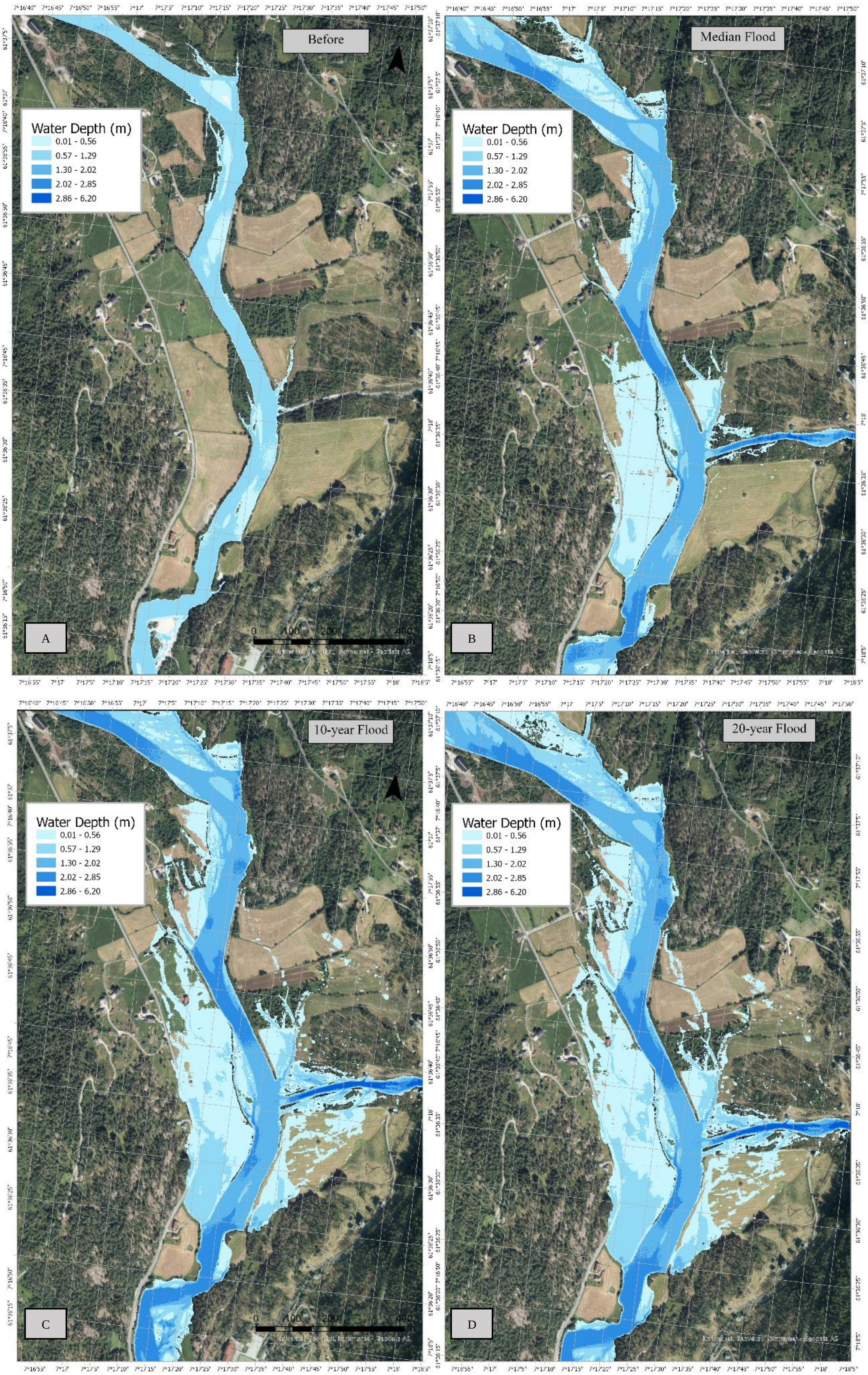

Figure 26: Impact Area 3- Farmland in Hesjevoll downstream of Geistedøla, Tributary 3, with mean annual water levels (A), Median (B), 10-year (C), and 20-year (D) floods

Impact Area 4, Section 2 (Figure 27): The area in Figure 27 has 2 bridges over the main river and one bridge over tributary 5 on the west side, as well as the Jostedal school on the east side of Figure 27. However, with the median flood simulation, there are not many visibly affected areas. But the water levels in the main river rises by several meters and the Tributary 5,

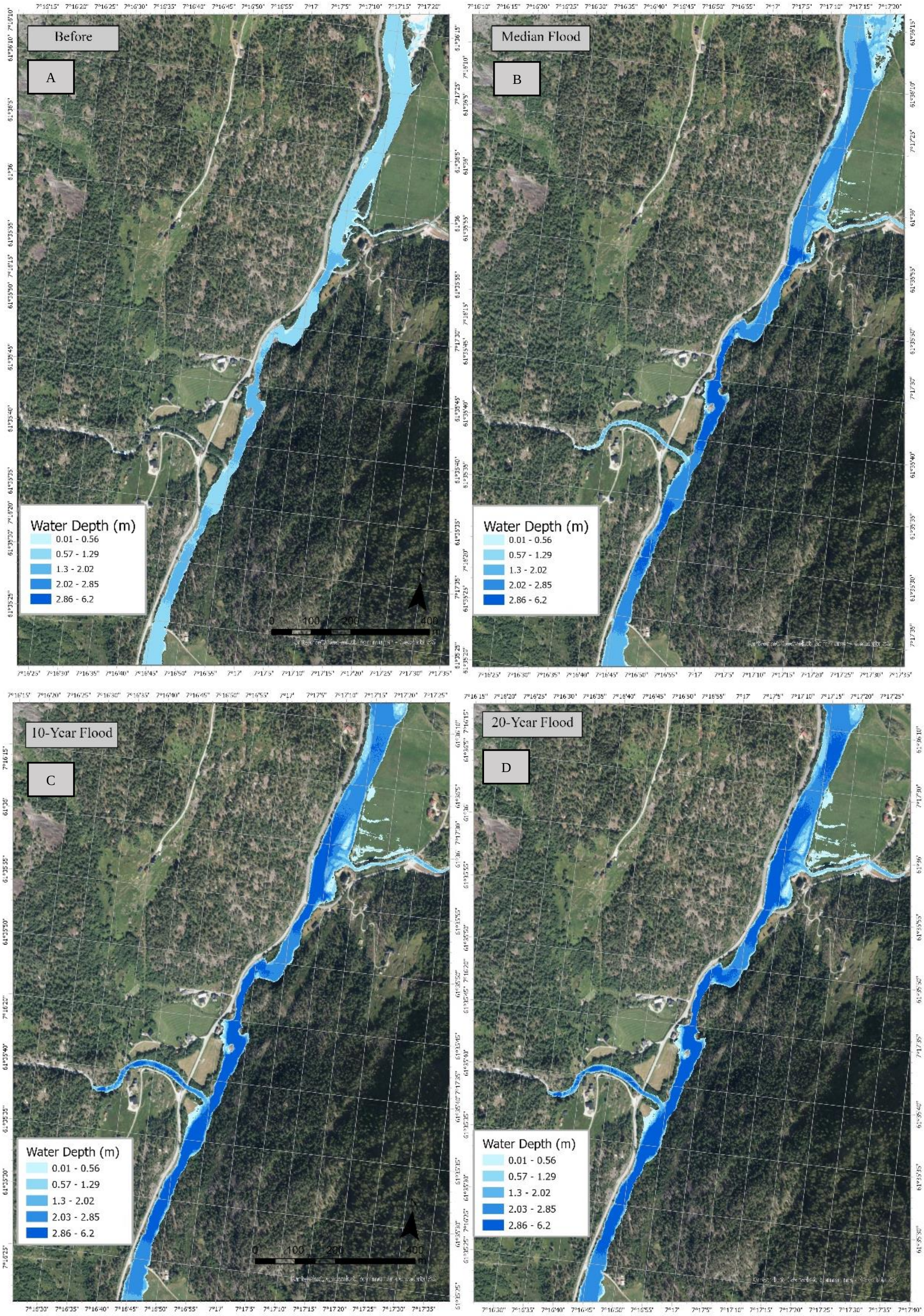

Figure 27:Impact Area 4 - Høgebru bridge, Tributary 4 and Sagrøyelva (Tributary 5) with Mean annual water levels (A), Median (B), 10-year (C), and 20- year (D) floods

Sagrøyelva is activated and full. The water levels in the main river stays the same for 10- and 20- year scenarios. The 10- and 20- year flood does move closer to the roads and the Tributary 5, Sagrøyelva, rises by more than a meter. Water levels under the bridge at Sagrøyelva rises from 1.85 m during median flood to 2.71 m and 2.73 m during 10- year and 20- year flood, respectively, which leaves only a 20 cm different from reach the bridge. The water levels under the Høgebru bridge rises from 2.9 m during median flood to 3.4 m and 3.5 m during the 10- and 20- year floods. The bridge itself is however still 2 m away from the flood water levels.

Impact Area 5, Section 3 (Figure 28): Tributaries 6 (on the east) and 7 (on the west) joins the main river at the Farmland before the flood marker at Sperle (Figure 28). Both the tributaries contribute significantly to the main river during the floods, the water level rises by 1 meter in the main river during the median flood. The Tributary 6 on the east side has a water depth of 2.27 m in a shallow part of the tributary with less than 0.5 m river depth and uneven slope, causing water to flow into the surrounding area (Figure 28B). Similarly, in Tributary 7, water level rises to 9.96 m in a narrow part of the tributary with a depth of 5 m causing water to flow into the surroundings. The water levels under the bridge in Tributary 7 rises to 4.5 m, potentially flooding the bridge, since the river depth under the bridge is only 2.2 m. Parts of the farmlands on either side of tributary 7 are affected but the water levels stay below 0.3 m throughout and rises between 1-5 m where the tributary breaches into the surrounding area.

The 10- and 20-year floods shows drastic change in flood water compared to the median flood. For both the 10- and 20- year flood the main river rises by half a meter. The water levels in tributary 6 rises up to 2.6 m and 2.8 m during the two floods and the water depth in the neighbouring farm stays within the same range as the median flood, rising up to 1.2 m near the breach area and below 30 cm throughout. The river water depth in the tributary 7 goes up to 14.82 m from 9.96 m in median flood (Figure 28C and 28D). A higher volume of water can be seen moving into the farms from the tributary. The farmland gets completely inundated, still with lower water levels and only a bit high levels between the range 0.64-1.51 m in some of the parts. The water levels under the bridge in tributary 7 rises to 5.5 m during 10-year flood and 5.8 m during 20-year flood causing potential damage to the bridge or flooding it. During both the simulations, the road is inundated near the tributary 7 with water levels go up to range 1.52-2.31 m. The downstream also has some significant water flowing in the surrounding areas, however the water levels stay in the lowest range except for the small channels.

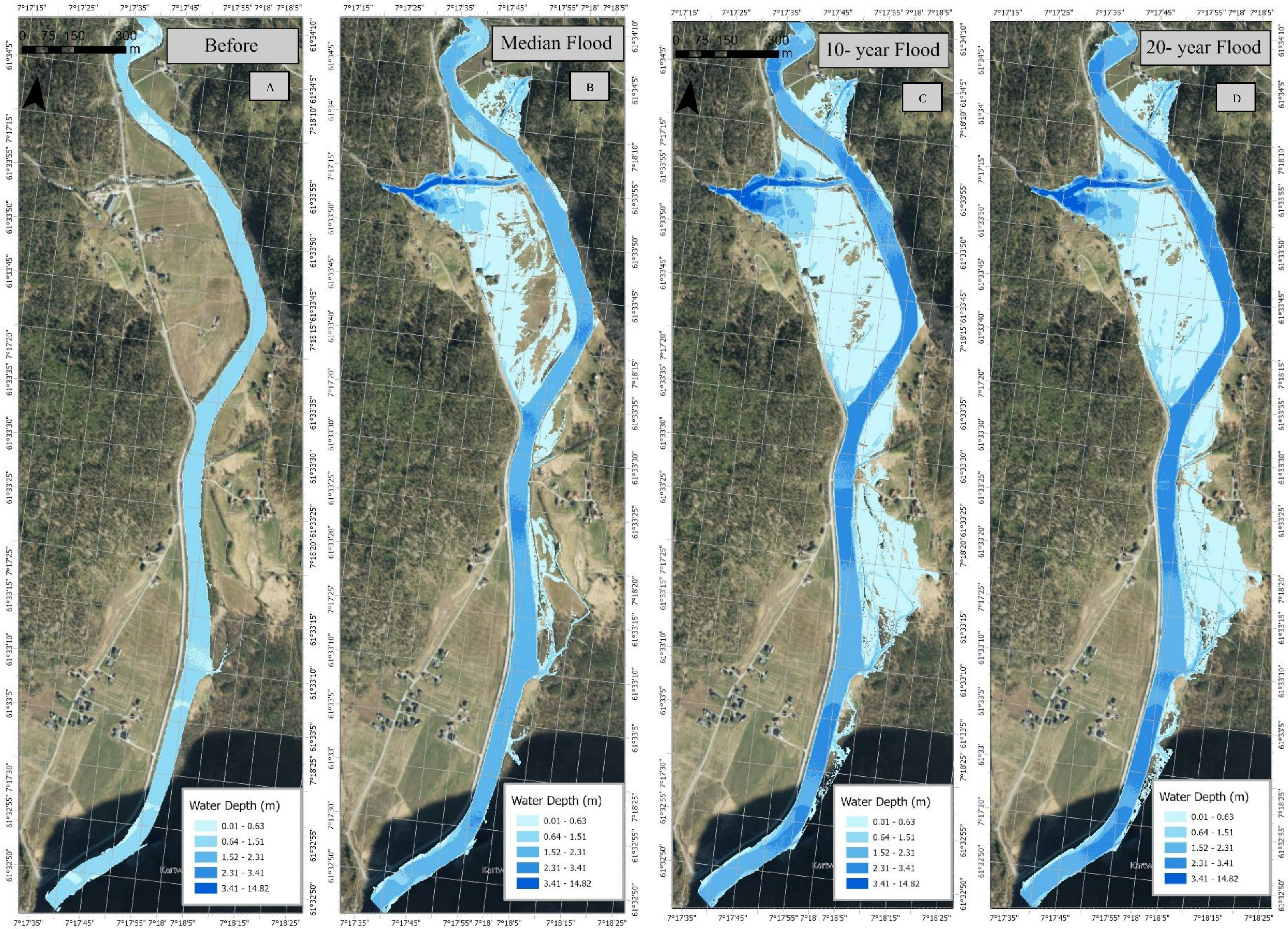

Figure 28: Impact Area 5- Tributary 6 and 7 joining the Main River at Sperle with Mean annual water levels (A), Median (B), 10-year (C), and 20-year (D) floods

Impact Area 6, Section 4 (Figure 29): Figure 29 shows the area called Fossøy in the valley. This is a part of the valley which had severe impacts during the 1979 flood. The flood marker is located just before the tunnel along with posters about the history of the flood. The area at the bottom of Figure 28 is connected to Figure 29. The median flood simulation does not show any impact on the flood marker region, however the rise in water levels in the river is very noticeable. The water levels rise from the range 0.70-1.49 m to the range 1.50-2.21 m, and up to 2.22-2.69 m further downstream. Areas with houses and small farmlands are affected with low water levels.

A significant difference in the 10- year and 20- year flood simulations can be seen by the marker. The area just before the tunnel, where the flood marker is located, has water flowing over the road and into the farmland. Though the water levels are in the lowest range, but the difference is significant. This is happening potentially due to the bottleneck that occurs right after the tunnel. The difference in water levels can be noticed in the main river for the 10-year and 20-year simulations. However, this difference cannot be seen in Figure 28, for the exact same location, this is because the simulation designed for the two figures (28 and 29) fall under different river sections. Figure 28 falls under Section 3 of the river, which ends before it reaches the bottleneck, Figure 29 falls under Section 4 of the river which simulates the impacts of the bottleneck, causing water to move into the farmlands with 20-year flood.

Besides this difference at the bottleneck, the rest of the river has same water levels for both the floods. The affected areas with the 10- and 20- year floods are however, much more than the median flood. Water in the two areas on the right have extended as well as the water level rises between 0.5 m to 1 m. More sections of the road on the west seems inundated, still with the lowest water range.

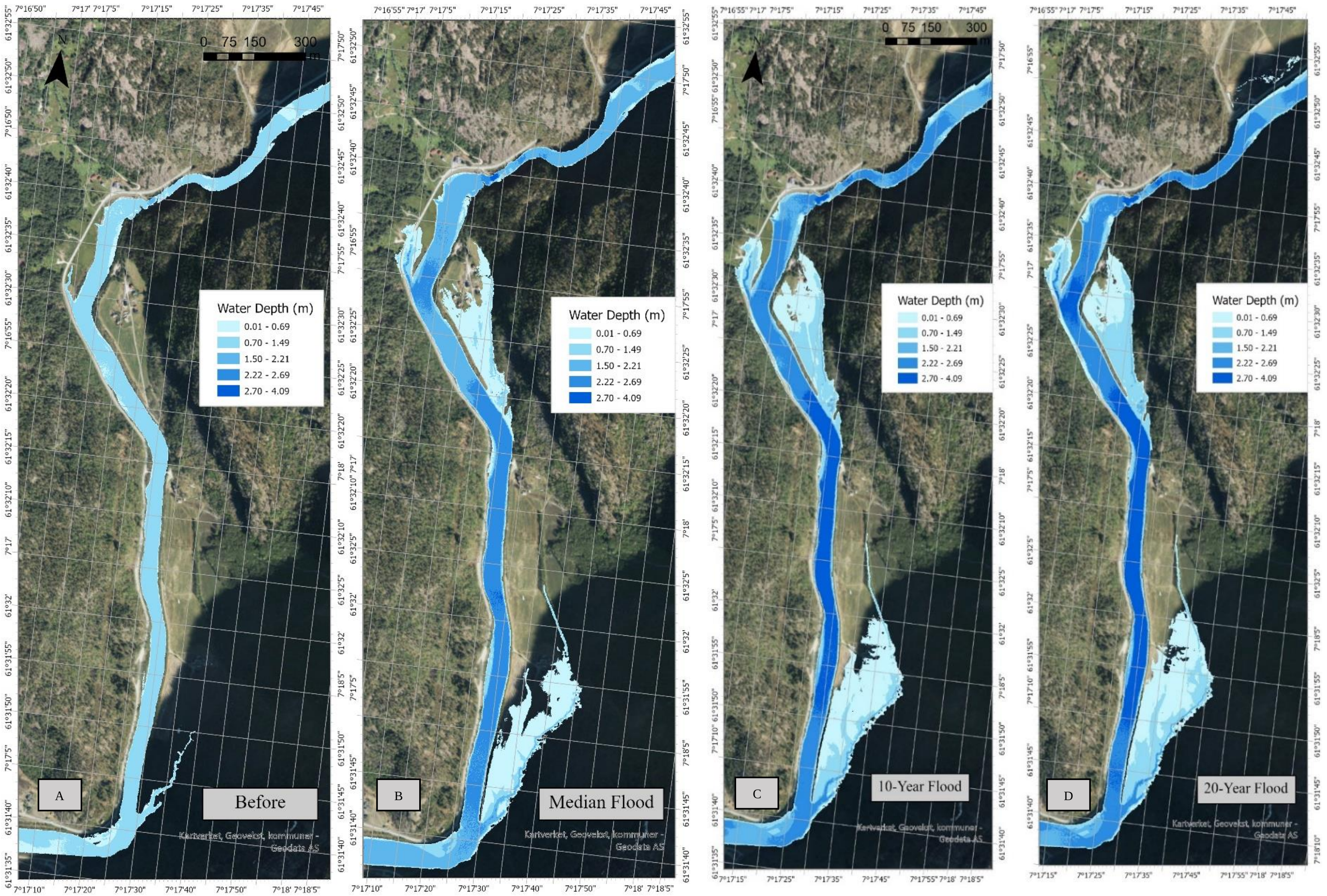

Figure 29: Impact area 6- Flood marker at Fossøy and downstream impacted area with Mean annual water levels (A), Median (B), 10-year (C), and 20-year (D) floods

Impact Area 7, Section 5 (Figure 30): The second gauging station in the Jostedøla river is at Myklemyr. Figure 30 shows another vital bridge on the river at Husøy and Tributary 8 joining the main river. The gauging station is located just across the bridge. According to NEVINA RFFA 2018 flood values, a median flood at Myklemyr station show a water flow of 234 m^3/s and the median flood simulation from this study shows a water flow of 239 m^3/s (Figure 31) when the median flood occurs. A 10-year and 20- year flood values by NEVINA at Myklemyr station are 325 m^3/s and 361 m^3/s, respectively. The maximum flow in the hydrograph during the floods in the simulations were 310 m^3/s for 10- year flood and 339 m^3/s for 20-year flood (Figure 31).

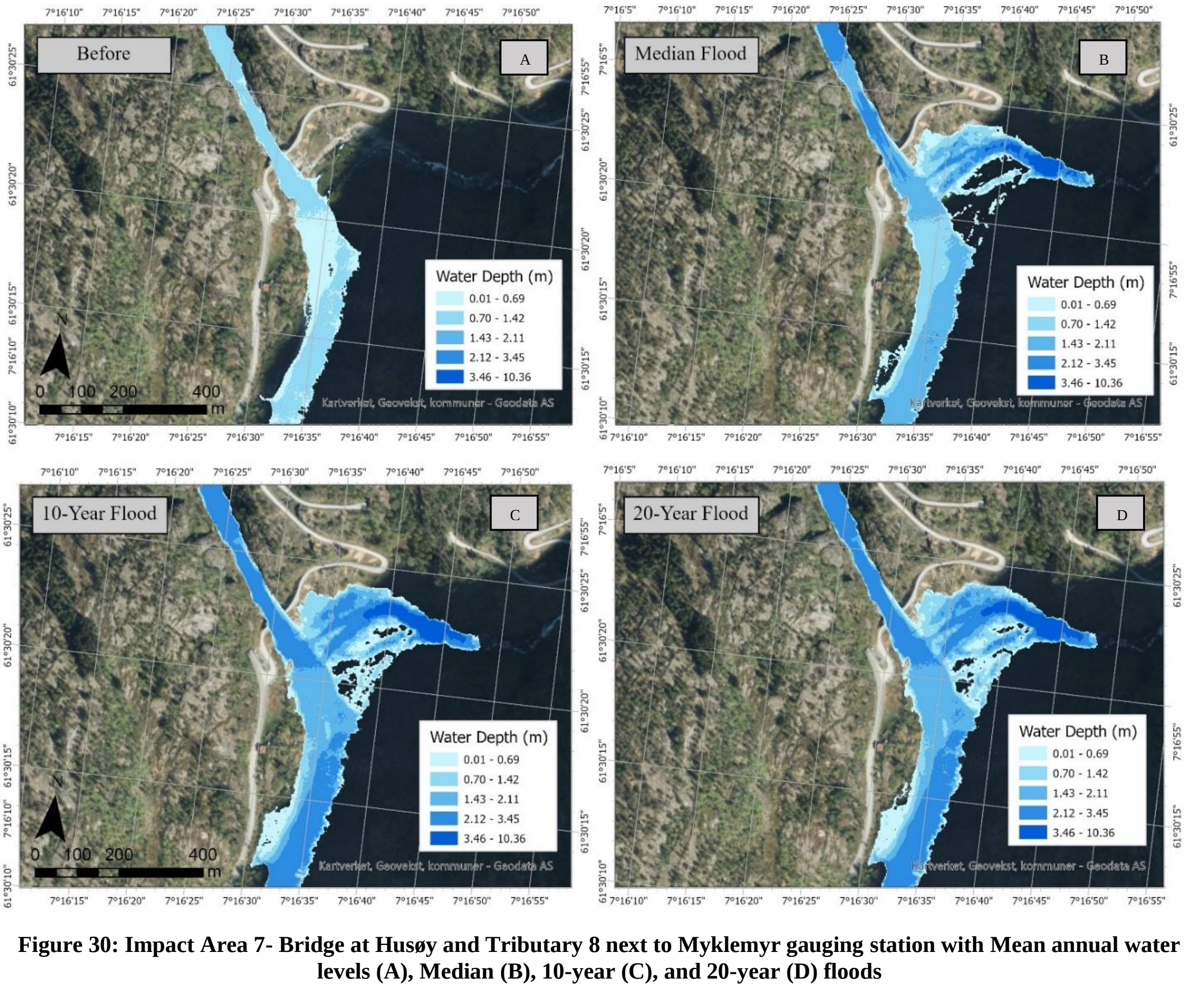

Figure 30: Impact Area 7- Bridge at Husøy and Tributary 8 next to Myklemyr gauging station with Mean annual water levels (A), Median (B), 10-year (C), and 20-year (D) floods

As the river approaches the bridge at Husøy, water levels rise from 1.30 m to 2.15 m in median flood. Similar to tributaries 6 and 7, tributary 8 is activated and has a water depth between 2.94-8.39 m (Figure 30B) in a shallow and unstable terrain, causing the water to flow into the surrounding area. Water levels of the main river near the Myklemyr gauging station rises by half a meter for the 10- and 20- year flood compared to the median flood (Figure 28C and 28D). The area around the tributary 8 has more water flowing into the surroundings with water levels between 1.43-3.45 m. On the southern part, water is flowing towards the main road but with low levels. The water level under the Bridge at Husøy rises to 2.5 m and 2.6 m for the 10-year and 20- year floods, respectively.

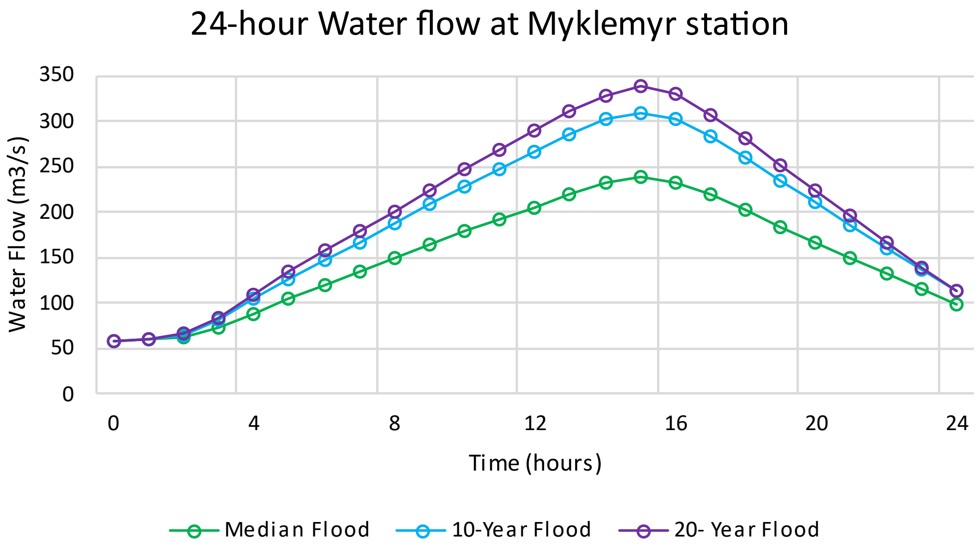

Figure 31: Hydrograph of Median, 10-year and 20-year flood simulations at Myklemyr station

Impact Area 8, Section 5 (Figure 32): Figure 32 shows the three floods affecting the road along the river as well as the farmland at Alsmo. The water levels in the main river rises from range 0.01- 0.73 m before floods to 0.74-1.35 m range during median flood and higher ranges during 10- and 20-year floods. The road along the northwest side of the river has some water flooding it and moving into the farmland. The water bodies west of the river is slightly filled up during the median flood (Figure 32B). However, the impact is low with water levels limited to the lower range. During the 10- and 20- year floods the waterbodies next to farm has more water than the median flood going up to the range 1.43-2.11 m during the 20-year flood (Figure 32C and 32D). Difference in water depth for 10- year and 20- year flood is quite visible on the maps. The water also spread to a larger area for both the floods, with 20-year flood having more coverage. The water levels on the main river, however, does not differ much but it rose about half a meter compared to the median flood. The water on the road has extended further towards the housings flooding the field near the house during 10- and 20-year floods.

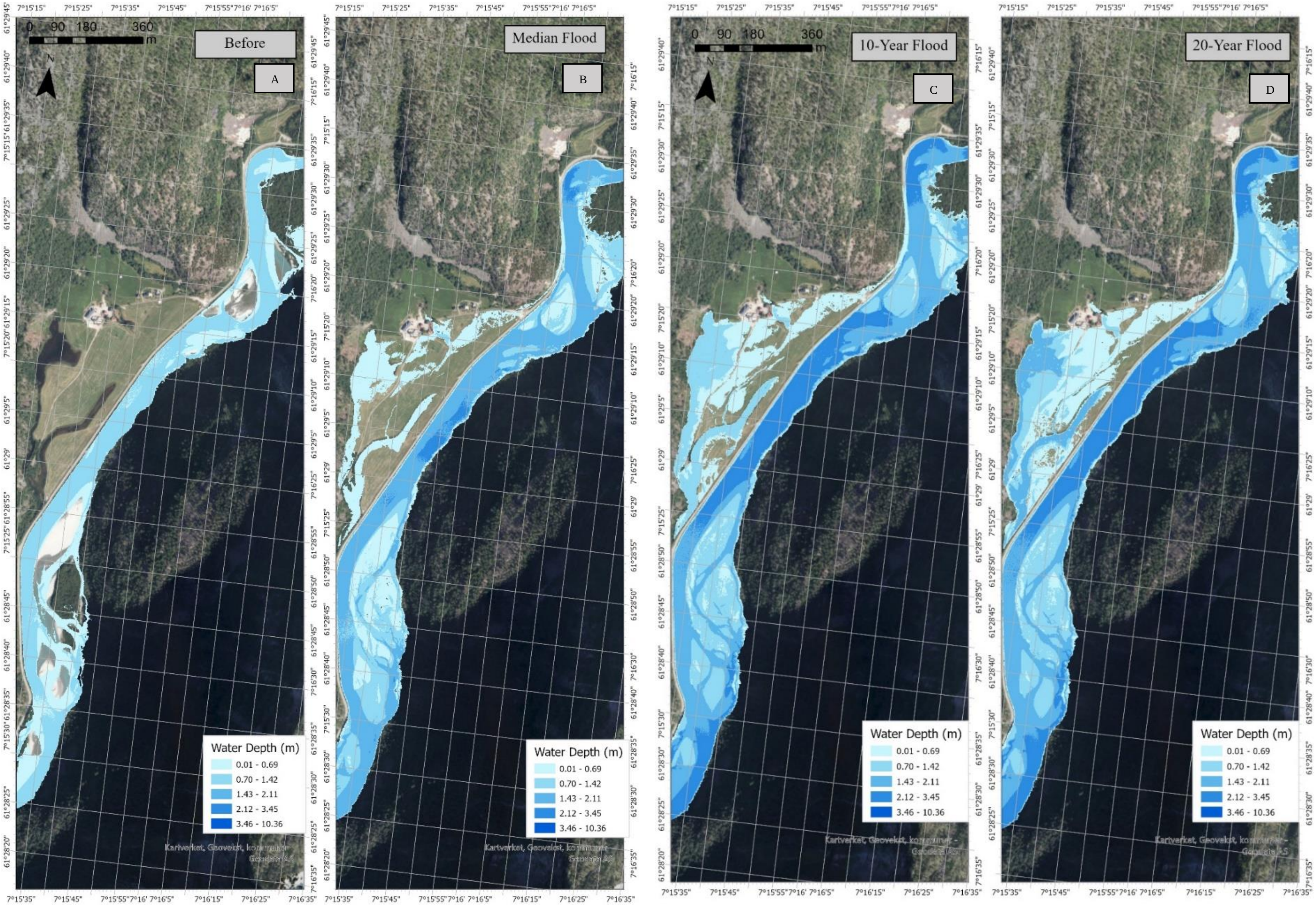

Figure 32: Impact Area 8- Affected Road and Farmland at Alsmo with mean annual water levels (A) Median (B), 10-year (C), and 20-year (D) floods

Impact Area 9, Section 6: The last affected area for the floods is at Gaupne, where the river flows into Gaupnefjorden (Figure 33). Historically, this area has been least affected by floods (NVE, 1981). Similarly, with the Median flood simulation, not many affected areas can be seen, but an area southwest of the river, before it joins the fjord, seem to have some flood water. Like all the areas in the median flood simulation the water levels are in the minimum range. Unlike the median flood, the 10-and 20-year flood simulations have impact at the end of the river in Gaupne. The extent of water flowing into the town is more in 20-year flood than the 10-year flood. However, the water levels stay with in the lower ranges and up 1 m. The water levels in the main river rises from range 2.23-2.87 m in the median flood to range 2.33-5.67 m during the 10-and 20-year floods.

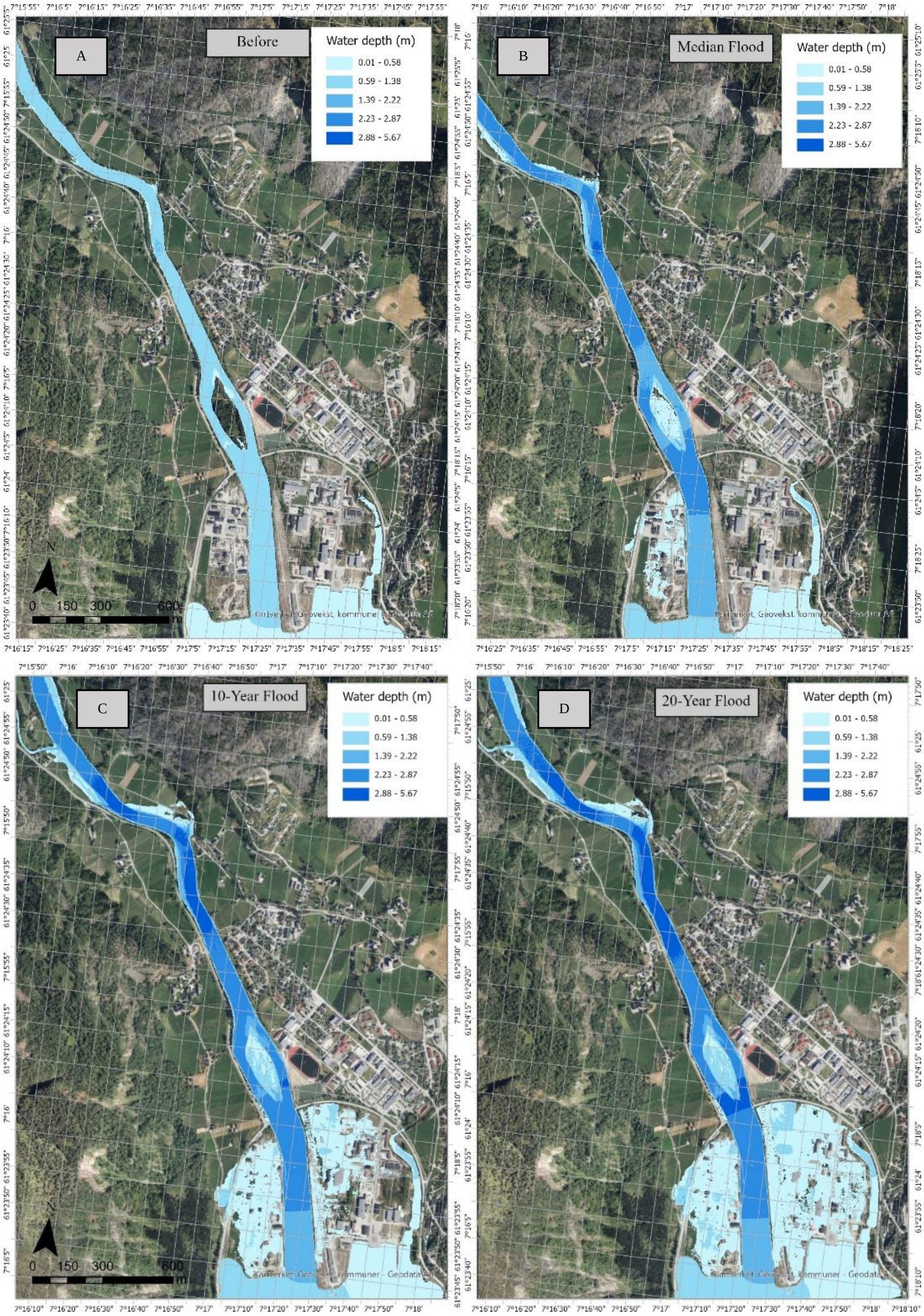

Figure 33: Impact Area 9 - Jostedøla flowing into Gaupnefjorden with Mean annual water levels (A), Median (B), 10- year (C), and 20- year (D) Floods

3.2 Resistive capacity of current flood protection installations under future floods in Jostedalen

This section presents model results for Jostedalen under a flood scenario of the same magnitude and a higher magnitude than that from 1979 and zooms in on the areas that are at risk of being flooded and damaged. The analysis specifically scrutinizes the efficiency of the existing flood protection infrastructures under the pressure of 50-, 100- and 200- year floods. Not only the higher magnitude flood simulations can help us identify how different sectors of the river would respond to a higher intensity flood but can also show which river sectors may need further protection under the anticipated intensification of weather extremes driven by the changing climate. To keep the narrative and location analyses consistent, the results from this scenario are presented in the same order and Impact area as the results in the previous section of the results, risking of becoming slightly repetitive. However, the focus is only on the most affected regions.

Impact Area 1, Section 1: The upstream sector of the main river and tributary 1, Breelvi, originating from the Nigardsbreen lake (Figure 34) shows the 50- 100- and 200- year floods at the Nigardsbreen camping. The water levels in the river rises to range 2.17-3.14 m and higher near the bridge in the south for all the three scenarios. The farm on the east has more water covering land compared to the minor floods. The most significant affect can be seen near the road on the west along the Breelvi river coming from the Nigardsbreen lake where the river Breelvi flows over the road and potentially causes damage. The water levels in all the three simulations however rises between 10-22 cm on the road with the velocity of the water in the stream being 3.8 m/s and water flow of 1.3m^3/s which is not enough to break through the road. Although the 200-year flood simulation predicts a mere 2-cm rise in the water levels on the road compared to the 50- and 100-year scenario, it does not account for the potential increase in the water flow due to intensifying melting of the glacier upstream.

The water levels under the Elvekrok bridge in the southern part of the map rises to 2.60 m for 50-year flood, 2.63 m for 100-year flood and 2.65 m for 200-year flood (Figure 34). As the areas affected by the flood remain essentially the same as for the 3 floods, a similar observation can be made for the camp where water levels only differ by 1 cm from the results of the 50-, 100- and 200-year flood experiments. For all the 3 flood scenarios, the Camp site is infiltrated with flood water, with water levels range between 10-20 cm.

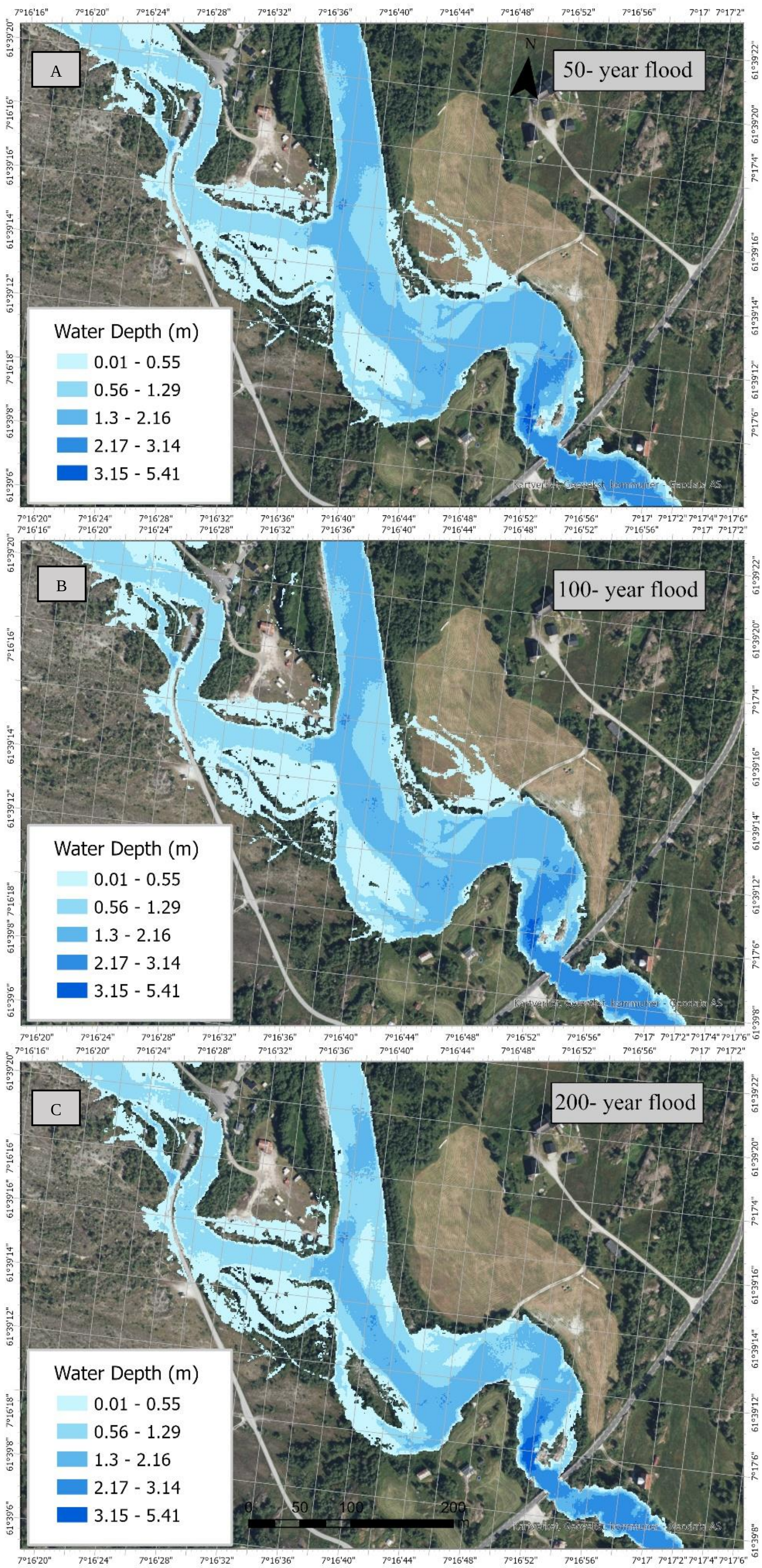

Figure 34: Impact Area 1- Nigardsbreen Camping and Confluence of Rivers Jostedøla and Breelvi (Tributary 1 from originating the Nigardsbreen lake) with 50- year (A), 100-year (B) and 200-year (C) floods

Impact Area 2, Section 2: The floods show more impacts on the downstream, as the second tributary joins Jostedøla (Figure 35). The flood water from the high intensity simulations shows more affected areas compared to the minor flood scenarios. The Jostedal campsite and the two neighbouring farms (Figure 35), have more inundation with water levels rising to range 0.56 m to 1.31 m. The water levels in the main river rises to range 1.32- 2.1 m and the flood extents further into the farms. The farm on the west has more water flowing in and the water levels go up to 1.3 m closer to the channel flowing in from the river.

The camping place (northwest of the map) has more water flowing in near the cabins by the riverbank. The water levels at the camp site moves further in and rises to 27 cm during 50-year flood and 31 cm during 100- and 200- year floods near the cabins. Due to the flood protections by the riverbanks, most of the camp is protected however, water levels still rise and can potentially cause damage to the infrastructure closer to the river. The floods effect a larger extent of the farm in the middle with water levels rising between 22-50 cm during 50- year flood, 22-70 cm during 100- year flood and 36-74 cm during the 200- year flood, with the upper ranges being closer to the southeast riverbank.

Impact Area 3, Section 2: As the flood moves downstream (Figure 36), the farm at Hesjevoll (Figure 36), is completely inundated with water levels rise to 50 cm and in the middle of the farm up to 1.5 m near the riverbank for the three floods. The road along the farm gets inundated as well as the surroundings of the building in the middle of the farm. As the floods increase in magnitude the road on the east and the red building in the middle of the farm is barely visible. The water levels on the road gets as high as 1 m during the 200-year flood. As the floods intensify, water moves further north into the surrounding farms. The smaller farms in the north are flooded with water levels between 0.6 m to 1 m (Figure 36C). The water levels in the main river rises to 2.06 m, 2.95 m, and 3.05 m during the 50- 100 and 200- year floods, respectively.

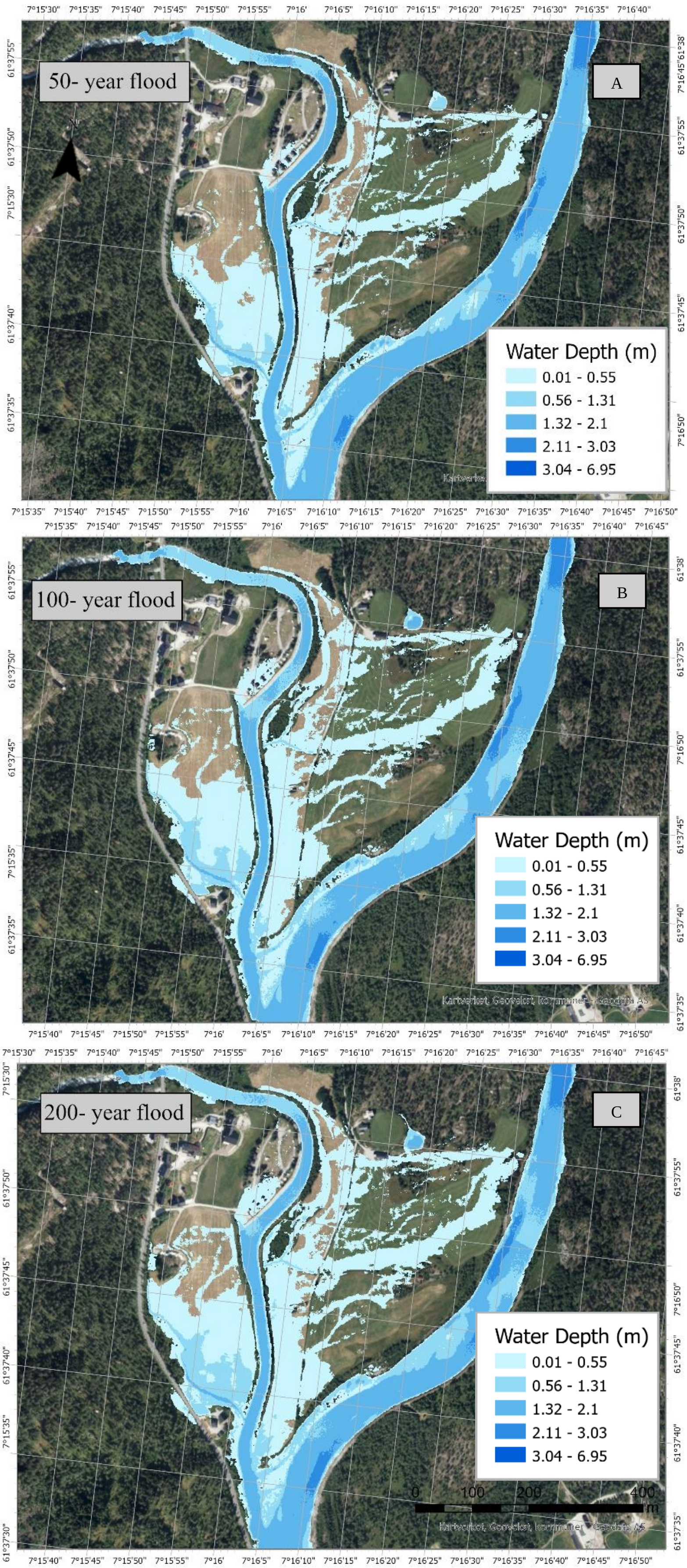

Figure 35: Impact Area 2- Jostedal Camping and Confluence of Jostedøla and Tributary 2 on the west with 50- year (A), 100-year (B), and 200-year (C) floods

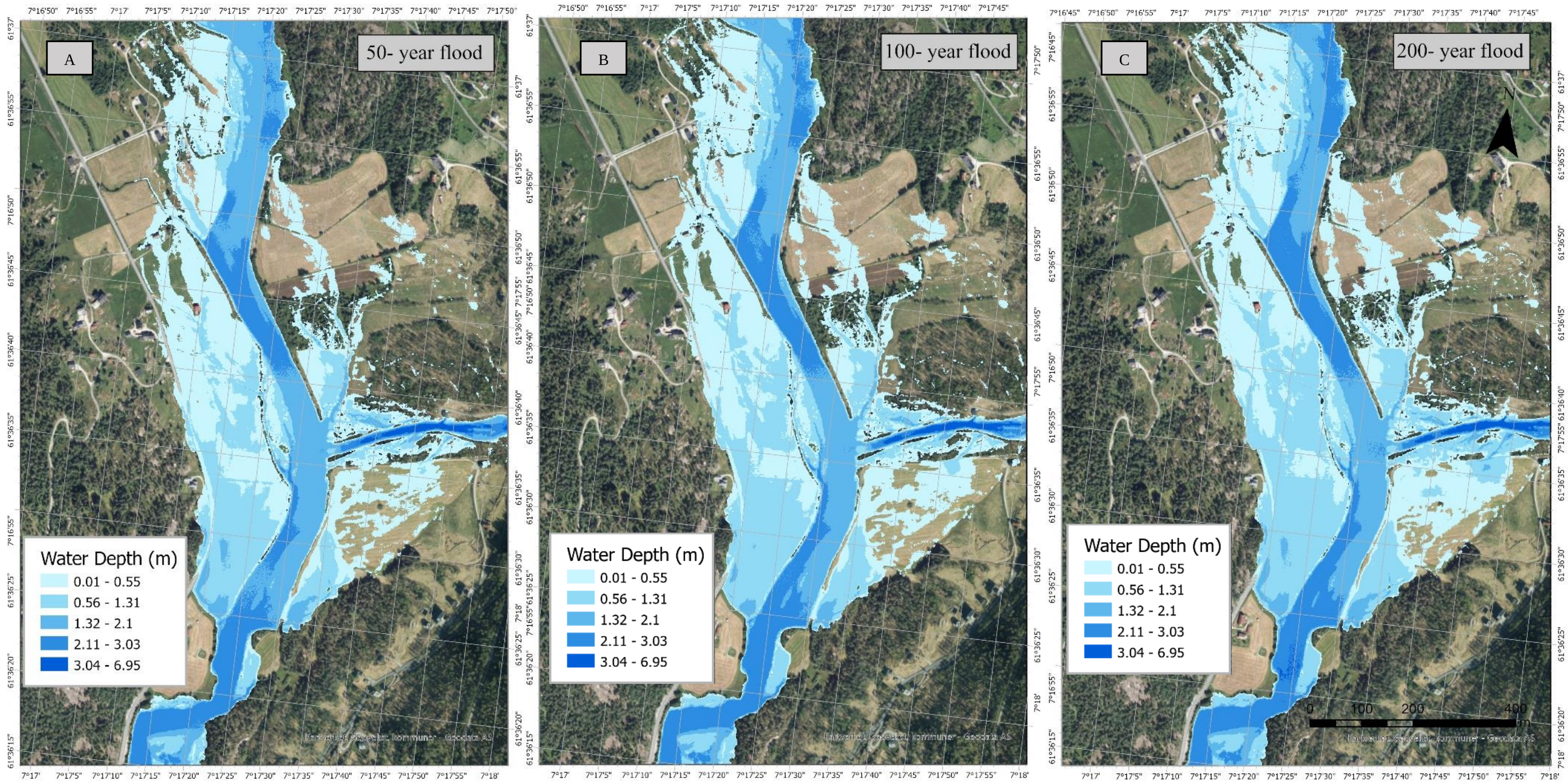

Figure 36: Impact Area 3- Farmland in Hesjevoll downstream of Geistedøla, Tributary 3, with 50- year (A), 100-year (B), and 200-year (C) floods

Impact Area 4, Section 2: Figure 37 shows the 4th impacted area in the valley. No significant change in the extent of flood water spread can be noticed in the maps, however, the water levels change throughout as the floods intensify. This was one of the most affected areas during the 1979 flood and has gone under severe terrain modification and flood protection measures. The Høgebru bridge is located here along with the smaller bridge over Sagrøyelva river (tributary on the west). The water levels in the main river rises between 4 m to 5.13 m near the Høgebru bridge during the higher intensity floods. Water levels under Høgebru bridge rises to 3.71 m (50-year flood), 3.85 m (100-year flood) and 4 m (200- year flood) during the floods. The bridge is approximately 1.7 m higher than the flood water levels.

On the other hand, the water levels under the Sagrøyelva bridge rises to 3 m for both 50- and 100- year flood scenarios, potentially causing the 2.9 m high bridge to be flooded. Given the higher magnitude of the 200- year flood the bridge might be severely affected as the water under the bridge goes up to 3.02 m, same as the other 2 flood scenarios, potentially damaging the bridge and flowing into the surrounding areas.

Impact Area 5, Section 3: During the high intensity floods the farm at Sperle gets completely inundated (Figure 38) The water levels in the tributary 7 (on the west) rises to 14.85 m, 14.88 m and 15.4 m as the flood magnitudes increases causing water to flow down into the surrounding areas and flooding the farm and damage the bridge downstream. Water flows down from the breach at the banks of tributary 7 with a velocity of 15 m/s and the water levels go up to 8.3 m (in the south) and 5.8 m (in the north) on the two sides of the tributary for the 3 scenarios. Both the farms get completely submerged with water levels get as high as 85 cm (50-year simulation), 97 cm (100- year simulation) and 1 m (200- year simulation) during the floods. The road on the west gets submerged as well, with water levels going up to 1.6 m near the tributary and 0.93m further down the road. The tributary 6 (on the east), contributes to some flood water in the farm next to it, the levels go up to 28 cm only in the 200- year flood, for the other 2 floods the water levels stay in the lowest range. Further down on the east side of the main river, the areas get flooded with same flood extent for the 3 scenarios, the water levels stay within 0.6 m.

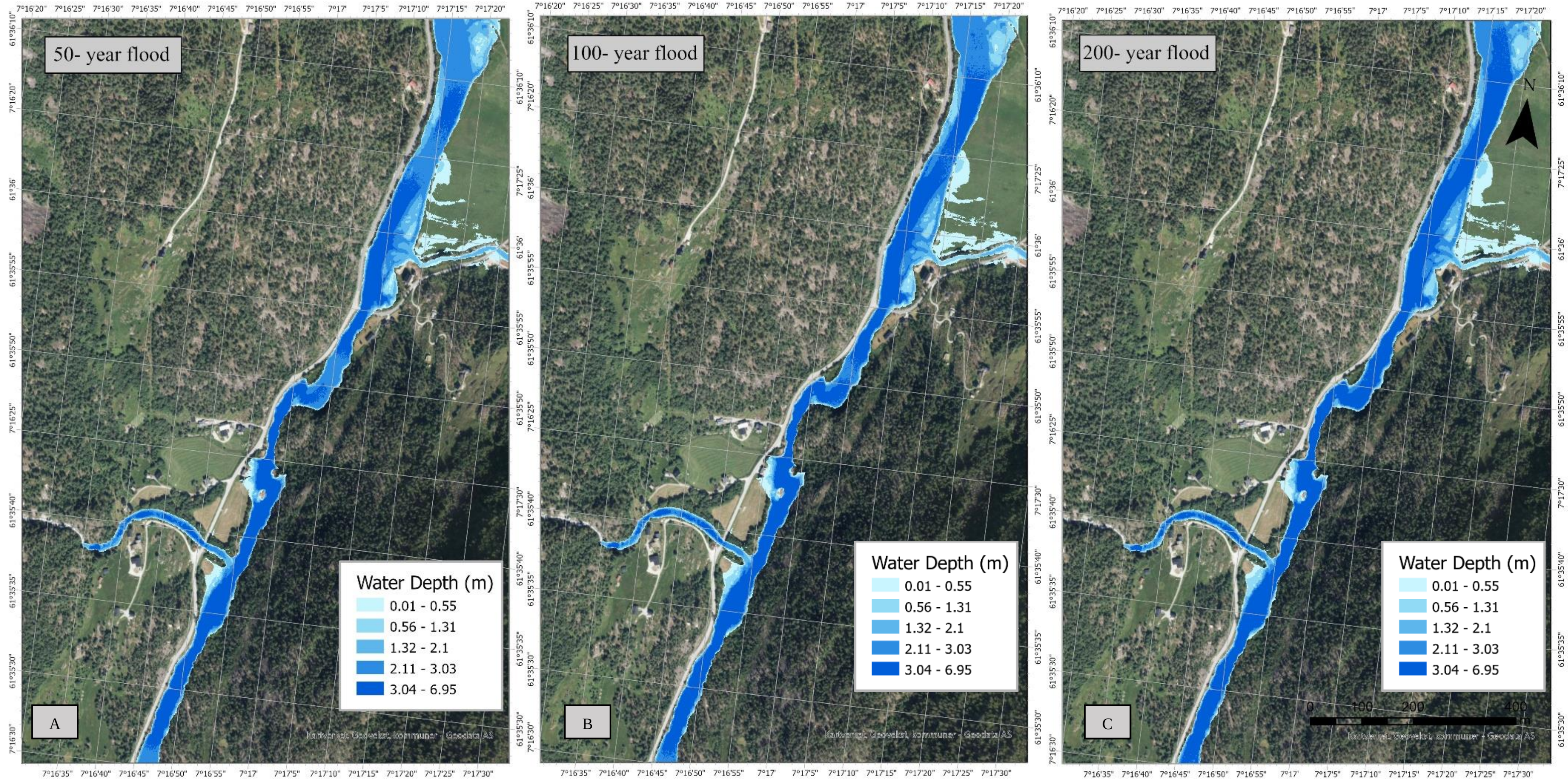

Figure 37: Impact Area 4 - Høgebru bridge, Tributary 4 and Sagrøyelva (Tributary 5) with 50-year (A), 100-year (B), and 200- year (C) floods

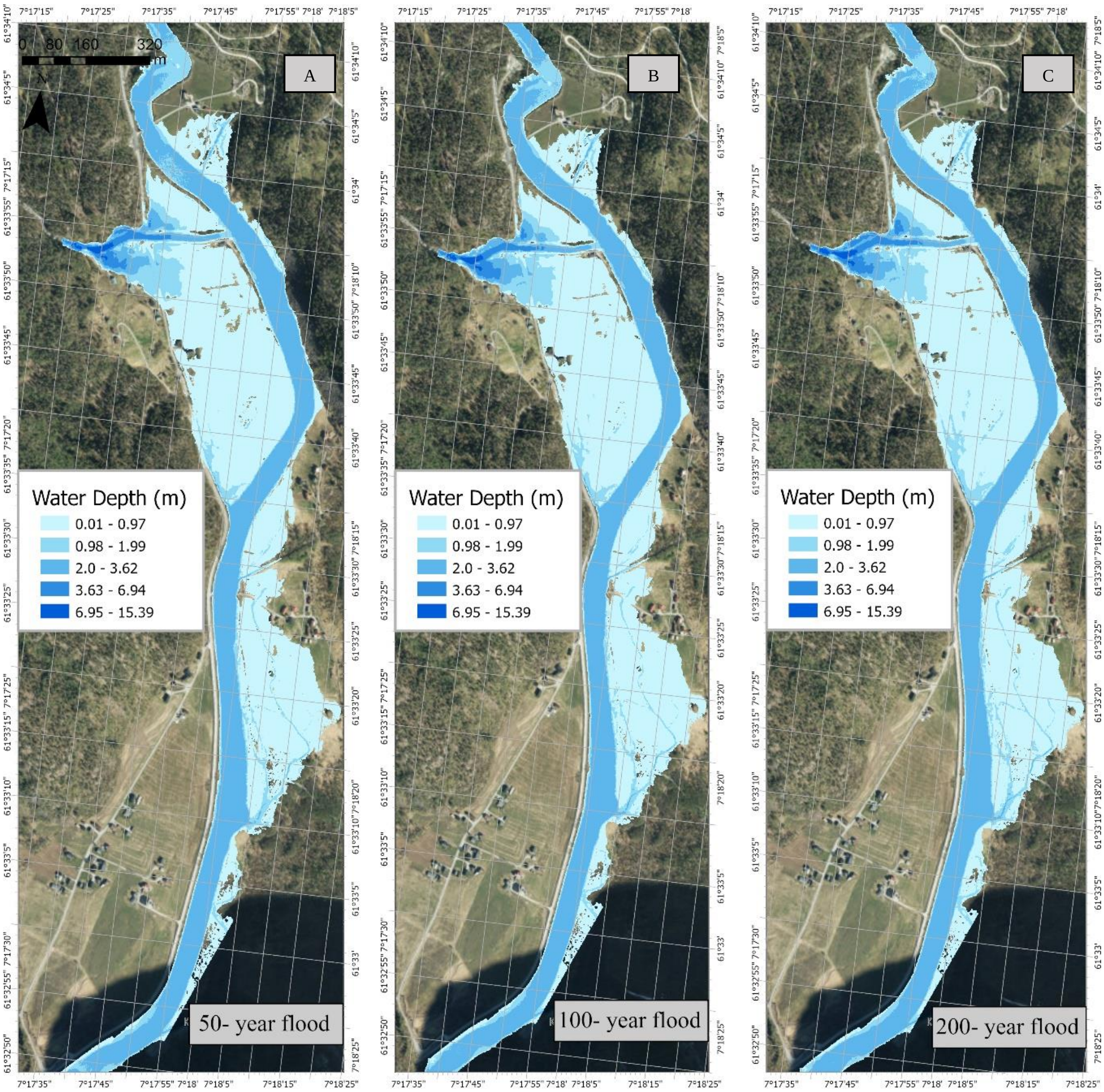

Figure 38: Impact Area 5- Tributary 6 and 7 joining the Main River at Sperle during 50-year (A), 100-year (B), and 200-year (C) floods

Impact Area 6, Section 4: As the flood moves down the river, it approaches a bottle neck at Fossøy. The bottle neck is right after the tunnel, northeast of the map (Figure 39). The water level in the main river rises to 2.50 m - 2.86 m near the marker and flows into the road though a small opening (marked in red) and a small part of the farmland. The water levels at the marker rise to 2.23 m for 50-year flood simulation, 2.70 m for 100-year flood simulation and 3.25 m for the 200- year flood simulation. As the floods intensify more area near the marker gets flooded with water levels rising to 1.64 m and 1.86 m during the 100- and 200- year floods, respectively. For the 50-year flood, the extent of water infiltration is lower, nevertheless the water depth is still up to 1m.

After passing the bottle neck the water levels in the main river rises to the highest range (Figure 39) Water flows into the main road on the northwest and floods the two fields east of the river at Fossen. The water levels under the bridge, that connects the northern field to the main road, 3.30 m, 3.41 m, and 3.52 m for 50-, 100- and 200- year flood, respectively, leaving about 1.3-1.5 m difference between the bottom of the bridge and the river. The water levels in the two fields go up to 1.73 m, during the 50- and 100- year simulations and 1.84 m during the 200-year simulation potentially causing damage to the land and the settlements.

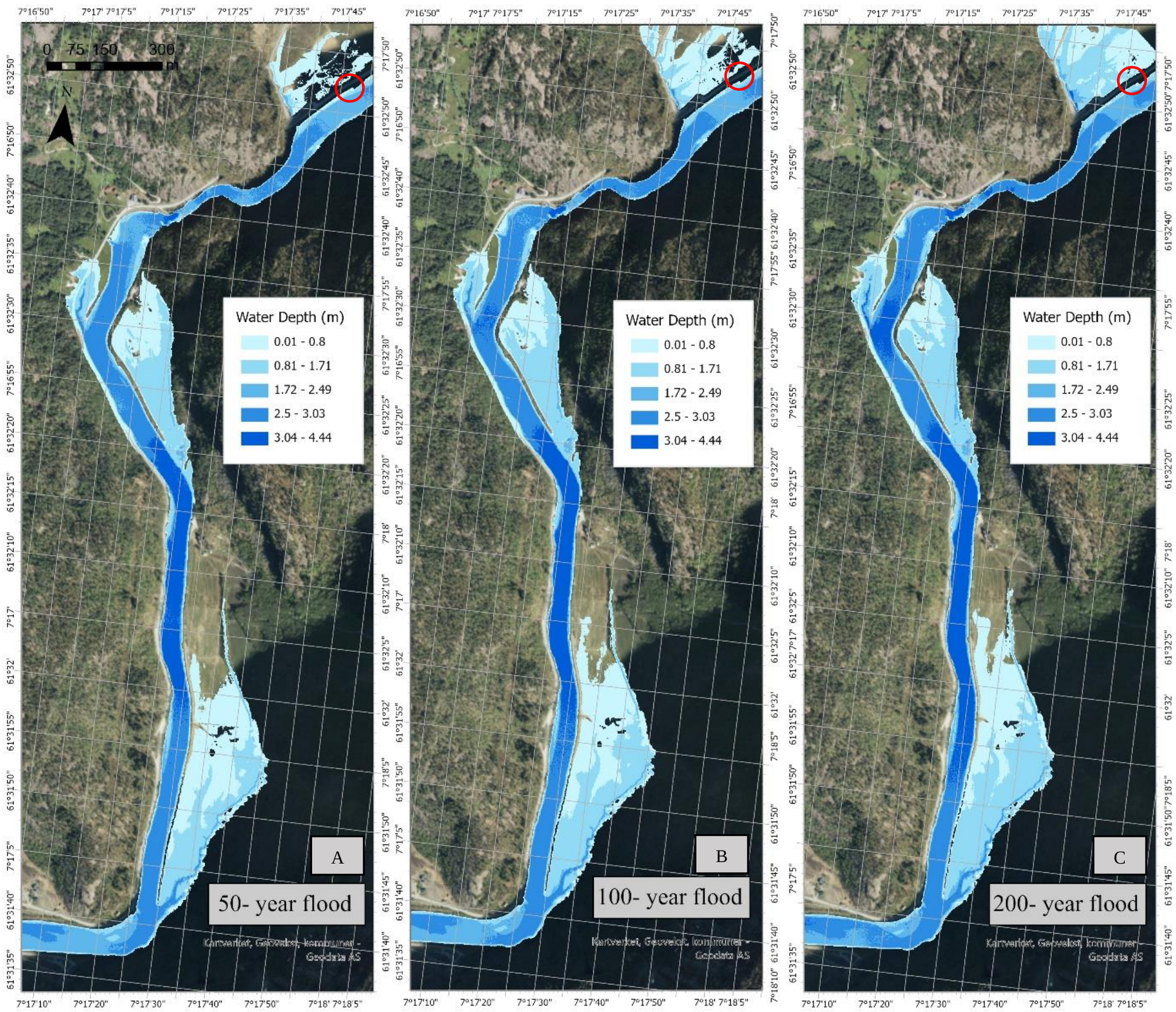

Figure 39: Impact area 6- Flood marker at Fossøy and downstream impacted area with 50-year (A), 100-year (B), and 200-year (C) floods

Impact Area 7, Section 5: The higher magnitude floods near Myklemyr station rises the water level of the river up to range 2.20 -3.28 m (Figure 40). NEVINA 50-year, 100- year and 200-year flood values at Myklemyr station are 408 m^3/s, 445 m^3/s and 428 m^3/s, respectively. The maximum flow in the hydrograph during the flood in the simulations were 362 m^3/s for 50- year flood simulation, 384 m^3/s for 100-year flood simulation and 411 m^3/s for 200- year flood simulation (Figure 41). The water levels under the bridge at Husøy rises to 2.7 m, 2.8 m and 2.9 m as the flood intensity increases.

Impact Area 8, Section 5: As the flood intensity increases from minor floods to major floods the land at Alsmo gets completely inundated (Figure 42), while the water levels go up to 1.23 m during the 50-year flood, the water levels reach up to 2.19 m outside the waterbodies during the 100- year flood and up to 3.28 m during the 200- year flood. The main road (in the north) gets inundated with 71 cm, 76 cm and 83 cm water as the flood magnitude increases potentially damaging the road. The water moves through the road and into the housing areas, causing inundation of more than 1 m water in the surrounding field during the 200- year flood. The water level in the waterbodies inside the field rises to 3.28 m spilling into the land and flooding the field as well (Figure 42C).

Impact Area 9, Section 6: As the floods approach the end of the river at Gaupne, the water levels in the river rises to 3.71 m, 3.83 m, and 3.92 m in order of increasing intensity (Figure 43) before submerging the town in flood water. Higher volume of flood water flows into the town compared to the minor floods. Water levels in the town around settlements rises to 0.97 m during 50-flood, 1.05 m during 100-year flood and up to 1.11 m during 200- year flood potentially causing damage to property and infrastructure. The water levels in the main river rises to 3.92 m. The flood water infiltrates through the road and floods the small farm area on the southwest, with water levels going up to 1.5 m and submerging the road as well in all three scenarios. During the 1979 flood, this part of the town was not as developed as it currently. Thereby, if a flood of similar 50- , 100- and 200-year flood approaches the valley, this location will be risk of flooding and potential damage to the infrastructures and property

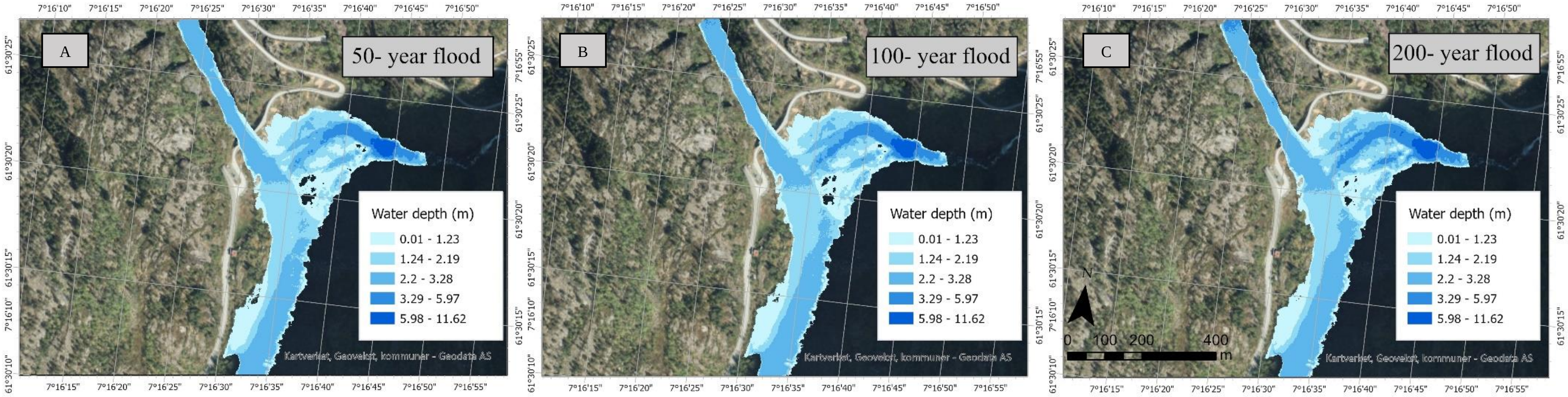

Figure 40: Impact Area 7- Bridge at Husøy and Tributary 8 next to Myklemyr gauging station with 50- year (A), 100-year (B), and 200-year (C) floods

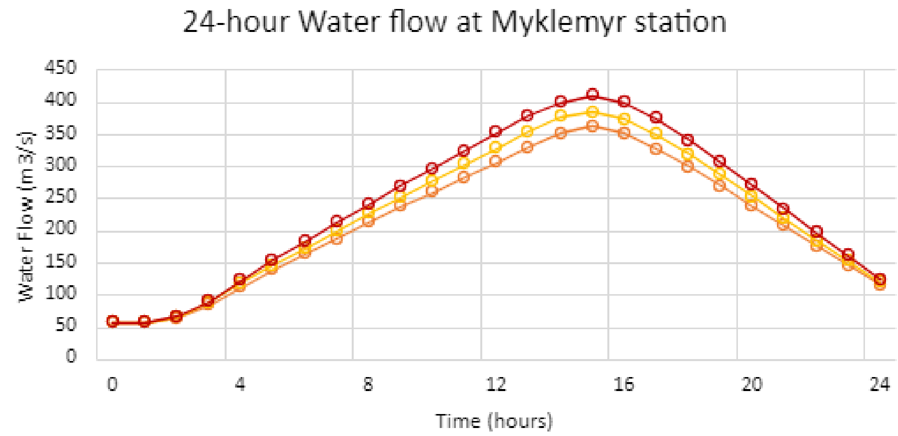

Figure 41: Hydrograph of 50-, 100- and 200- year floods at Myklemyr station

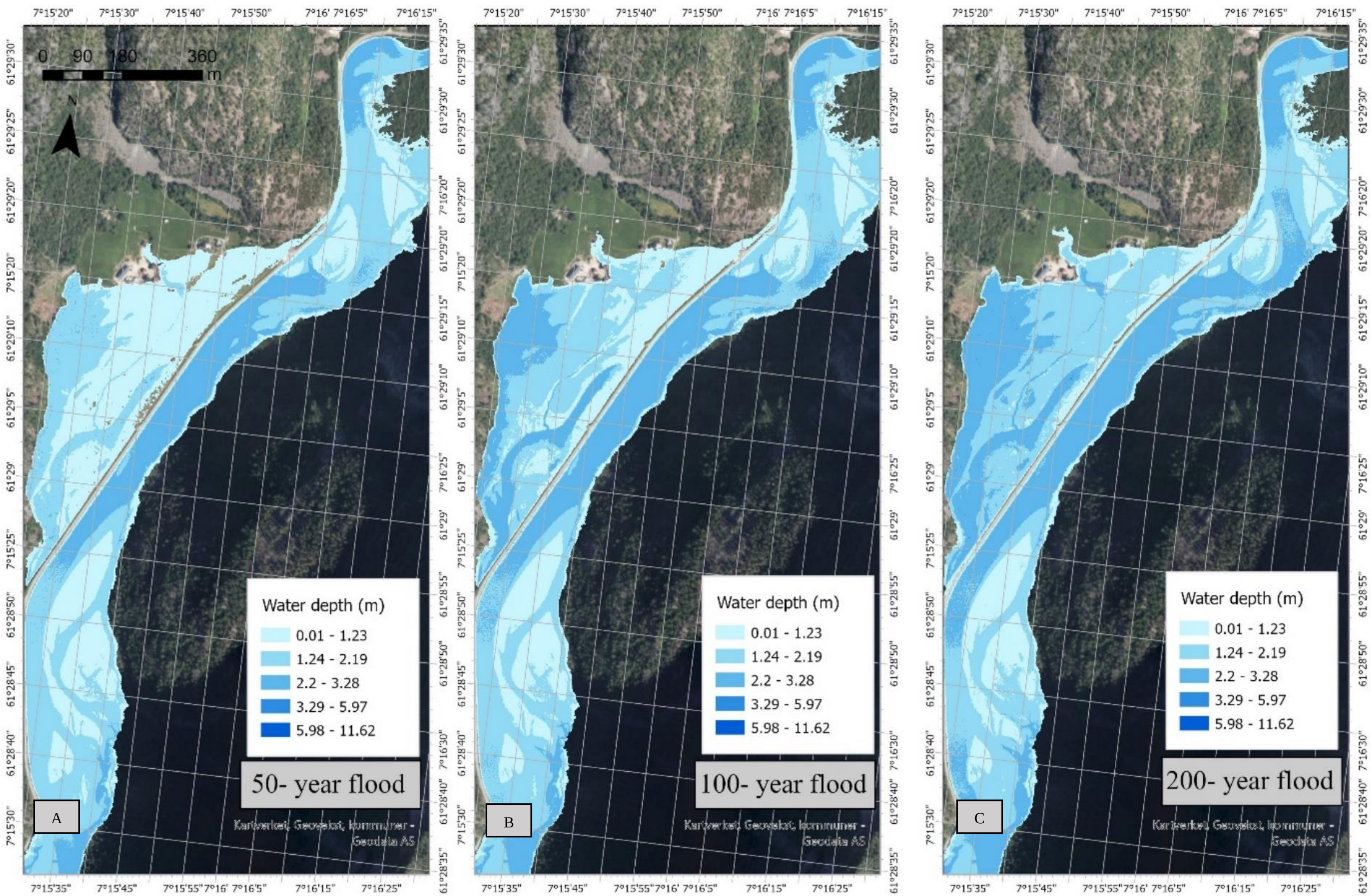

Figure 42: Impact Area 8- Affected Road and Farmland at Alsmo with 50- year (A), 100-year (B), and 200-year (C) floods

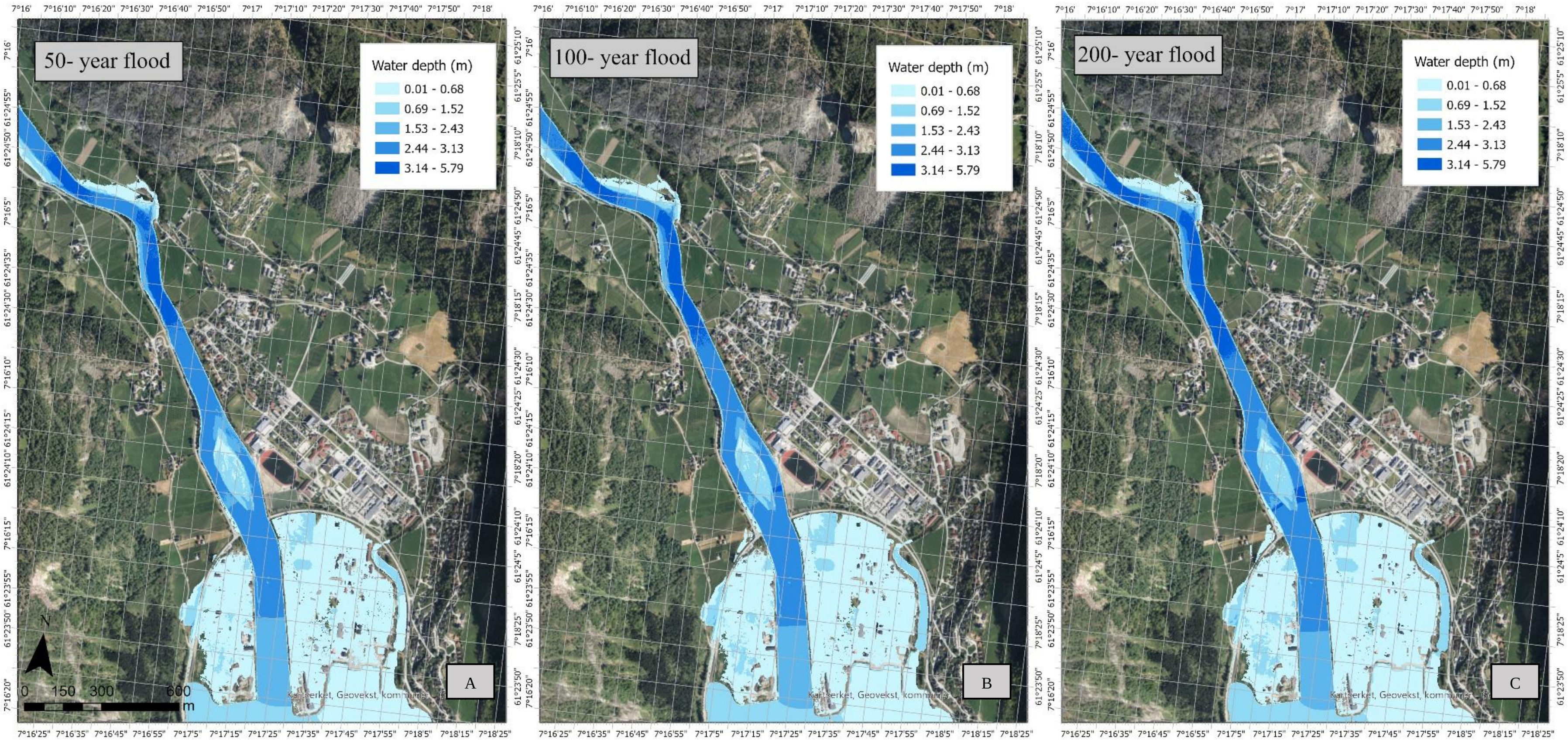

Figure 43: Impact Area 9 - Jostedøla flowing into Gaupnefjorden with Mean annual water levels (A), Median (B), 10- year (C), and 20- year (D) Floods

3.3 Capacity of Hjelledalen against high magnitude future floods

This sub-chapter presents the results of adapting the hydrological model set up for Jostedalen to Hjelledalen. Being the two wings of Jostedalbreen national park, the two valleys have very different response to weather and floods. Along with being the lesser documented and monitored valley, Hjelledalen, has had minimum flood protection measures installed in the region, however, it is very susceptible to high magnitude floods. This section presents the vulnerability of Hjelledalen and its lack of capacity to withstand future high intensity floods.

The Hjelledalen region is less densely populated than Jostedalen, therefore the area of interest comprises around the last 8 km river of Hjelledøla with Videdøla joining from the east and Sunndøla from the south. From the interviews during the summer 2021 fieldwork, it was brought to attention that junction of Videdøla and Sunndøla at the Folva adventure camp and the Oppstryn school downstream have previously experienced small floods from the river and potentially the glacier lakes of Tystigbreen. A master thesis by another GOTHECA member submitted in June 2021, specifically focuses on this study area on the impacts of glacier lake outburst floods (Svendsen, 2022). Based on the evidence of the vulnerability of these locations, high intensity (50-, 100- and 200- year) flood simulations like Jostedalen, were implemented in Hjelledalen to identify the capacity of the valley to withstand these higher magnitude floods.

The first area of Impact is at the Folva adventure camp at the junction of Sunndøla and Videdøla where they meet Hjelledøla (Figure 44). As the flood approaches the water level in the main river rises to 2- 3.5 m, with a bit higher water levels during the 200- year flood. the 3 fields north of the river gets flooded with water levels varying from 0.10-1.76 m in 50- year flood, 0.13-1.85 m in 100- year flood and 0.20-1.93 m in 200- year flood. All the three scenarios flood the front field of the Folva camping area (right after the junction), with water level going from 38 cm to 45 cm to 50 cm with increasing order of flood magnitude. The flood water then moves into the camping ground with water levels for 50- and 100- year floods staying with in the lower water level range and moving up to 0.53 m during the 200- year flood simulation (Figure 44D). Some water from the Sunndøla on the south, seems to flow into the camping area but it’s very low in volume and the water level stay below 10 cm, this could be because of the flood protection installed here by NVE. As the floods move downstream, the extent of floods increases with intensity and the water levels rises with in the first two ranges. Water from the river floods both sides of the road causing potential damage the farms along the road and the road itself.

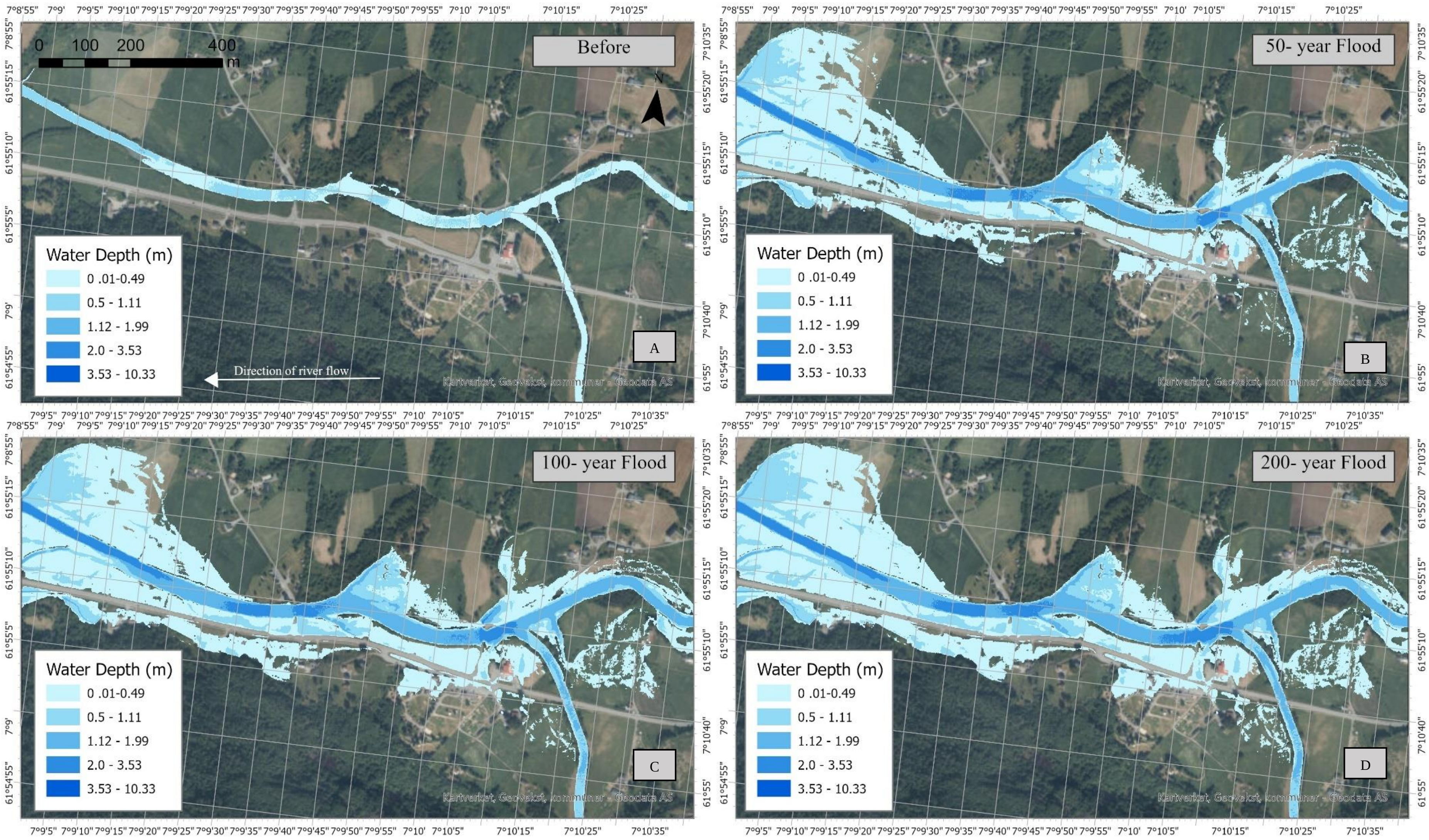

Figure 44: High intensity floods at Folva, Hjelledalen, mean annual water levels (A), 50- year (B), 100- year (C) and 200- year floods (D)

The second impact is located at the Hjelle (Figure 45). The farmlands at Hjelle after Folva, gets complete submerged in flood water, with water levels on the eastern part rising to 1 m for the 3 floods and remaining within 0.7 m in the curved farms downstream. The water gets closer to the main road on the south; however, it does not go beyond.

As the flood moves down towards the town in Hjelle, the football field near the Oppstryn school by the fjord get flooded. As the floods intensify from 50- to 200- year, more parts of the football field get flooded with water level rising to 12 cm (50- year flood) 18 cm (100- year flood) and 24 cm (200- year flood). In the 100- and 200- year flood scenario, the other field on the south of the river, near the fjord, gets a little water from the floods, with more water during the 200- year scenario (Figure 45D) rising to 30 cm.

The outcome of the flood simulations and the experiences of the people interviews, it is evident that the Hjelle and Folva region of Hjelledalen are at high risk from 50-, 100- and 200- year floods. Based on past experiences from minor floods, the flood protection measures work to some extent however they are not equipped enough if a higher magnitude flood occurs in the valley

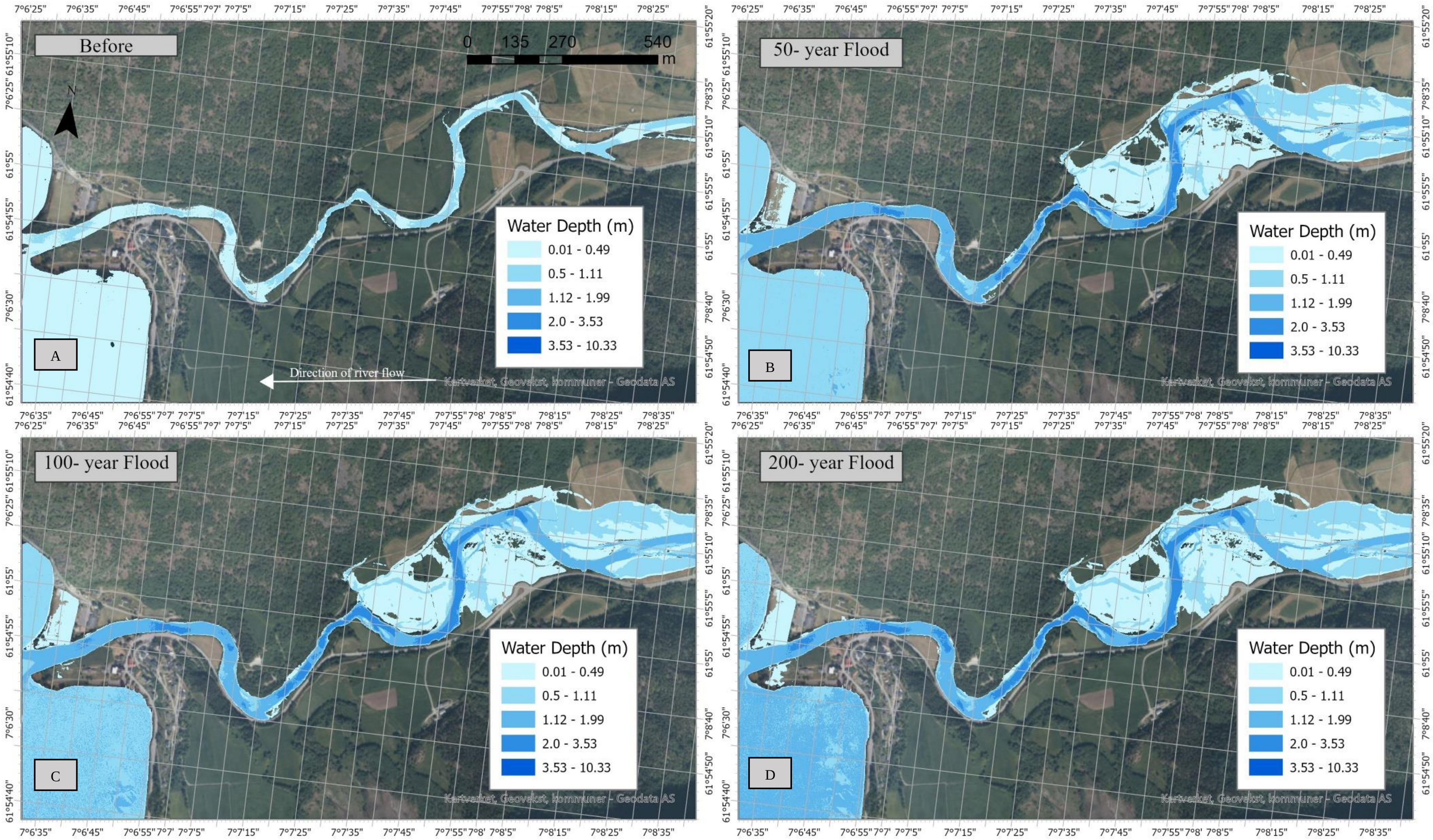

Figure 45: High intensity floods at Hjelle, mean annual water levels (A), 50- year (B), 100-year (C) and 200-year (D) floods

4 Discussion

This chapter interprets and explains the results of this thesis. The chapter is divided into 3 sub-chapters, each sub-chapter intends to answer the research questions of this study, starting with the interpretation of the 1979 Jostedalen flood reconstruction. The discussion then moves towards the impacts of similar and larger magnitude flood in the valley and whether the current flood protection measures can handle a more intensive flood. And finally, the discussion will focus on the implementation of the same hydrological model set up on the Hjelledalen region for the most intensive floods and how installing flood protection measures can reduce the impacts.

4.1 Reconstructing the magnitude and extent of the 1979-Jostedalen flood through hydrological modelling and historical evidence

The overarching focus of this study was to recreate the historical 1979 flood in Jostedalen valley and see how a flood of similar and higher magnitude would impact the valley in the present. Due to its intensive damage and elaborate documentation, the 1979 flood became the centre of this thesis. Since the flood occurred 43 years ago, there has been several terrain modification and installation of flood protection infrastructure in the valley.

The chapter discusses and presents reconstruction of the 1979 flood with the 50-year and 100-year flood simulations. These two floods are of particular importance as they are the closest reconstruction of the largest flood that occurred in Jostedalen valley in 1979. The flood of August 15th, 1979 was the most devastating and impactful flood in the valley. Following the damages caused by the flood, several terrain changes and flood protection measures have been taken in the valley. Investigation by NVE (1981) after flood concluded that this was a 100-year flood, however, according to modern RFFA by NVE NEVINA, the flood of 1979 is now categorized under 50-year flood. Therefore, to recreate the closest scenario of the flood, both the 50-year and 100-year simulations have been paired together for reconstruction and better analyse. The simulations have been designed over a modified terrain to best suit scenario of the terrain in 1979 since high resolution LiDAR-based DEM from before the 2007 are not available for the region. After modifying the terrain and removing the flood installations along the valley, the actual flood of 1979 was recreated.

Based on evidences from NVE's post-flood investigation report in 1981 (NVE, 1981), all active and inactive gauging station along the river and flood markers in the valley a validation map for Jostedalen (Figure 46) was made. Post-flood photos of damage left behind were marked in the map after verifying the locations from the report NVE (1981) and Google Map Street View. Each section of the river has at least 1 photo during the flood or a gauging station, with exception of section 6 of the river. No photos could be matched with the section 6 of the river. The NVE report mentions that there were significantly less damaged in the outlet of the river, this could be because parts of the town in the impact zone did not exist back then.

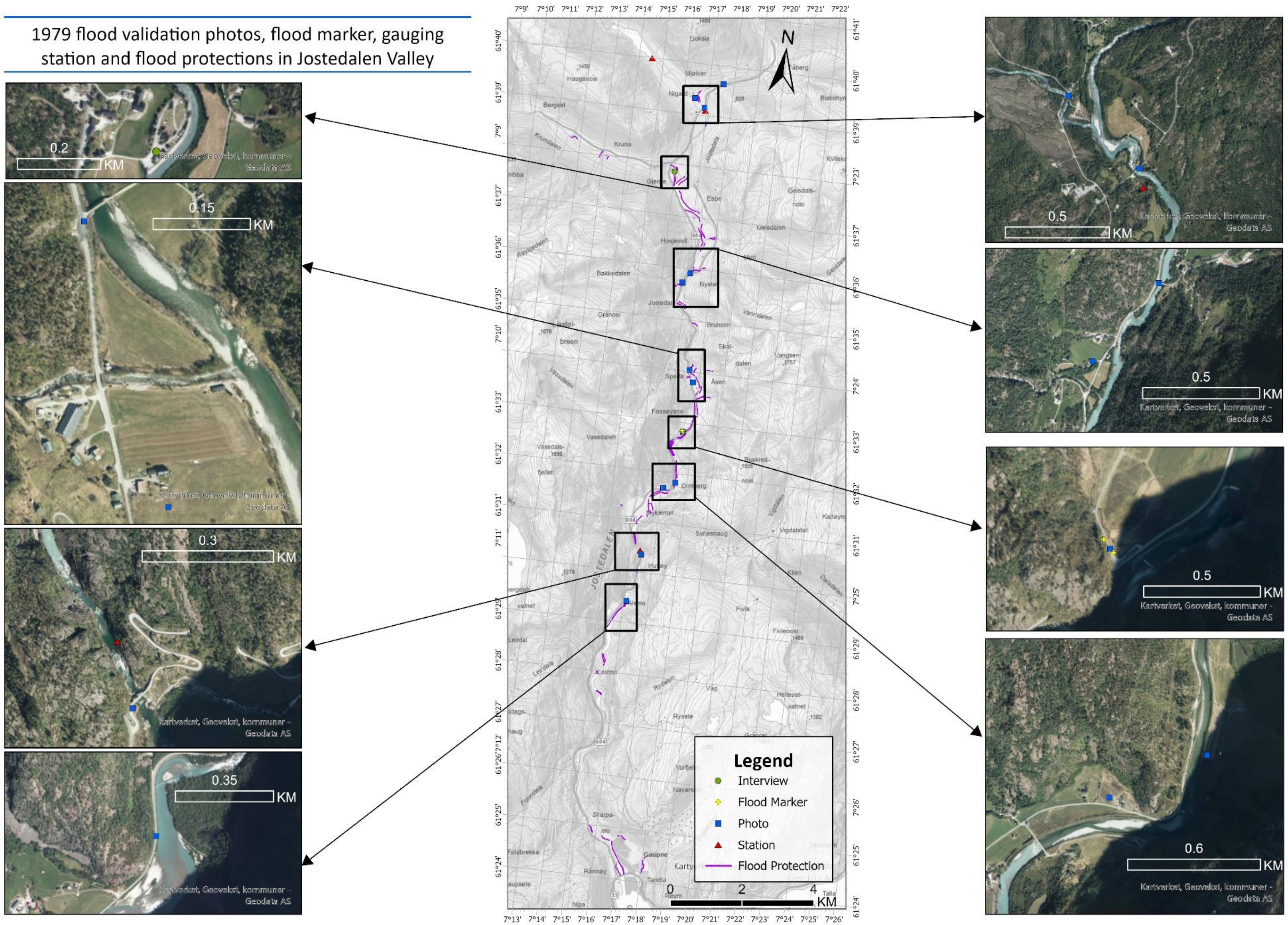

Figure 46: 1979 flood validation and flood mitigation map of Jostedalen

Affected Area 1, Section 1: The first reconstructed affected area was at the river junction of Jostedøla and Breelvi (tributary 1 from Nigardsbreen lake) (Figure 47). The first 2 locations on the validation map (Figure 46), is in this affected area (Figure 47). During the 1979 flood, the water levels in the tributary Breelvi rose to 1.32 m due to glacier melt from the higher temperature and heavy rain fall for the 12 hours before the flood hit on the midnight of 15th August. The reconstructed scenario shows the water flow in the tributary increasing and the river flows through the road (marked in red circle Figure 47) and makes a new channel (Figure 48A). In the 50- and 100- year simulations, the water levels on the road rise to 75 cm and 80 cm, causing the road to be damaged.

The next location on the validation map is at the Elvekrok bridge (Marked in yellow circle Figure 47), where the foundation of the bridge collapsed, and the deck collapsed (Figure 48B). The water levels under the bridge during the simulations rises to 2.5 m and 2.6 m, having a 2 m difference between the flood level and the bottom of the bridge. However, given the narrow width of the river before the bridge, the water levels and water flow increases, causing the banks to erode from the increased flow due to the heavy rainfall and glacier melt.

One of the short comings of the model can be seen here, where the interaction of the river with the sediment load and the riverbank erosion cannot be accounted for. Energy exerted by the river and the sediments it carries to cause collapse of roads and bridges cannot be measured from the simplified model set up. As the flood moves downstream, lack of sediment load contribution and riverbank erosion in the model can be seen.

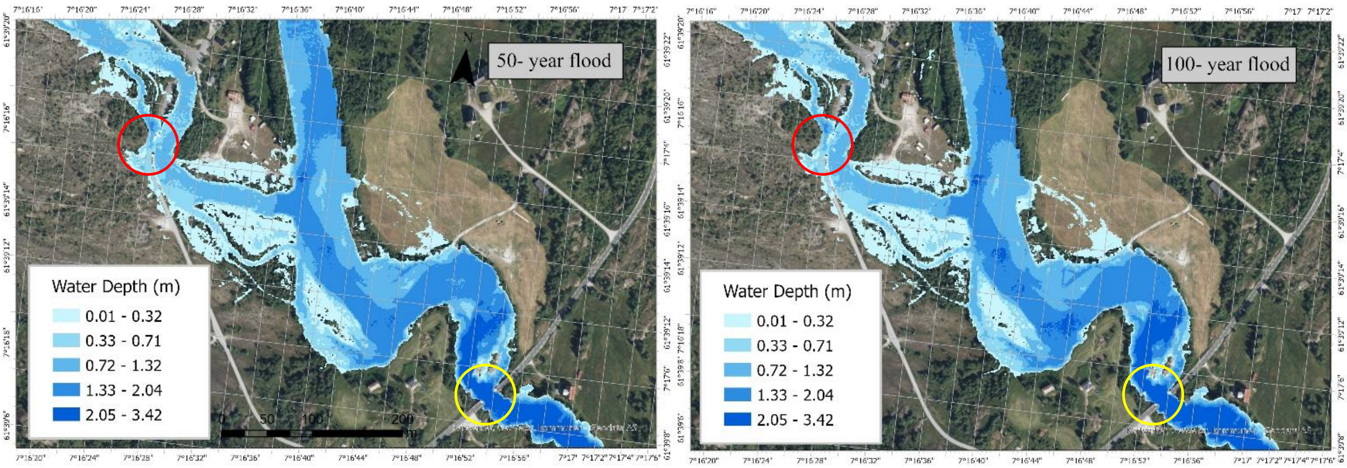

Figure 47: Reconstruction of 1979 flood at Affected Area 1- Nigardsbreen Camping and junction of Rivers Jostedøla and Breelvi (Tributary 1 from originating the Nigardsbreen lake)

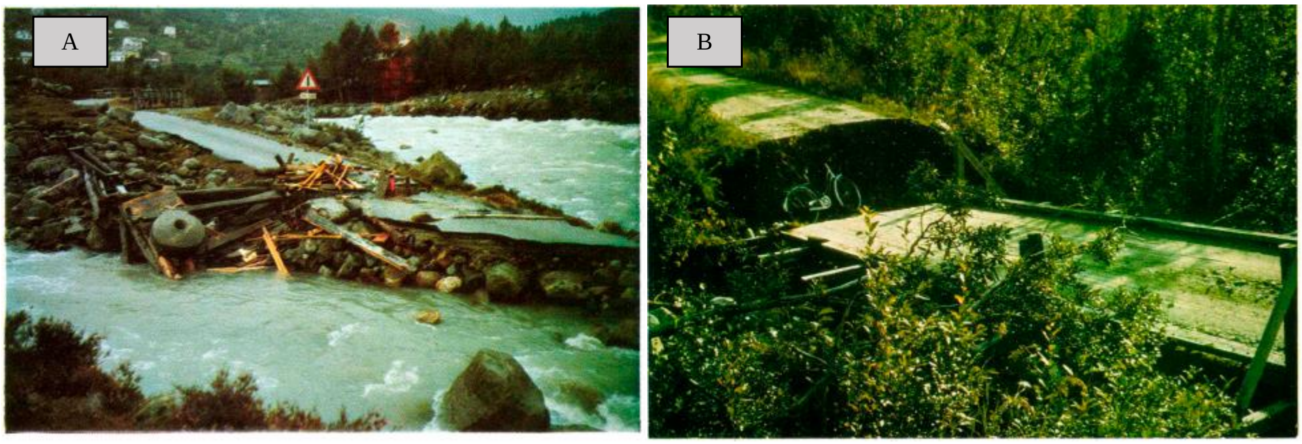

Figure 49: Photos of damage left behind by the flood in 1979 A) Breelvi breaking through the road & B) Elvekrok bridge collapse (NVE, 1981)

Affected Area 2, Section 2: The third location in the validation map that was flooded during 1979 flood is at Jostedal Camping in Gjerde. Water flow from both the rivers increases during the 50- and 100- year flood scenarios. Water in the main river rises to the range 1.29-2.05 m (Figure 49). The camp site (marked in red circle) gets completely submerged and the water levels rise to 48 cm for both the flood scenarios, causing significant damage to the camping place. According to the interview conducted with the camp owner in summer of 2021, on August 15th, 1979, the two cabins near the reception (marked in red circle) were damaged as water levels in the river rose and flooded the camping place. The guest in the newly established

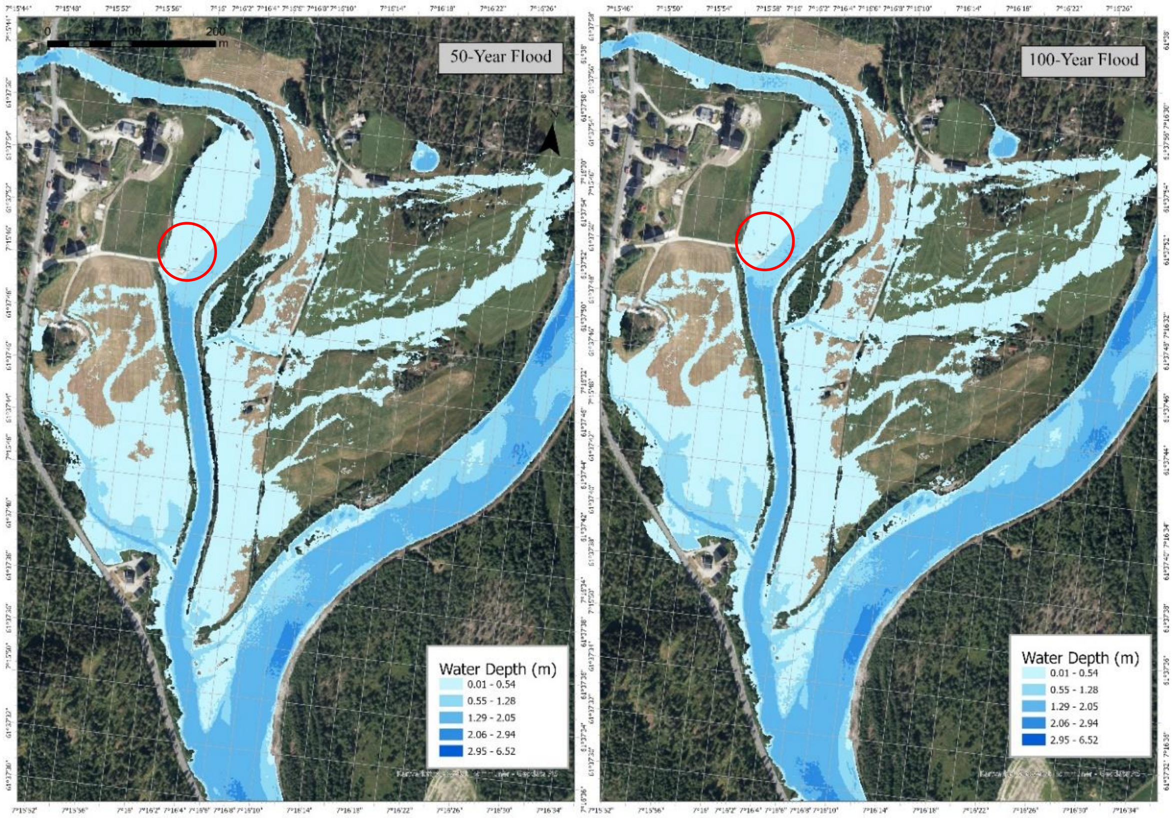

Figure 48: Reconstruction of 1979 flood at Affected Area 2 - Jostedal camping and the surrounding farms

campsite had to be evacuated immediately as the flood water infiltrated the campgrounds and the surrounding areas. As per the reconstructed simulations (Figure 49) the farm on the west side gets flooded with water levels ranging from 50 cm to 70 cm and the farm on the east side gets submerged in water with depth limiting to 50 cm. The camp owner also commented that the flood had left behind huge amount of mud and sediments as well as flooding people's homes downstream, labelling it as the most devastating experience for the community in the valley. Following the catastrophic flood, flood protections were installed in this area by NVE.

Affected Area 3, Section 2: As the flood moved downstream, it completely inundates the farms at Hesjevoll downstream of Geistedøla tributary (on the east) (Figure 50). No validation photos of this location were found; however, the flood simulations show a very high extent of damage left by the 50- and 100- year simulations. The big farm on the south gets flooded with water levels reaching up to 1.3 m and the water levels on the road along the farm gets as high as 50 cm and submerging the area around the building in the middle of the farm (Marked in red, Figure 50). Similar water level rise can be seen for the farm north of Geistedøla potentially causing severe damage to the fields with sediment, mud, and excess flood water. According to the flood brief published by NVE (1981) "*the water flooded over cultivated land, the water levels reached both farm buildings and residential houses, and roads were broken. The residents had evacuated in an emergency leaving their homes and get to safety on higher ground*".

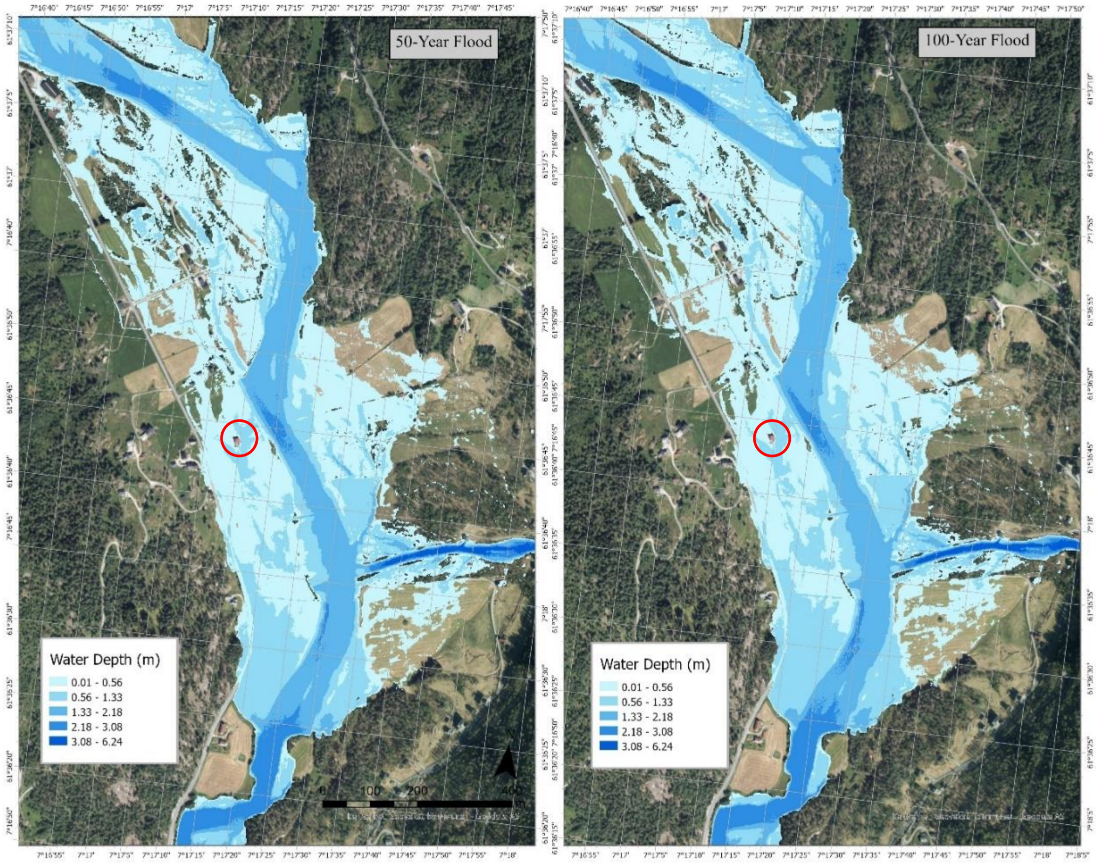

Figure 50: Reconstruction of 1979 flood at Affected Area 3- Farmland in Hesjevoll downstream of Geistedøla, Tributary 3

Affected Area 4, Section 2: The Høgebru bridge and the Sparebank building at Sagrøy suffered severe damage during the 1979 flood (Figure 52). The reconstruction of the flood in this area, represents the actual flood damage as the water levels rise in the main river and the tributary Sagrøyelva (on the west, Figure 51) to 3-6.4 m range. The water level under the Høgebru bridge (marked in yellow) rises to 3.6 m and 3.7 m during the 50- and 100- year flood simulations, leaving about 1.6 m difference before reaching the bridge. During the flood 1979, according to the NVE (1981) report, this bridge collapsed completely due to heavy water flow (Figure 52A). Since the model does not consider the erosion of the riverbanks and the effect of the sediment load, it is hard to assume whether the bridge collapses from the simulations.

Nevertheless, the extreme impact of the Sagrøyelva can be seen in the simulations, as the water levels in the tributary rises it flows into the property to the north (marked in red, Figure 50). Proceeding the extreme rainfall on the night of 14th August 1979, the water levels in the tributary rose drastically, Figure 52B and 52C shows pictures of the Sagrøyelva river flowing through the basement of a Sparebank building and flooding the entire front of the building, which is also evident in the simulations.

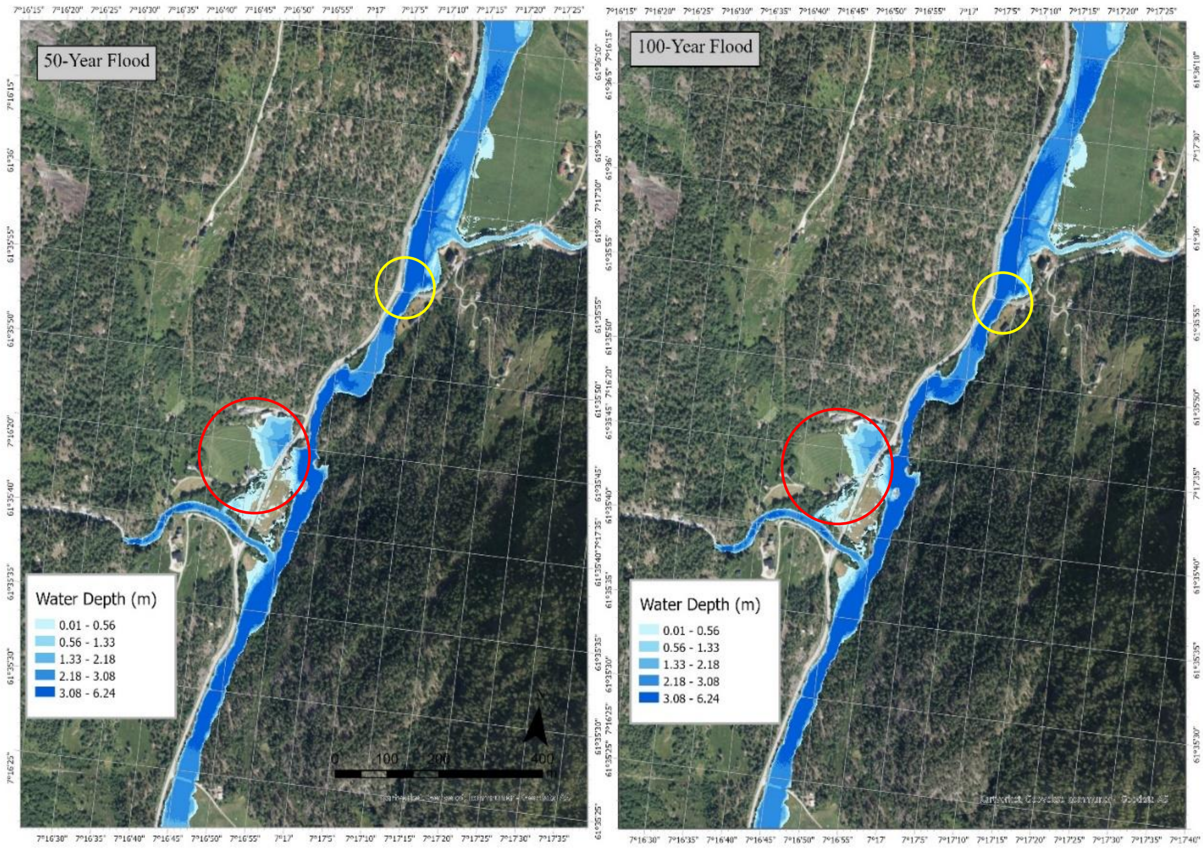

Figure 51: Reconstruction on 1979 flood at Affected Area 4- Høgebru Bridge and Sparebank building near Sagrøyelva (Tributary 5)

Figure 52: Damage left behind by 1979 flood at Sagrøy: A) Remains of Høgebru bridge (Photo: NVE, 1981), B) Sagrøyelva flowing through building basement (Photo: NVE, 1981), C) Damage left behind by Sagrøyelva (Photo: Hoel, 2013)

Affected Area 5, Section 3: The 4th location on the Validation map is at Sperle. During the flood, this location had 2 affected areas, at the bridge (marked yellow, Figure 53) and the farmland (marked red, Figure 53). According to the simulations of 50- and 100- year floods, the water under the bridge goes up to 2.5 m, the same bridge during the 1979 flood collapsed and sank (Figure 54A). The farmland, however, recreates the same scenario as the reality. As the water levels in the tributary 7 (on the west, Figure 53) rises to 14.8 m, with a river depth of 5 m and a narrow width, the water floods the surrounding area, leading to huge volume of water flowing into the farmland. Figure 54B shows a photo taken few days after the flood, the crops from the field were washed away by the flood and got trapped in the fences. The red marked area in Figure 53, is potentially the location of the fences and the crops fields.

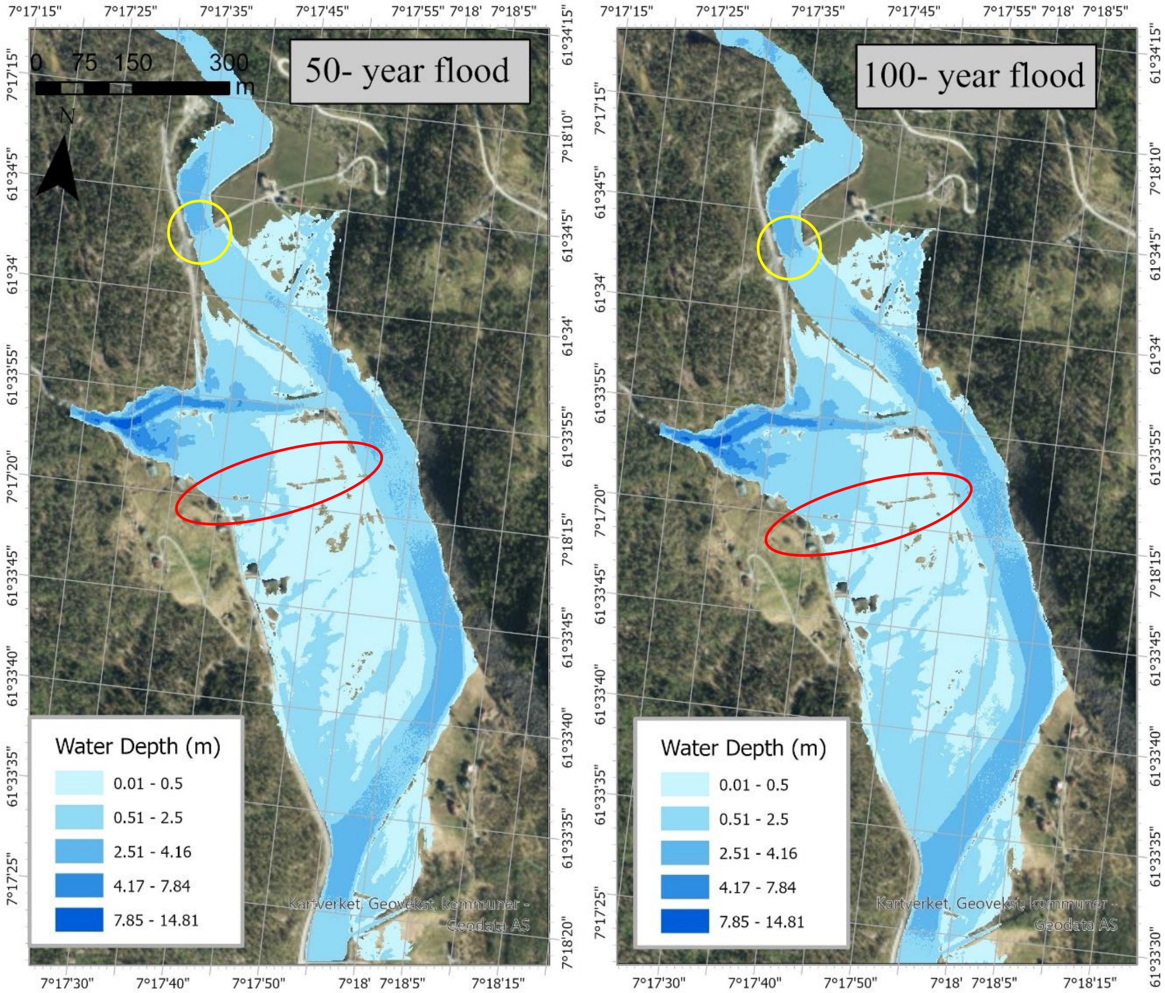

Figure 53: 1979 flood reconstruction at Affected Area 5, bridge, and farmland at Sperle

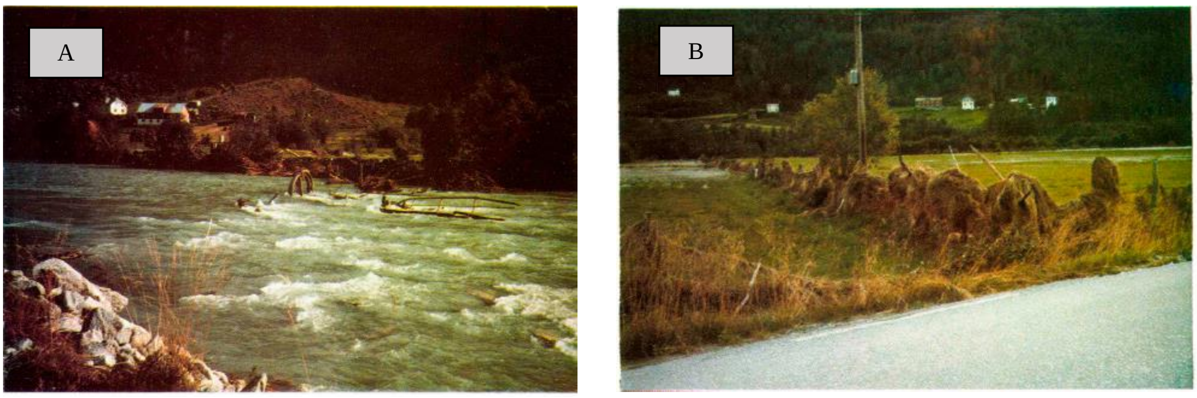

Figure 54: Photograph of A) Broken bridge over main river and B) Crops carried by the flood caught in fence (Photo: NVE, 1981)

Affected Area 6, Section 3 & 4: The 5th validation location along the river that was at Fossøy, where the flood markers in the valley is located. The red marked area is where the flood marker (Figure 55) for the 1898 and 1979 floods are located (Figure 56). The reconstruction simulations yet again, matches the actual flood scenario. The farm next to the marker gets completely flooded with water levels ranging from 20 cm to 80 cm. During the 1979 flood, the water in this area rose to 2.35 m (Figure 56), however, in the reconstruction the maximum water level goes up to 1.74 m next to the flood marker and the water levels in the rises to 4.16 m. The flooding in this area occurred mainly due to the bottle neck after the marker, as the water in the river got stuck in the narrow curve, the water on the upstream flooded the farm and the houses.

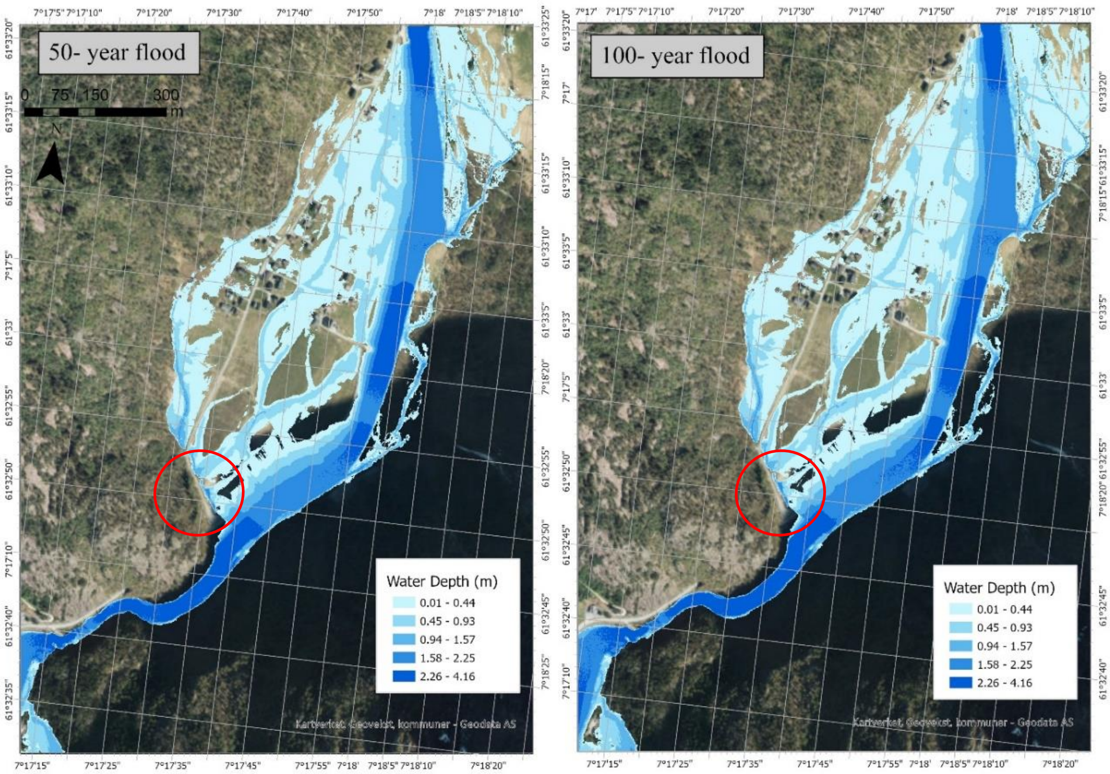

Figure 55: Past reconstruction of 1979 flood at Affected Area 6, Flood marker at Fossøy

Figure 56: Flood marker of Jostedalen at Fossøy, (Photo: Barnhaugen Media)

Affected Area 7, Section 4: The private properties and the smaller farmlands at Fossøy after the marker, were the 6th location along the valley that suffered severe damage from the flood. from the simulations of 50- and 100- year floods (Figure 57), the two farms on the east were complete flooded with water levels rising between 0.94 - 2.5 m. Figure 58 shows an image of post flood farmland and a farmer standing on his wrecked land with the bridge in the back broken and disconnecting him from the main road. This image is from on the two farms marked in Figure 57. Though the damage to the bridge was not simulated in the model but the water under the bridge rose to 2.8 m, and the bridge itself was only 60 cm above the flood levels.

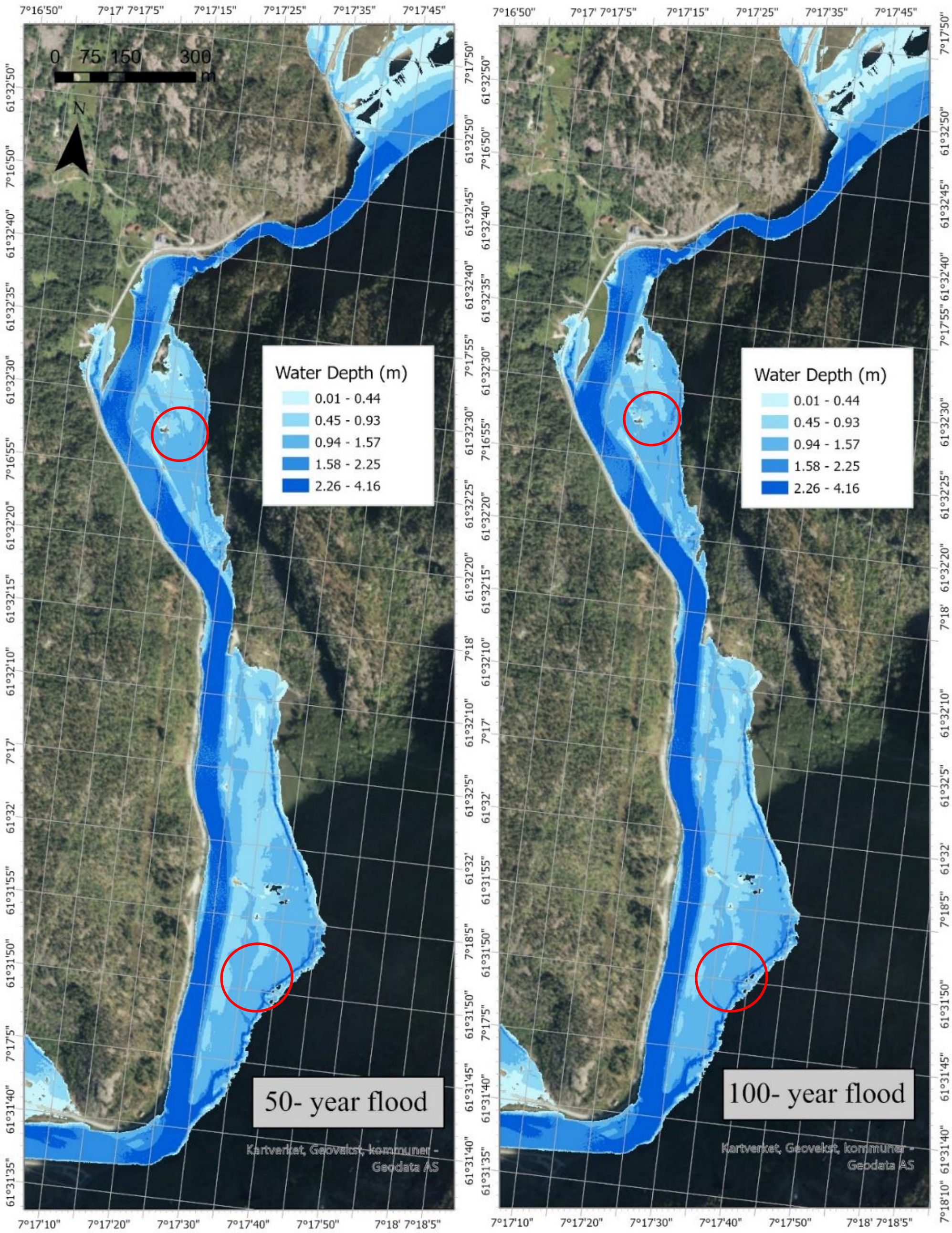

Figure 57: Reconstruction of 1979 flood at Affected area 7- farms at Fossøy

Figure 58: Photo of a farmer standing by his destroyed land (NVE, 2018)

Affected Area 8, Section 4: The next affected area on the validation map is at Myklemyr (Figure 59). This area had gone through flood mitigation modification due to the damage left behind by the 1979 flood. The simulations for reconstruction show that majority of the area was flooded with water level 0.45- 1.30 m. The photo in Figure 60, shows the ruins left behind by the flood at Myklemyr, this could be one of the two marked area on the map, Figure 59. The post flood brief from NVE (1981) mentions that one of the households could not evacuate in time, therefore by the time they were leaving, the water levels around the house were already too high and they had to stay inside overnight and could not leave.

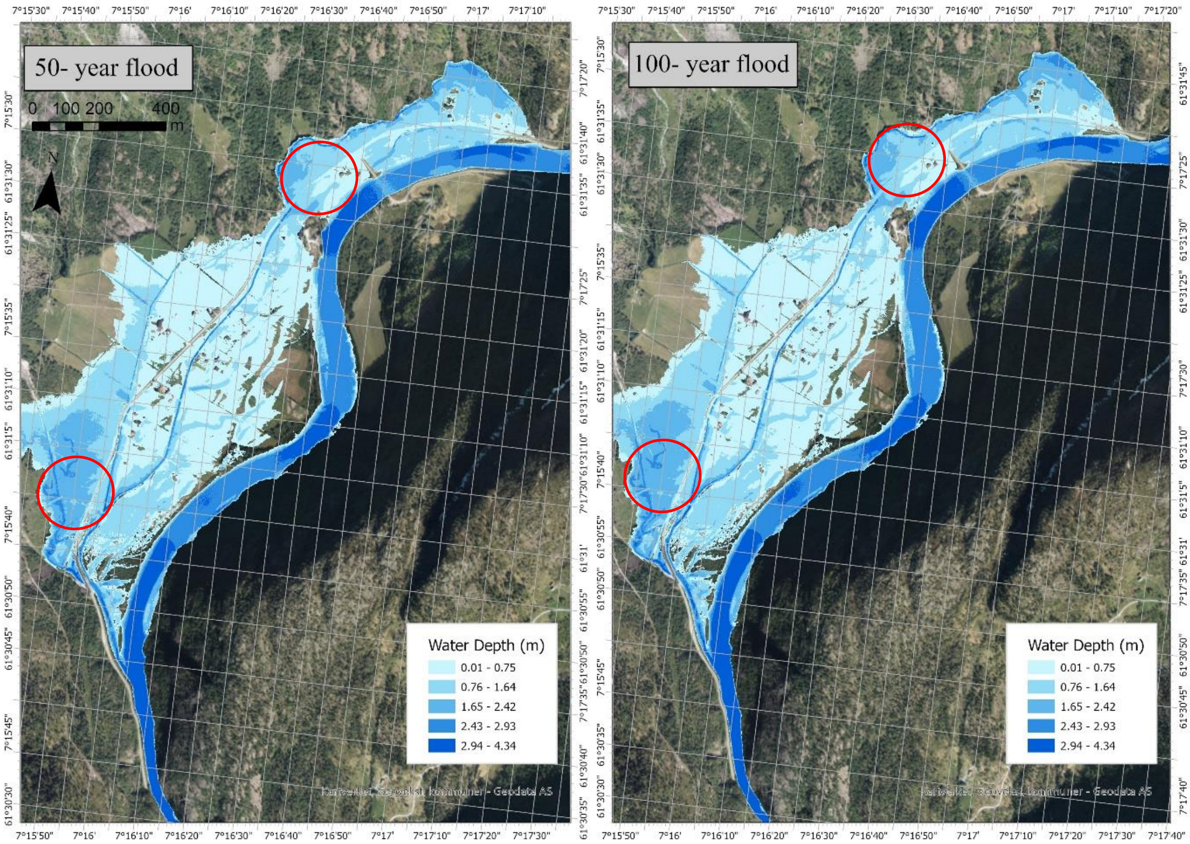

Figure 59: 1979 flood at Affected area 8- flooded farms at Myklemyr

Figure 60: Damaged land near Myklemyr after 1979 flood (Photo: NVE, 1981)

Affected Area 9, Section 5: The bridge near Myklemyr station at Husøy (Figure 61), was a particularly well documented site, since the NVE gauging station was located here. The water flow during the flood in 1979 was recorded to reach 409 m^3/s, prior to the water levels in the river rising so high that the station could not record anymore (NVE, 1981). In the 50- and 100-year reconstructed flood simulations, the maximum water flow was 374 m^3/s and 398 m^3/s the at the station, respectively. Next to the station the peak flood water levels were measured to be 6 m in 1979 and in the simulation, it went up to 3.10 -3.20 m for the 2 floods scenarios.

The Bridge at Husøy was one of the broken bridges during the flood in 1979. In Figure 62A the broken bridge can be seen from an aerial photograph. The close-up photo (Figure 62B) shows that the foundation of the bridge was severely eroded causing the bridge to collapse. The photos are from the marked region in Figure 61. In the simulations for the reconstructed floods, the damage to this area is not so visible (Figure 61), the water levels under the bridge at Husøy rises to 2.7 m for 50-year and 2.8 m for the 100- year floods, leaving a 4.2 m distance between the water levels in the river and the bottom of the bridge.

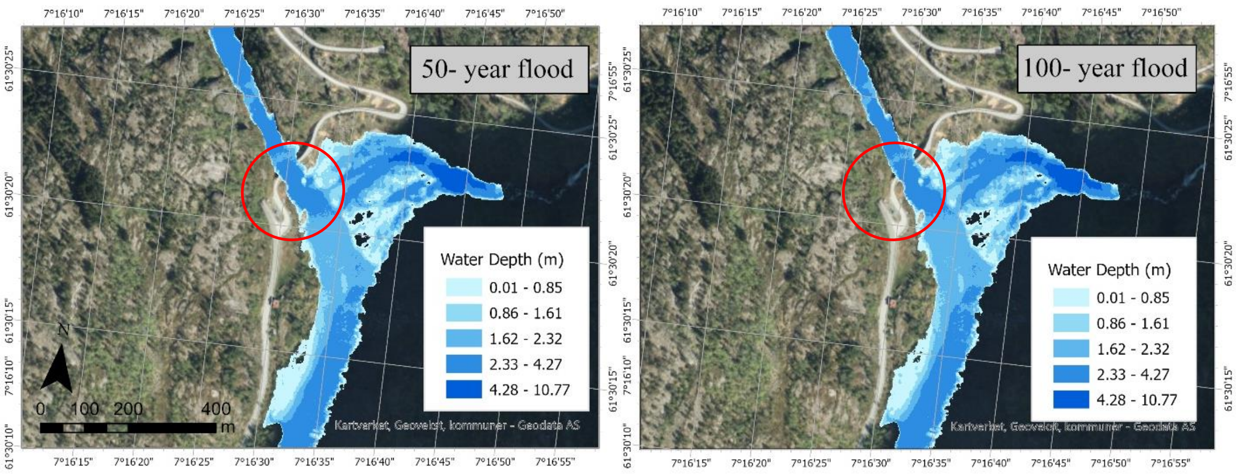

Figure 61: Flood reconstruction at Affected area 9 -Bridge at Husøy and Tributary 8 next to Myklemyr gauging station

Figure 62: A) Aerial image of broken Bridge at Husøy B) Close-up of remains of the bridge (Photo: NVE, 1981)

Affected Area 10, Section 5: As the flood passes through Husøy causing the bridge to collapse, the flood water flows into Alsmo (Figure 63). As the flood moves downstream, it flows into the main road causing the water levels on the road to rise to 40 cm (marked in red, Figure 63) in the simulations. Figure 64A and 64B are a picture taken 2 days after the flood, showing the eroded and broken roads near Alsmo. The farm and private property on the west get completely flooded with water levels getting as high as 2 m (Figure 63). The front of the houses leading to the main road gets blocked with water and the waterbodies on the west filled up with 2.6 m of water.

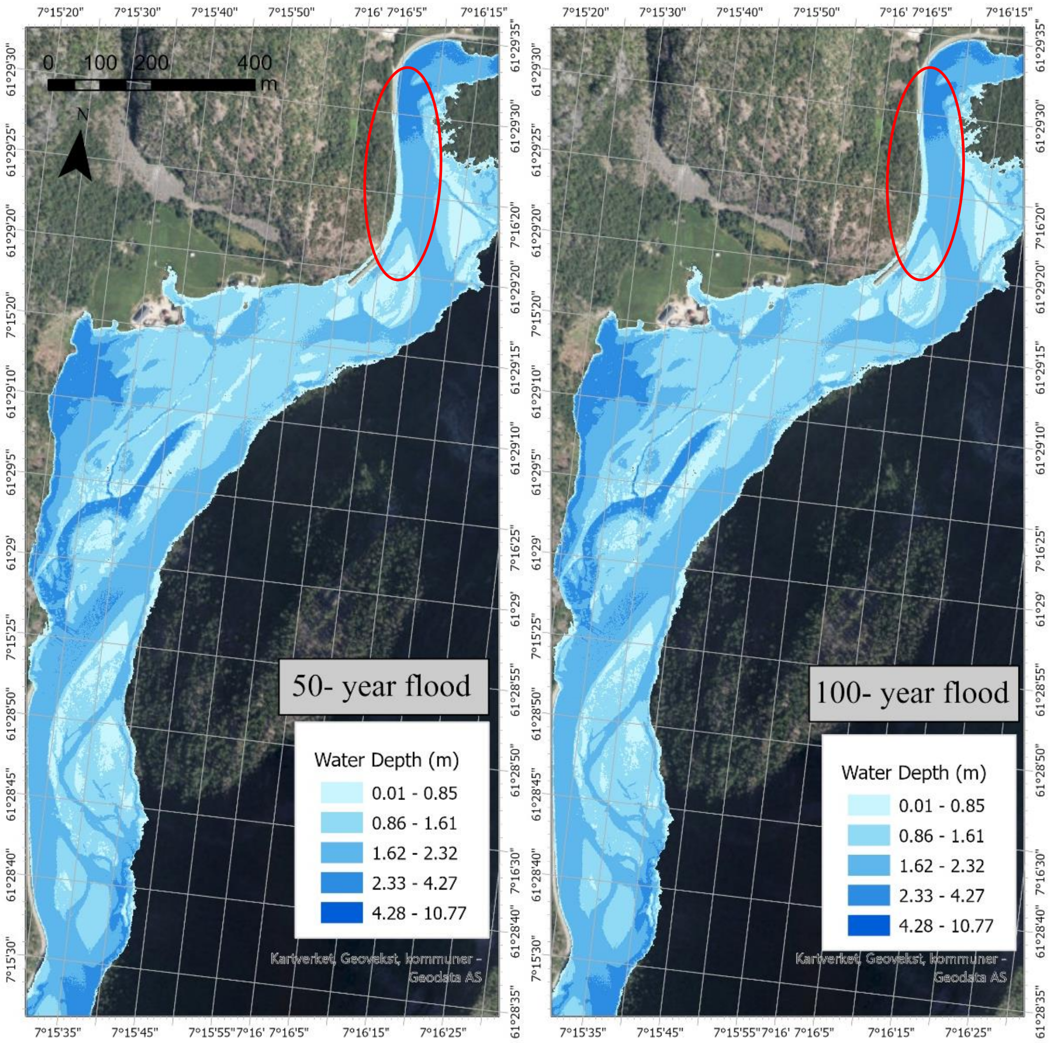

Figure 63: Affected Area 10- Road and Farmland at Alsmo

Figure 64: Main Roads eroded by the flood in 1979, (Photo: NVE, 1981)

Affected Area 11, Section 6: The affected Area 10, is the end of the river Jostedøla in the town of Gaupne. As per the flood report by NVE, this area suffered the least amount of damage during the 1979 flood. Figure 65 shows the reconstruction of the past flood; however, most parts of this area did not exist 43 years ago. Figure 66 is an image showing the aerial photos of Gaupne from 1966 and 2019, the settlements were not as dense as it in the present and most of the area was still part of the fjord. Therefore, the simulation in the southernmost part of the map, do not represent the past scenario. However, the eastern part of the did exist in 1979, and the flood simulations for both 50- and 100- year floods, show water infiltrating the parts of town, which in the past were farmlands (Figure 66). The water levels go up to 1 m in some places but remain below 50 cm throughout.

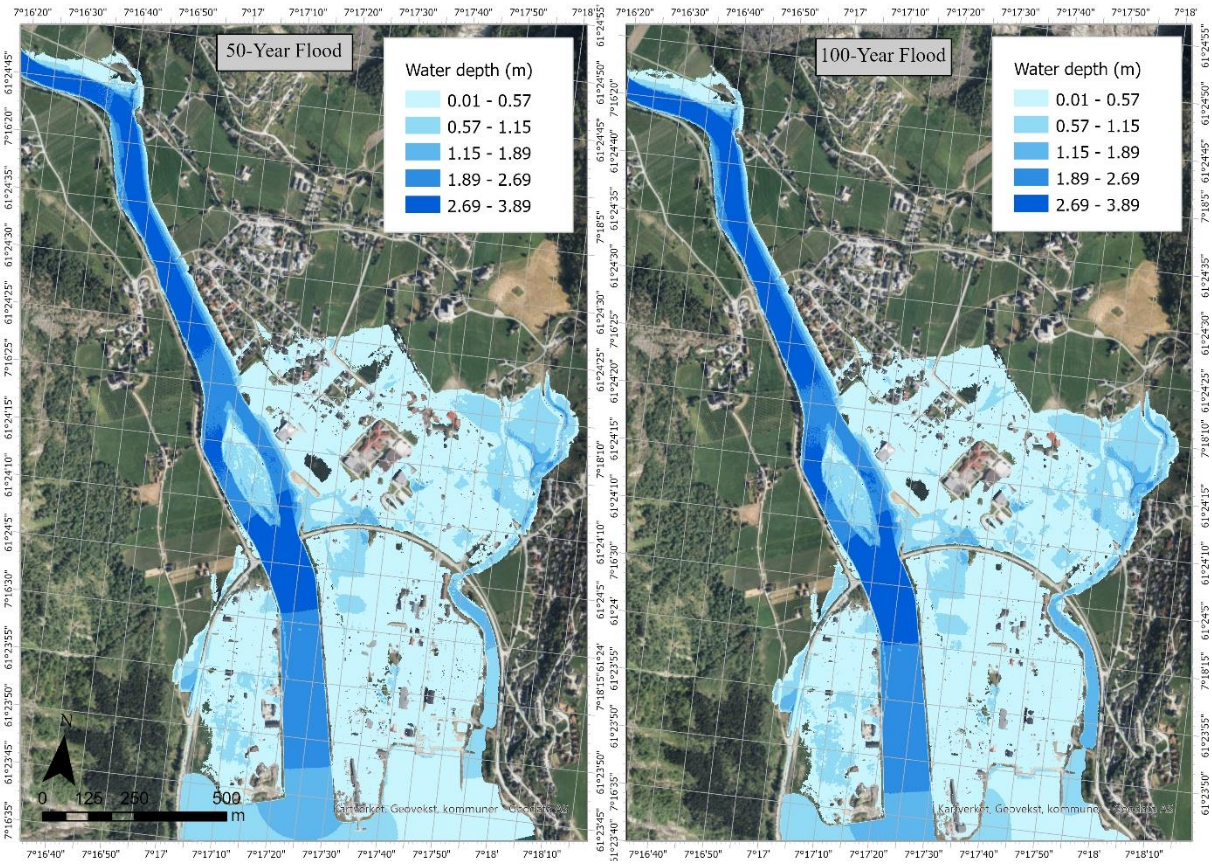

Figure 65: Affected Area 11- 1979 flood reconstruction at Gaupne

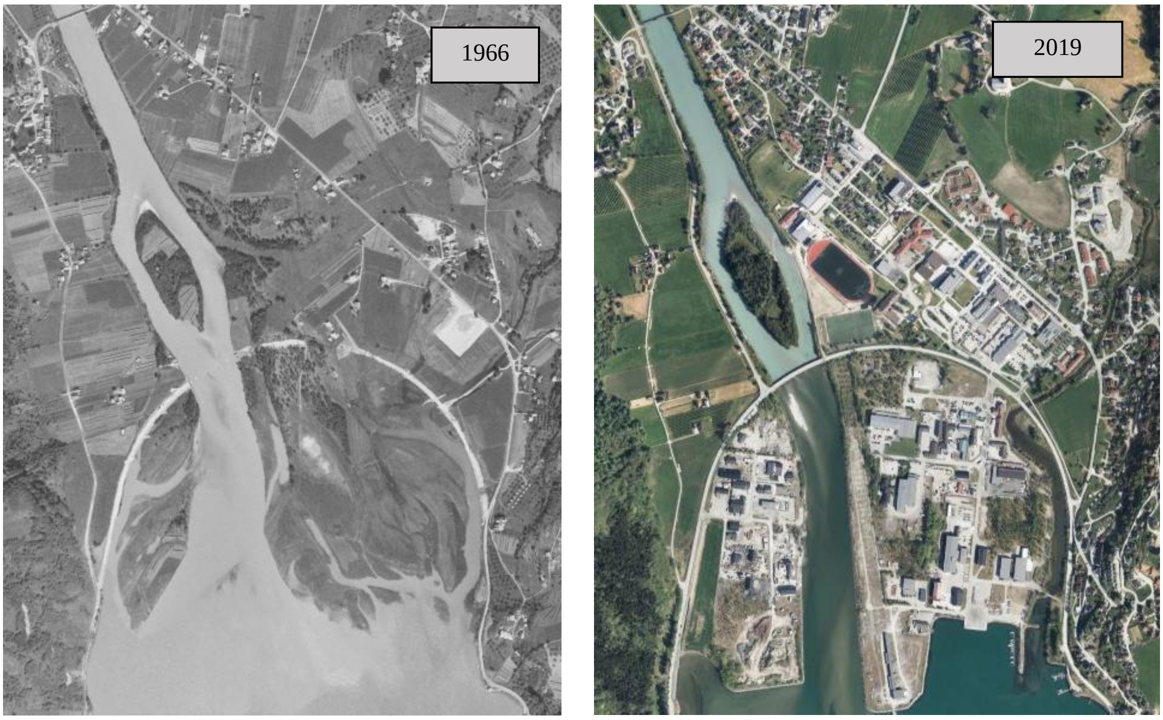

Figure 66: Aerial photos of Gaupne from 1966 and 2019 showing land use change (Photo: Norge i Bilder)

4.2 On the efficiency and effectiveness of the flood protection installations against future floods in Jostedalen

Following the most devastating flood in Jostedalen, several flood mitigation measures were taken by NVE to protect the valley and the community against further damages. Most of these mitigation measures included erosion protection and levees on the riverbanks (Figure 46) (NVE, 2022b). This section will discuss about the efficiency and the effectiveness of the flood protection measures installed along the valley. Based on the results from chapter 3.2 and the flood reconstruction in 4.1, this sub-chapter will focus on which protection measures are effective against the future high magnitude flood and which are ineffective against major and/or minor floods.

Maintaining the same order as the previous sections, the discussion will flow as the river flows downstream from the Junction of Breelvi and Jostedøla to Gaupnefjorden. The flood protection installed near the Nigardsbreen Camping at the junction of Breelvi and Jostedøla, are in the northern part of the camp (Figure 46), which has no protection to the camp itself from the two rivers. In the present-day minor and major flood simulations in sub-chapters 3.1 & 3.2 and the past reconstruction in 4.1, the camp is flooded near the southern banks in every scenario, therefore, this location is at risk and might need flood protection installations from minor 10- and 20- year floods (Figure 24C and 24D), as well as high magnitude 50-, 100- and 200- year floods (Figure 34).

The first location where the flood protection has been effective is at the Jostedal camping place in Gjerde. From the reconstruction of the past flood and the interview of the camp owner, it was evident that the high intensity 50- and 100- year floods greatly impact the camping place, submerging the entire campground. Nevertheless, after the installation of flood protection measures, this scenario changed. Simulations over the present-day terrain in chapter 3.2, provided evidence that the damage caused by the high intensity floods drastically decreases (Figure 35 (after protection) and Figure 49 (before protection)). The extent of water infiltration is not as far as it was in 1979 and the water levels go up to 31 cm during the highest flood value near the riverbanks, where there is opening for river rafting kayaking activities. The flood protection, however, do not work as well for the two farms on the west and the east. Even though the extent of flood is less with lower water levels during the high magnitude floods of 50-, 100-, and 200- year compared to the past flood, it is not completely protected. During the field visits in 2019 and 2021, the erosion of the riverbank and the flood protection installation was evident. While interviewing the camp owner, she said that some economic supports have been provided by NVE and the municipality to pave the riverbanks, but they could only help so much due to limited finance. The authorities suggested that maintenance must be done on personal finances, therefore a lot of money was invested on paving the riverbanks and to reduce costs rocks were brought from construction sites in the area.

The farm at Hesjevoll downstream of Geistedøla, has had flood protection installed since the 1979 flood (Figure 46), however, they have proven not be as efficient from the flood simulations. Even with low intensity median, 10- and 20- year floods (Figure 26), the farms get submerged with water levels 0.5 m to 2 m, with increasing intensity. As the higher intensity 50-, 100- and 200- year floods occur in the area, the impacts get worse with the flood moving further north, inland towards farm and the main road (Figure 36). Therefore, this is another location which is at high risk from floods and flood protection systems need to be upgraded.

The location of old Sparebank building next to Sagrøyelva tributary is the most terrain modified location along the river. Figure 67A shows the aerial image from 1964 of a small stream (Marked in red) flowing from Sagrøyelva into the private property. Given the destruction caused due to this stream (Figure 52B and 52C) in 1979, it was blocked off completely and covered with vegetation to mitigate any future flood being initiated through this stream. In the reconstruction, In the past reconstruction, Figure 51, it was very prominent how much this stream contributed to the flooding. However, in the present-day simulation without the stream (Figure 37), there was no impact in the same location from the high intensity floods. Therefore, blocking off the stream for flood mitigation works really well.

Figure 67: Aerial images of modified stream from Sagrøyelva

Similar to the farm at Hesjevoll, the farms at Sperle also have flood protection installed by the riverbank (Figure 46). And the same flood pattern can be seen at the Sperle farm as the Hesjevoll farm. The farms get flood even with minor 10- and 20- year floods, with lower levels water (Figure 28), as the major floods approach, the water levels increase to 85 cm (50- year simulation), 97cm (100- year simulation) and 1 m (200- year simulation), as well as increasing in extent (Figure 38). All the farms are extremely vulnerable to the even the minor floods. The tributary 7 is a huge liability to the area even with the flood protection along its banks. Thereby, a significant upgrade and maintenance of the flood protection installations is required in Sperle.

Further down the valley at the Flood marker in Fossøy, the flood protection works well for the farm and the housings in the area (Figure 38), for the high intensity floods. The same area was severely flooded in the reconstruction (Figure 55). However, the scenario is different for the lower part of the area where the flood reaches the bottle neck near tunnel (south of figure 38 and northeast of Figure 39), the higher magnitude floods impact the small region near the marker. In the present scenario with the flood protection, the water cannot move into the field, therefore in the main river, the depth increases causing the water to overflow as it reaches the bottle neck by the tunnel, and water floods into the marker area, with a small opening next to the road (marked in red Figure 39). The water levels at the marker up to 2.23 m and 2.70 m during the present day 50- and 100- year simulations compared to the past reconstruction, where it went up to 1.74 m for both floods, and for the 200- year it goes up to 1.84 m. Therefore, the protection before the tunnel is now as efficient for high intensity floods, as it is in the upper regions of Fossøy.

Due to the damages done by the 1979 flood in the two properties in Fossen, after the flood marker in Fossøy, flood protections were installed on the riverbanks (Figure 46). The flood protection, yet again, are not as effective against the minor and the major floods. Both the small fields and the settlement on the east gets flooded with 0.01-0.70 m water during the median, 10- and 20 year flood simulations (Figure 29) and as the floods intensify to higher magnitudes, the extent of flood increases and water levels rise to 1.8 m (Figure 39).

The most effective and efficient flood protection installation is at Myklemyr. No results or output of the farms at Myklemyr were presented in the sub-chapters 3.1 and 3.2, because neither the minor nor the major floods showed any impact on this area. However, once the flood protections along the banks of Myklemyr were removed for the reconstruction of the 1979, the impact was prominent (Figure 59). The entire area was submerged in water during the 1979 flood, therefore flood protection along the banks were installed by NVE (Figure 46). An overview of the minor and major flood simulations is presented in Figure 68. Compared to the results of the reconstruction in Figure 59, the 10- to 200- year flood simulations show almost no impact in this area. Therefore, the protective installations at Myklemyr are a great example of effective and efficient protection measure and maintenance efforts.

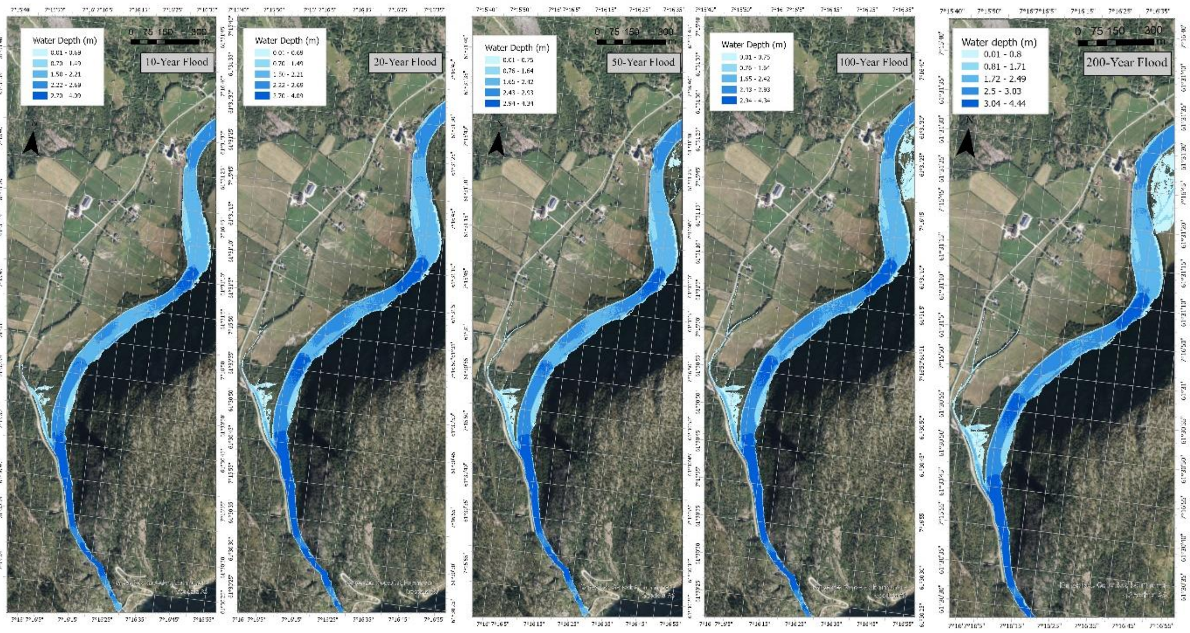

Figure 68: Minor and Major flood simulation outputs at Myklemyr, a positive impact of flood mitigation measure

The flood protection along the road and farm at Alsmo, do not response the best during the flood simulations. From the sensitivity analyses with minor floods in 3.1, it seems the roads get flooded from the main river; however, the farm gets flooded mostly from the waterbodies inland (Figure 32). Nevertheless, the water bodies are connected to the main river. As the floods intensify with higher magnitudes, the extent of damage increases as well as the water levels (Figure 42). Therefore, this is yet another location at risk from both minor and major floods and needs upgrading and maintenance of the flood installations.

The last location in the valley where the flood protection installations are located is at Gaupne. This location is of particular interest since parts of the town did not exist during the flood of 1979, therefore the protection measures are placed based on the areas that were affected in 1979 (Figure 65). The north-eastern part of the town was flooded based on the past reconstruction, as discussed in 4.1, this area was mostly farmlands, and from Figure 46 we can see that protection measures are installed on the riverbanks before the curved bridge until which the town was developed. Based on the Minor and Major flood simulations (Figures 33 and 43), it is evident that the southern part of Gaupne is at risk from all the 6 flood scenarios and need significant flood mitigation measures to avoid severe damage to the town and the community.

4.3 Testing resistive capacity of Hjelledalen by installing flood mitigation measures

Given the successful outcome of the terrain modified set-up of Jostedalen in 4.1, where the HEC-RAS model recreated the past flood by removal of flood protections, the study tried to implement the same set up to Hjelledalen by installing flood protection levee along some of the riverbanks to analyse whether they would be effective. From the NVE Atlas, few flood protection installations were identified near the Folva, at the Videdøla and Sunndøla meets. From the outcomes of 3.3 it was evident that the flood protections in upstream of Sunndøla (Figure 69), were quite resistive against the floods. The first mitigation measures were implemented in Sunndalen was in 1962 and 1969 (NVE, 2022b), according to the interviews with the farmer and an ex-employee at the museum, these mitigation measures have not been maintained since then. The valley downstream towards Hjelle is vulnerable to high magnitude floods even with the existing flood protection in the region (Figure 69). Therefore, based on the simulation for 3.3, some breaches were identified along the riverbanks (marked in red Figure 69) and levees of 1-2 m were added along the breaches in the river starting from the junction of the two rivers until the end at the fjord to see whether flood protection in these locations are the effective against high intensity floods. Most of the breach identified in the simulation has vegetation along the terrain which provides protection against floods and erosion even without having any artificial infrastructure (Esfahani & Keshavarzi, 2010). Therefore, the height of 1-2 m suggest levees could be even lower if the riverbanks already have vegetation, since the model is based on DTM and not DEM (which includes vegetation over the terrain), the vegetation is not taken into account.

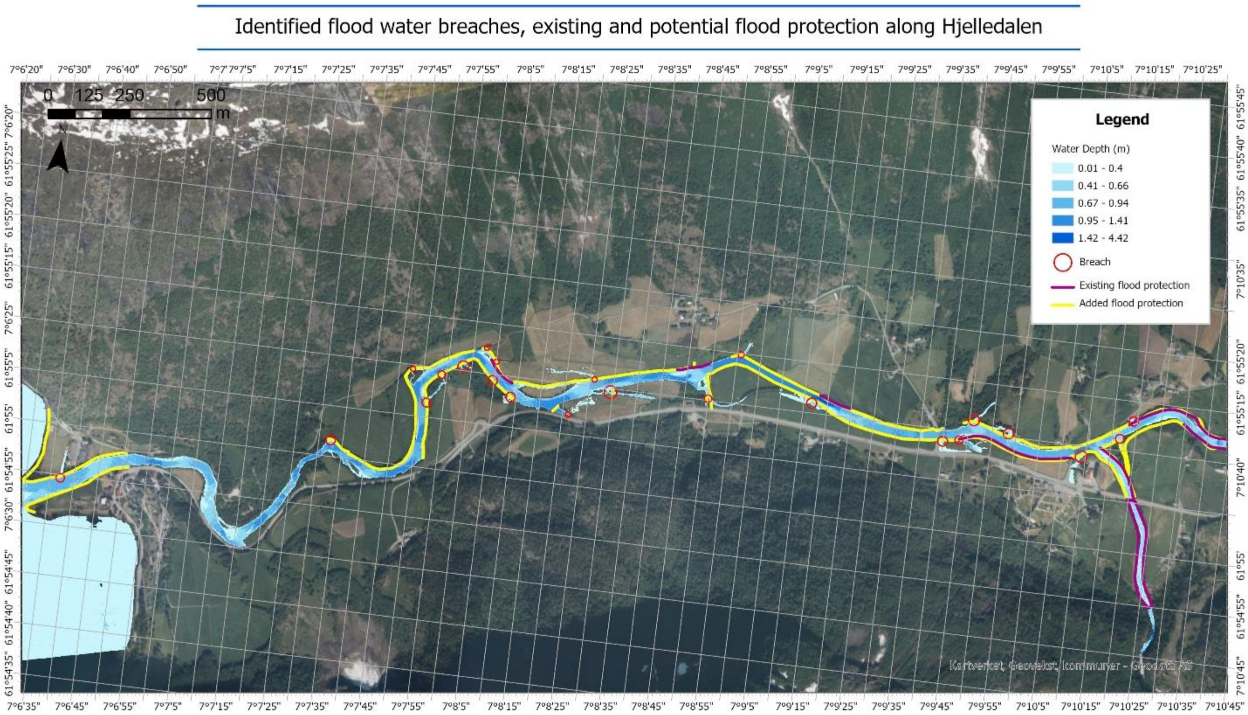

Figure 69: Identified flood breach zones, existing and newly added flood protections along Hjelledalen

Figures 70 and 71, shows the scenario of the high intensity floods at Folva and Hjelle after adding the flood protection along the river. The inundations simulated in section 3.3 decreases significantly but not completely. The water levels in the farms on the north near Folva, has decreased in extent and the water levels remain in the lower ranges for the 50-year flood, however as the floods intensify, the levees do not work as well, and the water levels rises to the higher ranges (up to 2.5 m in 200- year flood) yet the extent in limited near the riverbanks (Figure 70). On the southern part near the Folva adventure camp the flood protection along with the existing protection at Sunndalen (marked in purple in Figure 69) seem to work well for all the three scenarios, the flood, however, still infiltrates the area downstream, the water levels remain below 50 cm in most places and goes up to 70 cm near the banks. The water in the main river goes up to 4.16 m in the narrowest part of the river, causing the flood in the downstream through the channel in the farm in the west. Given the lower frequency of occurrence of these large floods, the water levels in most parts are quite manageable.

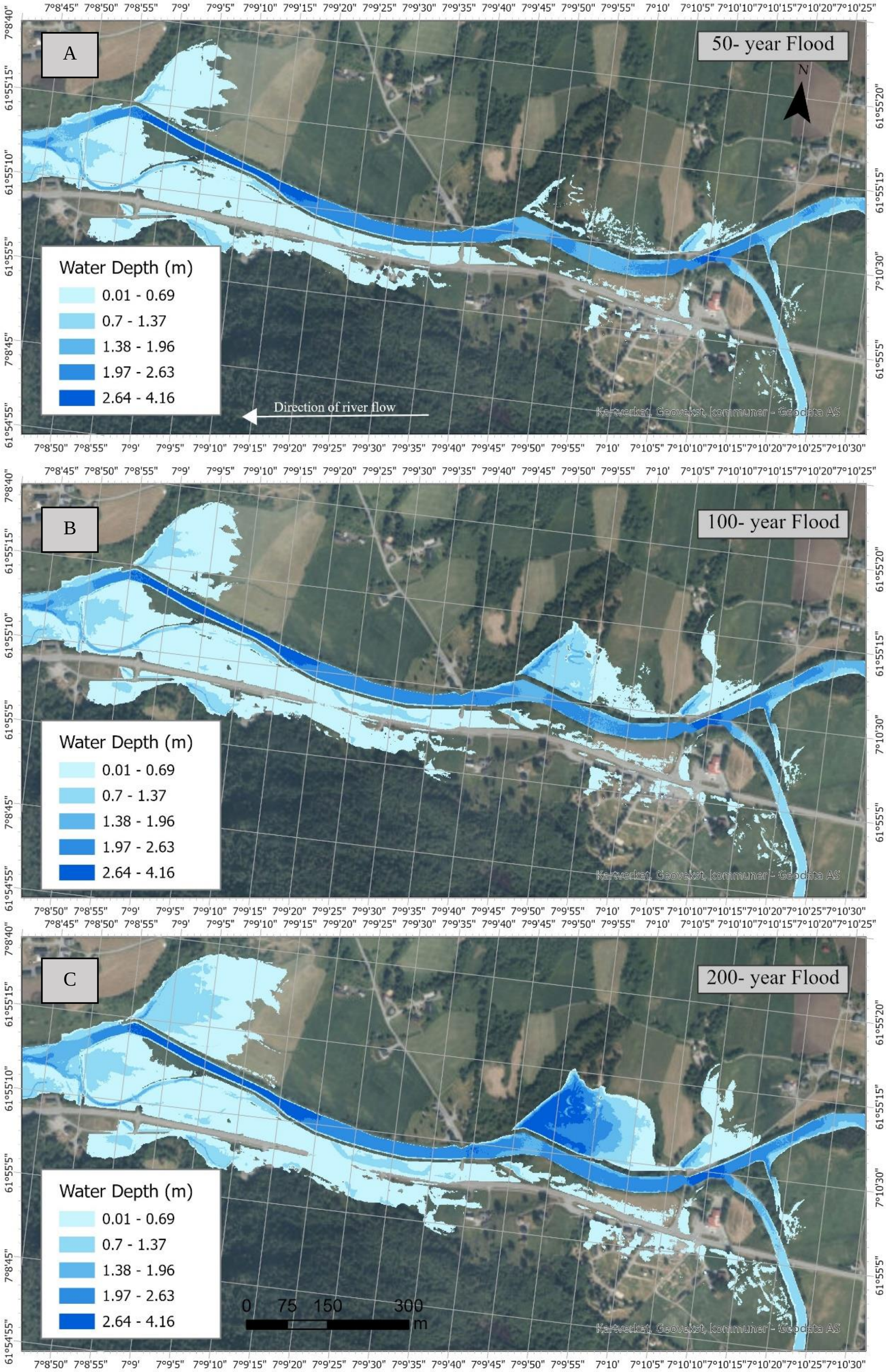

Figure 70: A) 50-, B) 100- and C) 200- year floods at Folva after installing flood protection along the river

As the flood moves downstream (Figure 71), the water is contained within the river for the farm on the northeast before the river starts to meander. As the river goes through the curves, the flood water takes longer to pass through, therefore, failing the levees and flooding the two smaller farms, however, the water levels in the southern farm rise to 70 cm for the 3 floods and levels in the northern farm stay within 50 cm. Given the flow of the river in this location, it is quite difficult to analyse how well the flood protections will respond, however, with increased vegetation cover along the banks, the impact to the fields can be reduced. The most effective flood protection in the valley seems to be at Hjelle near the school and the football field, where adding flood protection of maximum 2 meters can protect the entire area against the high intensity floods.

During the interview with the farmer at Folva, he mentioned that the floods during autumn have the biggest impact on the valley and mitigation plans having been going on to prevent the ‘normal’ floods but not the major floods, by normal flood its assumed that he talks about the minor floods. These mitigation plans were supposed to be implemented in Autumn of 2022 in Sunndalen, which is valley near Sunndøla. He also mentioned that the main problem is the sediments carried by the river during the floods that builds up in the riverbed and causes the water levels to rise. The most impactful floods occur in the autumn causing the water levels in Videdøla and Sunndøla to rise, these floods are using followed by snowmelt and heavy rainfall. He was also particularly interested in knowing how the valley would react to high intensity floods, especially in the downstream since that’s the area that has suffered more historically. The flood in 1953 was a particularly damaging one in the valley. The ex- employee from the national park validates the information given by the farmer, saying that following the flood in 1953, NVE tried to build riverside mitigation walls, to prevent future damages. The flood protection measures however has not been maintained or upgraded much since then.

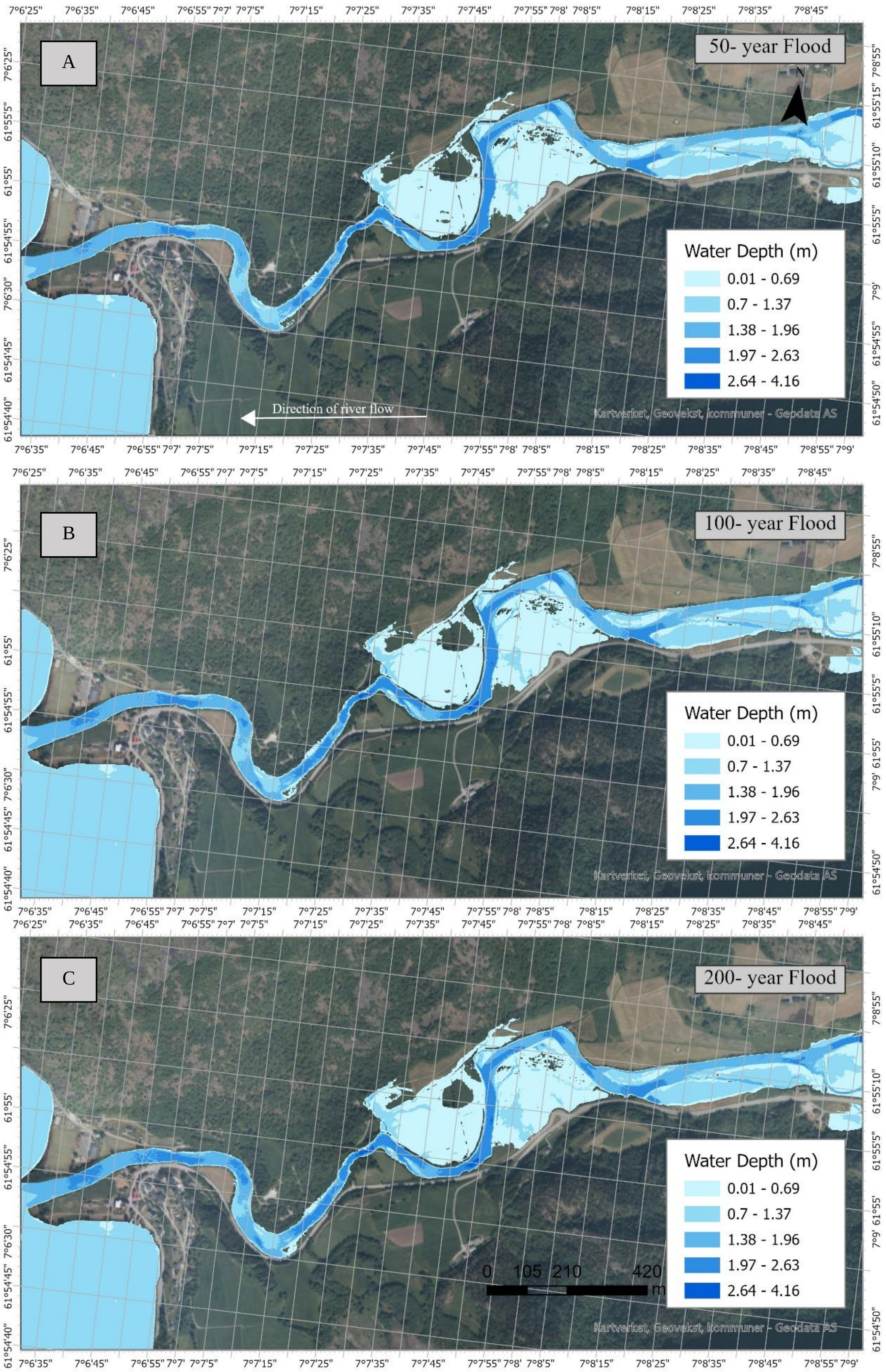

Figure 71: A) 50-, B) 100- and C) 200- year flood at Hjelle after installing flood protection along the river

5 Conclusions

This study has zoomed in on the catastrophic flood of 1979 in Jostedalen to create a bridge between the past and future and identify the areas at risk from future minor and major floods on both northern and southern sides of the Jostedalsbreen National Park. To compare the levels of preparedness to future floods in the valleys on both sides of Jostedalsbreen, the study has designed numerical experiments featuring a wide range of flood scenarios in the Jostedalen and Hjelledalen valleys with the HEC-RAS hydrological model. These experiments use high-resolution digital terrain models (DTMs), gauging station measurements and regional flood flow analysis of 2018 RFFA-2018 data to evaluate the sensitivity of different sectors of the valleys to minor and major floods, including future and past flood scenarios. Within these scenarios, diverse modification tools have been applied to either eliminate or incorporate flood protection systems and terrain changes within the valleys and in this way test their flood mitigation potentials. The newly engineered protection measures in the simulations have been adapted from existing constructions installed by the Norwegian Water Resources and Energy Directorate (NVE) in both valleys.

The outcomes of the sensitivity experiments for Jostedalen show that certain areas within the valley are at risk even from minor floods, albeit with low impacts on the community and non-hazardous water levels. These areas include a small part of the Nigardsbreen camping, farms at Hesjevoll and Sperle, housings at Fossøy and the low-lying part of Gaupne in immediate proximity of the fjord. As flood events intensify and larger magnitude floods occur in the valley, the extents of flood damage increase drastically with high water levels throughout many populated areas, regardless of the existing mitigation measures. Both camping places in the uppermost impacted areas get flooded, although water levels remain low and are restricted to the vicinity of riverbanks. In contrast, farms at Hesjevoll, Sperle, Fossøy and Alsmo get significantly inundated under high-magnitude scenarios when compared to the impacts of minor floods. As well as in the above-mentioned areas, the risks of flooding also increase in the main town of Gaupne.

On the northern side of Jostedalsbreen, in Hjelledalen, a high probability of land submergence and significant damage from high magnitude floods was discovered. Here, the numerical experiments with extreme hydrological forcing have tested the levels of resistance of the valley to major floods and have identified two areas prone to high impacts at Folva and Hjelle. Farms near the Folva camping place and the camp itself get easily flooded along with the downstream farms at Hjelle and the school football field near the fjord.

The model-based reconstructions of the 1979 flood have tested relative functionality and effectiveness of flood protection measures along the valley. The flood mitigation installation at Myklemyr has proven to be most effective since it prevents flooding of the area in all minor and major flood simulations. However, both the model-based reconstruction and the documentation from the past event show that this area was severely damaged by the historical flood that is again pointing at the significant and importance of these installations. This contrasts with the flood mitigation measures at Hesjevoll, Sperle, Fossøy, and Alsmo all of which clearly require extensive upgrades and maintenance since these locations get flooded in almost all simulations, regardless of the flood intensity. Given the development of a new town's district near the fjord, major flood protection installations are required in this part of Gaupne. In comparison to the flood mitigation measures on the southern side of the Jostedalsbreen National Park, the flood protection in Sunndalen, in the area close to Sunndøla at Folva, work well and keep the area relatively dry during the floods. Nevertheless, farms in the downstream and parts of Hjelle are still at risk of flooding when the hydrological forcing becomes too intense. However, the analyses of flood breach zones along the riverbanks and potential installations of levees have shown that the resistive capacity of the valley can be increased to some extent.

One of the limitations of this study is the use of water discharge data produced by flood flow analysis models as a forcing in the numerical experiments. This implies that the flood values prescribed as hydrographs are obtained from RFFA-2018 and are therefore predicted data (Wilson et al., 2011). Although they are validated against available real-time gauging station data, these estimates are not always sufficiently accurate. Besides, spatial patterns of precipitation play a key role in defining the volume and water flow in different sectors of the river and its tributaries during floods. Here, the analysis could not consider possible impacts of spatially diverse and topographically driven rainfall and glacier melt. Finally, in this study, the interpretation and simulation of the actual flood damage is restricted due to lack of sediment load carried by the river and topographic changes induced by the erosion of riverbanks during floods. Without the information on the energy exerted by the river flow through erosion and sediment entrainment, it is hard to analyse the extent of physical damage that the flood has on the infrastructure such as bridges, culverts, roads, and levees, and on agricultural lands and private property.

While setting up the model for the analyses presented in this thesis, several “sensitivities” of the model that did adversely impact the results of simulations were identified. Whatever highly efficient the model is in simulating floods, it has a number of drawbacks that become apparent when setting up local experiments. These include water leaks and gaps in the 2D geometry as well as under certain circumstances unphysical behaviour of fluids. The study has however demonstrated that designing the water flow area with minimum error in the mesh and careful computational settings can easily address these issues through a trial-and-error method, resulting in the best fit settings with a steady water flow for each experiment.

Following the growing availability of data on river regimes, run-off states, and water discharge, combined with the climate analysis data and surface mass balance models, the experiments presented here can be easily improved and adapted to any river system, whether or not it is fed by glacier systems. Based on the evidence from the reconstructed past flood, it is apparent that hydrological models with such high resolving capacity are great tools for flood simulations, including future projections and an identification of risk zones. With ever-developing versions of the HEC-RAS model, it is easier to modify the terrain by adding or removing levees, dams, and flood mitigation measures of diverse types. Increasingly more advanced and complex features of the model can help further studies to fill the identified gaps in this study to account for the impacts of river sediments and rainfall heterogeneities and thus produce predictions and reconstructions with a higher accuracy.

6 References

Bjarne Kjøllmoen, L. M. A., Hallgeir Elvehøy and Kjetil Melvold. (2021). *Glaciological investigations in Norway 2020* (31/2021). Retrieved from Oslo: http://publikasjoner.nve.no/rapport/2021/rapport2021_31.pdf

Brunner, G. W. (2021a). *HEC-RAS User's Manual*. Retrieved from https://www.hec.usace.army.mil/confluence/rasdocs/rasum/latest/foreword

Brunner, G. W. (2021b). *HEC-RAS River Analysis System Hydraulic Reference Manual*. Retrieved from https://www.hec.usace.army.mil/software/hec-ras/documentation/HEC-RAS%205.0%20Reference%20Manual.pdf

Brunner, G. W. (2021c). *HEC-RAS River Analysis System 2D Modeling User's Manual*. Retrieved from https://www.hec.usace.army.mil/software/hec-ras/documentation/HEC-RAS%205.0%202D%20Modeling%20Users%20Manual.pdf

Demiroglu, O. C., Dannevig, H., & Aall, C. (2018). Climate change acknowledgement and responses of summer (glacier) ski visitors in Norway. *Scandinavian Journal of Hospitality and Tourism, 18*(4), 419-438. doi:10.1080/15022250.2018.1522721

Drageset, T.-A. (2001). *Flood Calculation of Jostedøla*. Retrieved from chrome-extension://efaidnbmnnnibpcajpcglclefindmkaj/https://publikasjoner.nve.no/dokument/2001/dokument2001_01.pdf

Engeland, K., Glad, P., Hamududu, BH, Li, H., Reitan, T., Stenius, SM. (2020). *Local and regional flood frequency analysis* (NVE Report No. 10/2020.). Retrieved from

Esfahani, F. S., & Keshavarzi, A. R. (2010). How far must trees be cultivated from the edge of the flood plain to provide best river bank protection? *International Journal of River Basin Management, 8*(1), 109-116. doi:10.1080/15715121003714894

Gibson, S. (Producer). (2022). Using HEC-RAS Mapper Mods to REMOVE an Irregular Feature. Retrieved from https://www.youtube.com/watch?v=c4enO6qUynE

Gong, Y., & Rogozhina, I. (2021). High-resolution modeling of glacier mass balance and surface runoff in western Norway driven by bias-corrected climate forcing. *Hydrol. Earth Syst. Sci. Discuss., 2021*, 1-31. doi:10.5194/hess-2021-500

Goodell, C. (2014). The Measuring Tool. Retrieved from https://www.kleinschmidtgroup.com/ras-post/the-measuring-tool/

Goodell, C. (2015). 2D Mesh "Leaking". Retrieved from https://www.kleinschmidtgroup.com/ras-post/2d-mesh-leaking/

Goodell, C. (2019). Removing bridge decks from terrain surfaces. Retrieved from https://www.kleinschmidtgroup.com/ras-post/removing-bridge-decks-from-terrain-surfaces/

Hagen, J. O. (2019). Tystigbreen. Retrieved from https://snl.no/Tystigbreen

Hayat, H., Saifullah, M., Ashraf, M., Liu, S., Sher, M., Khan, R., & Adnan Ahmad, T. (2021). Flood Hazard Mapping of Rivers in Snow- and Glacier-Fed Basins of Different Hydrological Regimes Using a Hydrodynamic Model under RCP Scenarios. *Water, 13*(20), 2806. doi:https://doi.org/10.3390/w13202806

Hoel, O. L. (2013). Flaumen i 1979. Retrieved from http://www.historielaget.jostedal.no/?page_id=2720

Lim, K., Treitz, P., Wulder, M., St-Onge, B., & Flood, M. (2003). LiDAR remote sensing of forest structure. *Progress in Physical Geography: Earth and Environment, 27*(1), 88-106. doi:10.1191/0309133303pp360ra

Miriam Jackson, G. R. (2014). *Inventory of glacier-related hazardous events in Norway* (83 – 2014). Retrieved from Oslo: https://publikasjoner.nve.no/rapport/2014/rapport2014_83.pdf

NOAA. (2021). What is lidar? . Retrieved from https://oceanservice.noaa.gov/facts/lidar.html

NVE. (1981). *Flommen I Jostedal, 1 August 1979* (Rapport Nr 2-81). Retrieved from Oslo: chrome-extension://efaidnbmnnnibpcajpcglclefindmkaj/https://publikasjoner.nve.no/rapport/1981/rapport1981_02.pdf

NVE. (2018). Nedlasting av fagdata fra NVE. Retrieved from https://nedlasting.nve.no/gis/. Retrieved 11.09.22, from NVE https://nedlasting.nve.no/gis/

NVE. (2020). Glacier Monitoring: Nigardsbreen. Retrieved from https://www.nve.no/hydrology/glaciers/glacier-monitoring/nigardsbreen/

NVE. (2022a, 08.06.2021). Glacier Periodic Photo: Nigardsbreen-2297. Retrieved from http://glacier.nve.no/Glacier/viewer/gpp/en/nve/GlacierPictureInfo/2297

NVE. (2022b). NVE Atlas. Retrieved from https://atlas.nve.no/Html5Viewer/index.html?viewer=nveatlas#. Sikringstiltak, from NVE https://atlas.nve.no/Html5Viewer/index.html?viewer=nveatlas#

NVE. (2022c). Sildre. Retrieved from https://sildre.nve.no/map. https://sildre.nve.no/map

Oerlemans, J. (1992). Climate sensitivity of glaciers in southern Norway: application of an energy-balance model to Nigardsbreen, Hellstugubreen and Alfotbreen. *Journal of glaciology, 38*(129), 223-232. doi:10.3189/S0022143000003634

Oerlemans, J. (1997). A flowline model for Nigardsbreen, Norway: projection of future glacier length based on dynamic calibration with the historic record. *Annals of Glaciology, 24*, 382-389. doi:10.3189/S0260305500012489

Oerlemans, J. (2007). Estimating response times of Vadret da Morteratsch, Vadret da Palü, Briksdalsbreen and Nigardsbreen from their length records. *Journal of glaciology, 53*(182), 357-362. doi:10.3189/002214307783258387

Østrem, G., Liestøl, O., & Wold, B. (1976). Glaciological investigations at Nigardsbreen, Norway. *Norsk Geografisk Tidsskrift - Norwegian Journal of Geography, 30*(4), 187-209. doi:10.1080/00291957608552005

Pepin, N., Bradley, R. S., Diaz, H. F., Baraer, M., Caceres, E. B., Forsythe, N., . . . Mountain Research Initiative, E. D. W. W. G. (2015). Elevation-dependent warming in mountain regions of the world. *Nature Climate Change, 5*(5), 424-430. doi:10.1038/nclimate2563

Roald, L. A. (2021). *Floods in Norway* (1/2021). Retrieved from Oslo: https://publikasjoner.nve.no/rapport/2021/rapport2021_01.pdf

SeNorge. (2022). Daily theme map. Retrieved from https://www.senorge.no/map. from Varsom SeNorge https://www.senorge.no/map

SSB. (2022). Tettsteders befolkning og areal. Retrieved from https://www.ssb.no/en/befolkning/folketall/statistikk/tettsteders-befolkning-og-areal. Available from Statistik sentralbyrå Retrieved 10.10.22, from Statistik sentralbyrå https://www.ssb.no/en/befolkning/folketall/statistikk/tettsteders-befolkning-og-areal

Svendsen, S. (2022). *Potential physical and societal impacts of glacial lake outburst floods in Hjelledalen, Stryn, Norway.* (Master in Geography). Norwegian University of Science and Technology, Retrieved from https://hdl.handle.net/11250/3020015

Vaughan, D., Comiso, J. C., & Allison, J. (2013). Observations: Cryosphere. Climate Change 2013: The physical science basis. *Contribution of working group I to the Fifth Assessment Report of the Intergovernmental Panel on climate change*.

Wilson, D., Fleig , A. K., Lawrence, D., Hisdal, H., Pettersson, L.-E., & Holmqvist, E. (2011). *A review of NVE's flood frequency estimation procedures*. Retrieved from chrome-extension://efaidnbmnnnibpcajpcglclefindmkaj/https://publikasjoner.nve.no/report/2011/report2011_09.pdf

Zemp, M., Frey, H., Gärtner-Roer, I., Nussbaumer, S. U., Hoelzle, M., Paul, F., . . . Anderson, B. (2015). Historically unprecedented global glacier decline in the early 21st century. *Journal of glaciology*, *61*(228), 745-762.

Appendix 1

6.1 Data collection websites

Data	Link
Digital terrain Model	https://hoydedata.no/LaserInnsyn/
Gauging station data	https://sildre.nve.no/map
Regional flood frequency analysis	https://nevina.nve.no/
Orthophotos	https://www.norgeibilder.no/
Flood mitigation measures	https://atlas.nve.no/Html5Viewer/index.html?viewer=nveatlas#

NTNU

Norwegian University of
Science and Technology